UNIVERSITY OF CALIFORNIA SAN DIEGO

The Roles of Homeodomain Proteins SIX3 and SIX6 in GnRH Neuron Migration, Maturation, and Development

A dissertation submitted in partial satisfaction of the requirements of the degree Doctor of Philosophy

in

Biomedical Sciences

by

Erica Christine Pandolfi

Committee in charge:

Professor Pamela L. Mellon, Chair
Professor Alexander S. Kauffman
Professor Mark A. Lawson
Professor Alysson R. Muotri
Professor Nicholas J. G. Webster

2018

The Dissertation of Erica Christine Pandolfi is approved, and it is acceptable in quality and form for publication on microfilm and electronically.

Chair

University of California San Diego

2018

DEDICATION

This dissertation is dedicated to my grandparents for their unyielding love and support.

EPIGRAPH

Intelligence and proper education will give you independence of spirit.

Charlotte Bronte

TABLE OF CONTENTS

LIST OF ABBREVIATIONS

AOB	Accessory olfactory bulb
ACOV	Assay coefficients of variance
AVP	Arginine vasopressin
DEG	Differentially expressed genes
E_2	Sine oculis-related homeobox 6
FSH	Follicle-stimulating hormone
GBC	Globose basal cell
GnRH	Gonadotropin-Releasing Hormone
H & E	Hemotoxylin and Eosin
HET	Heterozygous
HBC	Horizonal basal cells
HPG	Hypothalamic-pituitary-gonadal
iORN	Immature olfactory receptor neuron
IHC	Immunohistochemistry
IHH	Idiopathic Hypogonadotropic Hypogonadism
IUCAC	Institutional animal care and use committee
KISS	Kisspeptin
LH	Luteinizing hormone
LHRH	Luteinizing hormone-releasing hormone
MASH1	Mammalian achaete scute homolog 1
ME	Median eminence
MOB	Main olfactory bulb
MOE	Main olfactory epithelium
MOS	Main olfactory system
MUP	Major urinary protein
Ngn1	Neurogenin1
OMP	Olfactory marker protein
QPCR	Quantitative polymerase chain reaction
ORN	Olfactory receptor neuron
ROI	Regions of interest
SCN	Suprachiasmatic nucleus

Six3	Sine oculis-related homeobox 3
Six6	Sine oculis-related homeobox 6
SUS	Sustentacular cells
VIP	Vasoactive intestinal polypetide
VNO	Vomeronasal organ
WT	Wild-type

LIST OF FIGURES

ACKNOWLEDGEMENTS

I would like to thank Professor Pamela L. Mellon for her support both personally and professionally. She has always been a mentor that has pushed me to work hard, in an effort to make her proud. I would also like to thank my undergraduate mentors Dr. Daniel Morse, and Dr. Ruben Alarcon, whose guidance has molded me as a scientist and as a person. I want to thank Dr. Alarcon for being the first person to believe in me, and Dr. Morse for being the first person to show me how to believe in myself. I would like to thank the members of my thesis committee: Professors Alexander S. Kauffman, Nicholas J. G. Webster, Mark A. Lawson, and Alysson R. Muotri, for their support, guidance, and time. I want to give special thanks to Dr. Mark Lawson for being a mentor and role-model for me, who was always there with advice for me, both professional and personal. In addition, I want to thank the Med-into-Grad initiative for giving me the opportunity to work in the clinic, alongside Dr. R. Jeffrey Chang who was been a wonderful mentor and fabulous friend throughout my graduate work.

Furthermore, I am appreciative of my close friends in the Mellon lab, Dr. Jessica Cassin, Dr. Lauren Chun, and Emily Ho, whom have filled my days with smiles, science advice, and gossip. I would like to give special thanks to Dr. Hanne M. Hoffmann for her instruction in learning essential techniques, and her guidance in writing grants and papers. I appreciate the constant advice and support from the members of the Department of Reproductive Medicine, including members of the Kauffman Lab, Lawson Lab, Thackray Lab, and Breen-Church Lab. Finally, I need to appreciate the mice who unwillingly donated their lives to this project.

I also want to acknowledge my friends and family for their support. I want to thank my brother, Dr. Ronald Pandolfi, for being a role model for me, and for always being willing to drop

everything to help me with whatever crisis I am dealing with. Additionally, I thank my mother for supporting me emotionally and for being my nurse whenever I'm sick. More notably, I thank her for instilling in me a value in education and independence. Furthermore, I want to thank my grandparents for their unyielding love and support, and for always believing in me. In addition, I am grateful to my Aunt and Uncle Rebecca and Steve Fitzpatrick for being a pillar of support that I can always rely on. Another family member I need to acknowledge is my cat Princess Monkey, for embodying unconditional love and friendship. Finally, I am delighted to thank my fiancé, Justin Smolian, for supporting my work and for filling my life with happiness and hope.

This work was supported by National Institutes of Health grants R01 HD082567 and R01 HD072754 (to P.L.M.) and by National Institute of Child Health and Human Development/National Institutes of Health P50 HD012303 as part of the National Centers for Translational Research in Reproduction and Infertility. This work was also partially supported by P30 DK063491, P42 ES101337, and P30 CA023100. I was also partially supported by National Institutes of Health R25 GM083275 and National Institutes of Health F31 HD098652.

Chapter 1 has been published in *Molecular Neurobiology* (Pandolfi, Erica C.; Hoffmann, Hanne M.; Schoeller, Erica L.; Gorman, Michael R.; Mellon, Pamela L. 2018.) Haploinsufficiency of Six3 abolishes male reproductive behavior through disrupted olfactory development, and impairs female reproductive behavior through disrupted GnRH neuron migration. 2018. Dr. Hanne Hoffmann assisted with the experimental design, wheel-running experiments, and paper composition. Dr. Erica Schoeller assisted with the behavioral experiments. Dr. Michael Gorman assisted with the wheel-running experiments. The dissertation author was the primary investigator and author of this material. Pamela Mellon supervised the project and provided advice. Chapter 1 also contains a review article accepted by *Neuroendocrinology* (Hoffmann, Hanne M.; Pandolfi, Erica C.; Larder, Rachel; Mellon, Pamela L. 2018), and a manuscript published in *The Journal of*

Neuroscience (Hoffmann, Hanne M.; Trang, Crystal; Gong P.; Kimura, Ikuo; Pandolfi, Erica C.; and Mellon, Pamela L. 2016).

Chapter 2 is currently being prepared for submission for publication of this material. Pandolfi, Erica C.; Jones, Samantha H.; Burow, Dana A.; Wilkinson, Miles F.; Mellon, Pamela L. The dissertation author is the primary investigator and author of this material. Dr. Samantha Jones contributed the single-cell sequencing data. Dr. Dana Burow contributed the analysis of the single-cell sequencing data. Dr. Wilkinson oversaw collection and analysis of the single-cell sequencing data. Pamela Mellon supervised the project and provided advice.

Chapter 3 is currently being prepared for submission for publication of this material. Pandolfi, Erica C.; Hoffmann, Hanne M.; Mellon, Pamela L. The dissertation author is the primary investigator and author of this material. Hanne Hoffmann assisted in making the *Six6flox* mouse, and in writing the manuscript. Pamela Mellon supervised the project and provided advice.

Chapter 4 is currently being prepared for submission for publication of this material. Pandolfi, Erica C.; Hoffmann, Hanne M,; Mellon, Pamela L. The dissertation author is the primary investigator and author of this material. Hanne Hoffmann assisted in making the *Six6flox* mouse, and in writing the manuscript. Pamela Mellon supervised the project and provided advice.

VITA

2013 Bachelor of Science, Biological Sciences, University of California, Santa Barbara

2018 Doctor of Philosophy, Biomedical Sciences, University of California, San Diego

PUBLICATIONS

Pandolfi EC, Hoffmann HM, Mellon PL. Deletion of *Six6* from Gonadotropin-Releasing Hormone (GnRH) Neurons Decreases GnRH Expression Resulting in Hypogonadism and Infertility. (In Preparation).

Pandolfi EC, Jones SH, Burow DA, Wilkinson MF, Mellon PL. Homeodomain Protein SIX3 is required for Development of the Main Olfactory Epithelium and Normal Olfaction. (In Preparation).

Hanne M. Hoffmann HM, **Pandolfi EC,** Larder R, Mellon PL. Haploinsufficiency of Homeodomain Proteins Six3, Vax1, and Otx2, Causes Subfertility in Mice Via Distinct Mechanisms. *Neuroendocrinology*. Accepted for Publication

Pandolfi EC, Hoffmann HM, Schoeller EL, Gorman MR, Mellon PL. Haploinsufficiency of SIX3 Abolishes Male Reproductive Behavior Through Disrupted Olfactory Development, and Impairs Female Fertility Through Disrupted GnRH Neuron Migration. (2018). *Molecular Neurobiology* 55, 8709-8727

Hoffmann HM, Trang C, Gong P, Kimura I, **Pandolfi EC**, and Mellon PL. (2016). Deletion of Vax1 from GnRH Neurons Abolishes GnRH Expression and Leads to Hypogonadism and Infertility. *Journal of Neuroscience* 55, 8709-8727

DeMartini DG, Izumi M, Weaver AT, **Pandolfi EC,** Morse DE. Structures, Organization, and Function of Reflectin Proteins in Dynamically Tunable Reflective Cells. (2015). *The Journal of Biological Chemistry* vol. 290 (24) p. 15238-49

DeMartini DG, Ghoshal A, **Pandolfi EC**, Weaver AT, Baum M, Morse DE. Dynamic Biophotonics: Female Squid Exhibit Sexually Dimorphic Tunable Leucophores and Iridocytes. (2013). *Journal of Experimental Biology* 216, 3733-3741

ABSTRACT OF THE DISSERTATION

The Roles of Homeodomain Proteins SIX3 and SIX6 in GnRH Neuron Migration, Maturation, and Development

by

Erica Christine Pandolfi

Doctor of Philosophy in Biomedical Sciences

University of California San Diego, 2018

Professor Pamela L. Mellon, Chair

Gonadotropin-releasing hormone (GnRH) is a primary and essential regulator of vertebrate reproduction. When GnRH neurons are compromised, GnRH expression is attenuated, producing the condition Idiopathic Hypogonadotropic Hypogonadism (IHH). IHH is characterized by infertility and/or delayed or absent puberty. When this condition is accompanied by anosmia, it is termed Kallmann syndrome. Although it is clearly a crucial factor in the reproduction of mammalian species, little is known about the genetic regulators of GnRH neuronal ontogeny. In

the work presented herein, we elucidate developmental and genetic mechanisms that control the migration and maturation of GnRH neurons, and therefore illuminate the novel mechanisms responsible for IHH. Furthermore, we have identified new genes influencing the relationship between nasal development and GnRH neuron migration- further elucidating the etiology of Kallmann syndrome. The two genes that are explored in the work presented here are the closely related homeodomain transcription factors, sine oculis-related homeobox 3 (*Six3*) and *Six6*. First, we present data demonstrating that *Six3* regulates GnRH neuron migration through actions external to the GnRH neuron. *Six3* heterozygous mice displayed disrupted migration of GnRH neurons and severe olfactory impairment. Interestingly when the role of *Six3* specifically within the GnRH neuron was investigated using a GnRH specific cre-recombinase, we found that *Six3* acts within the neuron to upregulate GnRH neuron number. In addition, we investigated the actions of the closely related gene *Six6. Six6* was found to be essential for survival of GnRH neurons and maintenance of fertility in a Six6 knock-out mouse. Six6 was found to play a similar role within the GnRH neuron in enabling fertility; however, within the GnRH neuron, Six6 acts to regulate GnRH expression. These investigations have enabled us to garner knowledge concerning the novel regulatory mechanisms of this fascinating hormone; and, has allowed us to shed light on the causes of infertility plaguing ~7% of all couples.

INTRODUCTION

GnRH Neurons in IHH

Understanding the ontogeny of GnRH neurons is imperative to understanding the regulation of human reproduction. Situated at the peak of the hypothalamic-pituitary-gonadal axis, this small population of neurons is responsible for releasing the decapeptide GnRH in a pulsatile manner. GnRH is released into the hypophyseal portal circulation to reach the pituitary, which responds by releasing luteinizing hormone (LH) and follicle-stimulating hormone (FSH) to stimulate production of gonadal steroids (1). These steroids provide feedback that regulate each previous step (the pituitary and the hypothalamus). GnRH neurons respond to cues about the environment, such as circadian rhythms, sexual maturation, and metabolic conditions, and fluctuate their release of GnRH accordingly (2). When GnRH is deficient, the HPG axis is disrupted, affecting fertility (3).

Idiopathic Hypogonadotropic Hypogonadism and Kallmann Syndrome

One example of a disruption in the HPG axis is idiopathic hypogonadatropic hypogonadism (IHH). The incidence of IHH is 1-10 per 10,000 births (2). IHH is engendered by a failure to activate secretion of GnRH during puberty, the developmental stage when GnRH is substantially increased in frequency and amplitude. The condition is characterized by infertility and delayed or absent puberty. When this condition is accompanied by anosmia (the inability to smell), it is termed Kallmann syndrome. Kallmann syndrome is a rare genetic disorder of complex and heterogeneous genetic etiology, characterized by the loss of fertility, absent or delayed puberty, and anosmia/hyposmia due to developmental errors in nasal structures and GnRH neurons (1,4).

GnRH neurons originate in the olfactory placode and migrate along olfactory axonal projections to reach the forebrain (5-7). Due to the topographical and migratory link between the GnRH neuronal population and the neurons of the main olfactory epithelium (MOE), it is not surprising that their fates are tied together and that both are compromised in the human developmental disorder termed Kallmann syndrome (4,8). Previous genetic analyses studying familial cases of Kallmann syndrome have revealed that there are multiple genes involved in the regulation of GnRH neuron migration and olfactory system development (9-11). Some cases of Kallmann syndrome have been linked to compound heterozygosity in patients (11).

Olfactory Development

Mammalian behaviors such as aggression, mating, and fear all depend on signaling within the olfactory system (12). Reproductive behavior in mice is dependent upon olfactory signaling to convey information about the sex, social, and reproductive status of conspecifics (13). This olfactory communication stimulates the necessary neuroendocrine responses that drive reproduction (14,15). Rodents contain two anatomically and functionally separate neuronal populations in the nose termed the main olfactory epithelium and the vomeronasal organ (VNO) (16). Complex chemosignals are received and processed by sensory neurons in the MOE that project to glomeruli in the main olfactory bulb (MOB), while the sensory neurons in the VNO project to the accessory olfactory bulb (16). Although there is overlap between these two anatomically distinct organs systems, it is generally believed that neurons within the MOE respond mainly to volatile odorants in the environment, whereas VNO neurons mainly process signals about non-volatile pheromones (14,16-18). The odorants that cue mating behavior in male mice are volatile odorants processed by the MOE (14,19,20). Previous research demonstrates that exclusive impairment of the MOE results in disrupted male reproductive behavior due to the inability to recognize estrus females (18,20-22). These experiments have bolstered the conclusion that the MOE is mainly responsible for the processing of mating odorants. While human mating

behavior is not largely driven by olfaction as it is in rodents and other mammals, olfaction is an essential part of our everyday lives, and therefore understanding the genetics of development of the olfactory system is essential (23). Furthermore, improper development of the olfactory system has been linked to abnormal sexual maturation in humans (23).

GnRH Neuron Migration

When GnRH neurons mis-migrate, they cannot locate correctly in the hypothalamus, release GnRH at the median eminence, or orchestrate proper reproductive physiology, resulting in IHH (24). GnRH neurons have a unique cellular origin; in mice, they are first detected on embryonic day 11.5 (e11.5) in the olfactory placode, only detectable with the onset of GnRH expression. GnRH neurons move from the nasal placode into the hypothalamus where they extend their axons into the median eminence (25). The complex developmental events leading to correct GnRH neuronal migration and survival are regulated by many factors including: Prokineticin-2, Prokineticin Receptor-2, SDF1/CXCR4, FGF8/FGFR-1, Plexin B1, Plexin C1, Neuropilin-2, Neuropilin-1, and several Semaphorins (7a, 4d, and 3a) (26-30). Migration and development are crucial components in the survival and travel of GnRH neurons; when disrupted, they can lead to impairment of the HPG axis manifesting as GnRH deficiency (31).

The Importance of Six3 and Six6 in GnRH Neurons

While mutations in several genes have been shown to cause IHH, over 68% of the cases of IHH are of an unknown genetic origin (2,32). As such, the genetic program underlying GnRH neuronal ontogeny is poorly understood; and new genes involved in GnRH neuronal development and IHH must be identified. To identify new genes of interest in IHH, the Mellon lab performed a microarray screen comparing RNA levels between GN11 cells and GT1-7 cells (33-35). GT1-7 cells are GnRH-secreting, immortal, differentiated, hypothalamic neurons. GN11 cells, another GnRH cell line, secrete low levels of GnRH, and represents the immature, migratory stage of the

GnRH neuron (36-39). Based on the divergent phenotypes of these two cell lines, new gene products expressed at different times in GnRH neuronal development can be identified.

Six6 was found to be one of the most differentially expressed genes of the ~2000 transcripts identified in this screening of GN11 and GT1-7 cells (33). Finding that *Six6* expression correlated with an increase in GnRH expression led our lab to hypothesize that SIX6 could play a role in the regulation of GnRH gene expression, implicating *Six6 (*a tissue-specific repressor and regulator of progenitor cell proliferation) (40) as a possible player in the hypothalamic control of fertility. The RNAseq screening also identified a second Six gene, *Six3*, to be preferentially expressed in GT1-7 over GN11, suggesting that this gene might play a role in GnRH neurons during development and into adulthood (33). The Six proteins are members of the mammalian Six protein family, that are composed of two highly conserved domains (41). These domains consist of a homeodomain (that mediates DNA interaction) and a Six domain (that modulates specificity for DNA binding) (42). While all Six genes show expression during embryogenesis, *Six6* and *Six3* are expressed solely in the developing eye (Six6), olfactory system (Six3), pituitary, and brain tissues, in particular the hypothalamus (Fig. 1) (43). A strong influence of Six6 on GnRH neurons and fertility has already been ascertained by the Mellon Lab. Our published data show that mice with a whole-body knock-out of *Six6* (Six6KO) exhibit a striking decrease in fertility in both male and female mice (Table1) (33). Additionally, a marked 90% reduction in the number of GnRH neurons in Six6KO mice was reported (33). Furthermore, Using transient transfections in GT1-7 cells, we have shown SIX3 and SIX6 to be direct regulators of the GnRH promoter-luciferase reporter, through binding directly to ATTA elements (33). When *Six6* was overexpressed via transfection in GN11 and GT1-7 cells, *Six6* caused activation of the luciferase reporter in both cell lines and induced overexpression of GnRH (33). The *Six3* gene was similarly tested and activated the GnRH E/P-luc in GN11 cells; however, in GT1-7 cells (the mature GnRH cells), *Six3* was found to be a repressor of the same reporter (Fig. 4) (33). A compelling relationship between the

effects of *Six6* and *Six3*, emerged in that the repressive effects of *Six3* could be eliminated by titrating in *Six6* (Figure 2). To fully understand the balancing act of *Six3* and *Six6* in GnRH development, their roles must be investigated both within and outside of the GnRH neuron.

Chapter 1: Haploinsufficiency of SIX3 Abolishes Male Reproductive Behavior through Disrupted Olfactory Development, and Impairs Female Fertility through Disrupted GnRH Neuron Migration

Abstract

Mating behavior in males and females is dependent on olfactory cues processed through both the main olfactory epithelium (MOE) and the vomeronasal organ (VNO). Signaling through the MOE is critical for the initiation of male mating behavior, and the loss of MOE signaling severely compromises this comportment. Here, we demonstrate that dosage of the homeodomain gene *Six3* affects the degree of development of MOE but not the VNO. Anomalous MOE development in *Six3* heterozygote mice leads to hyposmia, specifically disrupting male mounting behavior by impairing detection of volatile female estrus pheromones. *Six3* is highly expressed in the MOE, main olfactory bulb (MOB), and hypothalamus; all regions essential in the proper migration of the gonadotropin-releasing hormone (GnRH) neurons, a key reproductive neuronal population that migrates along olfactory axons from the developing nose into the brain. Interestingly, we find that the reduction in *Six3* expression in *Six3* heterozygote mice compromises development of the MOE and MOB, resulting in mis-migration of GnRH neurons due to improper olfactory axon targeting. This reduction in the hypothalamic GnRH neuron population, by 45% in adulthood, leads to female subfertility, but does not impact male hormone levels, suggesting that male infertility is not related to GnRH neuron numbers, but exclusively linked to abnormal olfaction. We here determine that *Six3* is haploinsufficient for MOE development, GnRH neuron migration, and fertility, and represents a novel candidate gene for Kallmann syndrome, a form of inherited infertility.

Introduction

Aggression, mating behavior, and fear responses depend on an intact olfactory circuit in mammals (44). Olfaction is required to distinguish sex, social, and reproductive status, as well as to express sexual behavior and induce neuroendocrine responses necessary for reproduction (13,45-47). In rodents, these odors are processed via two anatomically and functionally separate sets of neurons localized in the main olfactory epithelium (MOE) and the vomeronasal organ (VNO) (16). In the MOE, complex chemosignals are detected and differentiated by sensory neurons that project to glomeruli in the main olfactory bulb (MOB) (16). It is believed that MOE neurons respond mainly to volatile odorants in the environment, whereas VNO neurons respond mainly to non-volatile pheromones, with some overlap between the functions of these anatomically distinct organs (16,48). Interestingly, volatile odorants that cue mating behavior in mice are processed by the MOE (19-22,49), and exclusive impairment of the MOE results in disrupted male reproductive behavior due to the inability to recognize estrus females (19,50,51). Although humans do not need their sense of smell for reproduction, olfaction is an essential part of our everyday lives, and it is clear that proper development of the olfactory system is required for normal sexual maturation (23).

The development of olfactory neurons is closely linked to the development of the key reproductive neurons, gonadotropin-releasing hormone (GnRH) neurons (5,25,51-54). GnRH neurons originate in the primordial MOE (the olfactory placode), and migrate along olfactory nerves into the forebrain (5-7). Due to the topographical and migratory link between the development of the olfactory system and GnRH neurons, it is not surprising that their fates are tied together and that both are compromised in the developmental disorder termed Kallmann syndrome (4,8). Kallmann syndrome is a rare genetic disorder of complex and heterogeneous genetic etiology, leading to various degrees of subfertility, including complete infertility (hypogonadal hypogonadism), along with anosmia/hyposmia in humans (1,4). Genetic analysis

in familial cases of Kallmann syndrome has demonstrated that there are multiple genes involved in the process of regulating GnRH and olfactory neuron migration, including compound heterozygosity in patients (9,11). Despite recent advances, ~68% of the cases of Kallmann syndrome are of an unknown genetic origin, thus identification of new genes of interest in this condition is critical (11,55).

Several newly discovered genes (56,57) and haploinsufficiencies (32,58) that alter GnRH neurons in development in mouse models are candidates for hypogonadal hypogonadism without anosmia. One potential candidate for Kallmann syndrome is the homeodomain gene *Six3*, which is highly expressed in the MOE, MOB, and hypothalamus, areas essential for maintaining reproduction and olfaction (www.brain-map.org, consulted Feb 2017). Due to early postnatal lethality of *Six3* knock-out (KO) mice (59), they have only been studied during early embryogenesis, with a focus on craniofacial and eye development (60,61). Haploinsufficiency of *Six3* has been recently studied and shown to produce a phenotype in holoprosencephaly; demonstrating that dosage of SIX3 can be directly proportional to the severity of a phenotype (62-64). Here, we present the first study of the fertility of adult *Six3* heterozygote (HET) mice, finding that *Six3* haploinsufficiency alters male fertility, with various degrees of subfertility to infertility attributed to disrupted development of the MOE producing an incapacity to express normal sexual behavior.

Methods

Mouse lines and animal housing. All animal procedures were performed in accordance with the University of California, San Diego, Institutional Animal Care and Use Committee regulations.

Mice were group-housed with ~4 to a cage on a 12-hour light, 12-hour dark cycle (on 6:00 A.M., off 6:00 P.M.), with *ad libitum* chow and water. All mice were kept on a C57BL/6J mouse background. *Six3*-flox mice were provided by Dr. Guillermo Oliver (59). *Six3* KO mice were

created by crossing *Six3*-flox with a Zp3-Cre mouse (65) (https://www.jax.org/strain/006888), allowing germ-line recombination. *Six3*-flox mice were crossed with *GnRH*-Cre (66) mice to create *Six3*$^{flox/flox}$*:GnRH*^{cre} mice homozygous for the *Six3* deletion within GnRH neurons. The mice were killed by a CO_2 or isoflurane (Vet One) overdose. Unless specified, all animals used were ~3 months of age.

Behavioral experiments. All behavioral tests were performed during the first three hours of the dark phase using red light illumination. The experimenter was blind to the genotype of the subjects. Before each assay, the mice were habituated for 1 hour in a new cage with fresh bedding and no food or water. All females presented to males in behavioral tests were virgin ovariectomized and primed with 1 µg estradiol benzoate diluted in sesame oil at 9 A.M. the day before testing and 500 µg progesterone diluted in sesame oil at 2 P.M. on the day of testing.

Collection of tissue and histology. Diestrus ovaries, brains, olfactory bulbs, embryos, noses, ovaries, and testes were fixed overnight (~16 h) at 4°C in freshly made mixture of 6:3:1 absolute alcohol: 37% formaldehyde (Fisher F79-4): glacial acetic acid. Tissues were paraffin embedded and serially sectioned at 10 µm. Ovaries, testes, brains, and noses were stained with hematoxylin and eosin (H&E; Sigma-Aldrich). In ovaries, histology was examined and the number of corpora lutea in a single ovary per mouse was recorded blindly.

Immunohistochemistry. Adult brains, olfactory bulbs, and embryos were sectioned at 10 µm. Immunohistochemistry (IHC) was performed as described previously (42). Sections were immunostained with rabbit anti-GnRH (1:1000; Novus Biologicals, catalog number: NB300-506, RRID:AB_2110266), anti-peripherin (1:200; Abcam, catalog number: ab4573, RRID:AB_2171346), or rabbit anti-OMP (1:100; Santa Cruz Biotechnology, catalog number: sc-67219, RRID:AB_2158005). To increase the visibility of immunostained neurons, adjustments of brightness, contrast, and color balance were done with Image J (National Institutes of Health,

Health, Bethesda) and applied to the entire image. Peripherin quantification was conducted by counting all fibers within the MOE/MOB region in the HET and WT mice. Such analysis could not be performed on the KO mice, as all the fibers were contained in one large mass and could not be individually quantified. Counterstaining was performed using vector Hematoxylin counterstain (H-3401) for 15 seconds, followed by running tap water for two minutes. Slides were then incubated in bluing solution for one minute and then rinsed in distilled H_2O.

GnRH neuron counting and OMP staining were conducted throughout the entire embryonic head, and throughout the adult brain beginning with the front of the olfactory bulb (bregma 4.46) to bregma –2.80 (67). Each slide was collected and evaluated for GnRH and Olfactory Marker Protein (OMP) staining in a blinded manner using a Nikon Eclipse E400 microscope. Although all collected sections were assessed for staining, neuroanatomical landmarks were used to identify the regions of interest (ROI) as depicted in the corresponding figures. Slides were coded to blind the researcher to treatment group during analysis. In KO mice where recognizable structures were absent, images were taken in locations corresponding to where structures of interest are normally seen. Adult brains analyzed for GnRH include equal numbers of both male and female subjects, although a sex difference in GnRH neurons has not been recorded to our knowledge. Embryos were not sexed.

Lineage tracing. For lineage tracing, *Rosa*^{tdTomato} reporter mice (https://www.jax.org/strain/007908) were used (68) and mated to *Six3* HET and *GnRH*^{cre} mice to create the *Six3*^{HET}:*Rosa*^{tdTomato}:*GnRH*^{cre} line. IHC was performed with the anti-RFP antibody (1:1000, Abcam, catalog number: ab62341, RRID: AB_945213).

GnRH-pituitary stimulation tests. For two weeks prior to the hormonal challenge, mice were adapted to handling stress such that they would be unaffected by stress during serial sampling. Baseline tail blood was collected from male and female metestrus/diestrus WT and *Six3* HET

littermates. Ten minutes after receiving an IP injection of 1 µg/kg GnRH (Sigma #L7134) diluted in physiological serum, tail blood was collected again. For kisspeptin challenge, 20 minutes after *ip* injection of 30 nmoles of kisspeptin (Tocris #4243) diluted in physiological serum was injected, tail blood was collected again. The total volume of blood collected did not exceed 100 µL. Blood was collected between 11:00 AM and 12:00 PM and was allowed to clot for 1 hour at room temperature. Blood was then centrifuged for 15 min at 2600 X g. Serum was collected and stored at -20°C before Luminex analysis was used to measure LH. The LH assay detection limit was 0.24 ng/mL, inter-assay CV was 15.2 and intra-assay CV was 11.5. This experiment was conducted as previously described (57).

Sperm motility and total sperm count. Epididymides were collected in M2 media at room temperature (Sigma-Aldrich). One epididymis was cut in half and sperm were gently expelled by manual pressure. The numbers of motile and immotile sperm were counted in a hemocytometer 15 minutes after sperm were expelled. To immobilize motile sperm for a total sperm count, the hemocytometer was placed for 5 minutes on a 55°C heat block. The second epididymis was chopped into small pieces and left 30 minutes at room temperature in M2 media. The solution was filtered through a 70 µm filter (Falcon), and the sperm were diluted in PBS before counting the total number of sperm heads in one epididymis. This experiment was performed as described previously (32).

Vaginal plug formation, mating assay, generation of timed embryos, and estrous cycling. To monitor plug formation, a WT or *Six3* HET female mouse was housed with either a WT or *Six3* HET male mouse at 12 weeks of age and plug formation was monitored for ten consecutive days. Embryos were obtained using timed matings in which one male and one female mouse were housed together, and vaginal plug formation was monitored. If a plug was present, the day was noted as day 0.5 of pregnancy and used to collect embryos for timed mating at embryonic day

e13.5 or e17.5. A second cohort of virgin *Six3* WT and HET mice were housed in pairs, and the number of litters born and the number of pups per litter were recorded over a period of 14 weeks. Mice were assessed for estrous cyclicity as previously described (32). To assess estrous cyclicity, vaginal smears were performed daily between 9:00 and 10:00 A.M. on 120-day-old mice by vaginal lavage as described previously (32). A cycle was determined by counting the days from one estrus period to the next estrus period.

Determination of day of vaginal opening and preputial separation. Starting at 21 days-of-age, *Six3* WT and HET mice were inspected daily and pubertal onset was determined by the age at vaginal opening in females or by preputial separation in males as previously described (32).

Mounting assay. Male mice were habituated to new cages for 1 hour. Ovariectomized and estrogen primed female mice were then introduced to WT and HET male mice of 16 weeks of age. This test was conducted three times with only the third trial quantified and reported. Trials were conducted one week apart from each other, and the same estrogen primed females were used in all assays. Pairs were videotaped and behavior quantitated in a blind manner with incidences of mounting being recorded over a period of 15 minutes. Some of the same males were used in the mounting assay, the buried food test, and the habituation-dishabituation experiments.

Buried food test. A buried food test was conducted to check for gross malfunction of the main olfactory system as described previously (69). All mice were food-deprived overnight (18 hrs). A small piece of mouse chow was buried (~3 cm deep) at a random location in a clean mouse cage containing fresh bedding. One mouse was placed in the cage and timed for the latency to find the mouse chow during a period of up to 15 minutes. Mice were videotaped and behavior quantitated in a blind manner.

Sugar water test. Six3 HET and *Six3* WT mice were housed under normal conditions, except a second water bottle was placed on the cage that contained 4% dissolved sugar. Prior to beginning testing, mice were habituated to the presence of two drinking bottles (one containing 4% sucrose and the other water) for 3 days in their home cage. Following this acclimation, mice had the free choice of either drinking the 4% sucrose solution or plain water for a period of 4 days. The location of the bottles was switched each day to avoid a confounding factor of cage-side preference. The water bottles were weighed at the beginning of the study and at the end, the change in weight was reported.

Wheel-running behavior. To determine if *Six3* HET mice had normal activity on running wheels, *Six3* HET and WT male mice were housed individually in cages with running wheels. Food and water was available *ad libitum* during the entire experiment. After 1 week acclimation to the polypropylene cages (17.8 × 25.4 × 15.2 cm) containing a metal running wheel (11.4 cm diameter), locomotor activity rhythms were monitored with a Vitalview data collection system (Version 4.2, Minimitter, Bend OR) that compiled in 6 min bins the number of electrical closures triggered by half wheel rotations. Running wheel activity was monitored for 2 weeks on a 12h Light:12h Dark cycle. Cage changes were scheduled at 3-week intervals. Wheel-running activity was analyzed using ClockLab Analysis (ActiMetrics Software).

Territorial marking assay. Six3 HET and *Six3* WT male mice were placed in a clean empty cage to habituate for 1 hour. After habituation, the bottom of the cage was covered with Whatman paper for 15 minutes to record a baseline for normal urination. This paper was then removed, and the bottom of the cage was covered with a new piece of Whatman paper with 60 µL of estrus female mouse urine placed in the center of the paper. Male mice were allowed to mark the paper for 15 minutes. The Whatman papers were then dried overnight and sprayed with 0.2% ninhydrin diluted in 100% EtOH (Sigma) and air dried until urine spots developed a purple color. Papers were

photographed and images were converted to binary and the number of urine marks was determined using Image J software. The number of marks elicited by sensing estrus female urine was determined by subtracting the number of urine marks in baseline markings. This experiment was conducted as previously described (70).

Male countermarking behavior against a strange male's urine. *Six3* HET and WT males, who had been singly housed and who were sexually inexperienced, were placed in a cage lined with Whatman paper for 30 min. Fifty μL of male urine pooled from 5 adult male mice was placed in the center of the Whatman paper. The Whatman papers were then dried overnight and sprayed with 0.2% ninhydrin diluted in 100% EtOH (Sigma) and air dried until urine spots developed a purple color. Papers were photographed and images were converted to binary and the number of urine marks was determined using Image J software. The number of marks elicited by sensing male urine was determined by subtracting the number of urine marks in baseline markings. Urine was collected from male mice by holding mice by the scruff of the neck over a piece of clean parafilm.

Urine collection. Urine was collected from stimulator estrus female mice by holding mice by the scruff of the neck over a piece of clean parafilm. Female stimulator mice were prepared by ovariectomizing female mice and inserting a low-dose estrogen pellet of 0.05 cm diameter subcutaneously. On the day of urine collection, stimulator females were injected with 1 μg of estradiol benzoate diluted in sesame oil 24 hours before collection, followed by 500 μg of progesterone diluted in sesame oil at 2 P.M. Urine was collected at 6 P.M. Urine from 5 different mice of each sex was pooled into separate male and female urine collections on the day of testing. This experiment was performed as described previously (18,48).

Urine preference test. Preference for investigating the urine of one mouse sex over the other was assessed in a 5 min test during which male and estrus female urine were presented

simultaneously on pieces of filter paper. The odor presentations were attached to weigh boats that were placed at opposite ends inside a cage with either a *Six3* HET or WT male mouse. Tests were videotaped and seconds spent investigating the urine stimulus were quantitated in a blind manner. This experiment was conducted as described previously (71).

c-Fos immunohistochemistry. Prior to experimentation, males were isolated from female scent in a room separate from other mice for at least 2 days. On the day of the experiment, male mice were singly housed in a clean cage in a quiet room for three hours prior to female exposure. The male mice were then exposed (at 6:00 PM under dim red light) to urine (60 µL) collected from hormonally primed estrus stimulator female mice. The urine was placed just out of reach of the mice to prevent direct contact. After 90 minutes, males were killed, and brains were collected in fixative. Sections were stained with c-Fos antibody (Santa Cruz Biotechnology; catalog number sc-52 RRID:AB_10160513; 1:1000). Neuroanatomical landmarks were used to identify the counting region as depicted in the corresponding figure. Quantification was performed on biological replicates consisting of c-Fos nuclei within the defined region from a minimum of three unilateral sections. C-Fos-positive cells were quantified by an experimenter blinded to the treatment group. While the c-fos IHC produced a range of staining intensity, only those cells that were darkly stained were included in the quantification. The numbers from each biological replicate were then averaged across all the animals in that group. Slides were coded to blind the researcher to treatment group during analysis.

Resident–intruder aggression assay. Male mutant and control mice were isolated at 9–11 weeks of age for a period of 2 weeks before testing. Mice were singly housed in cages with bedding. Testing lasted 15 min, and began when a group-housed, sexually inexperienced, adult WT ‘‘intruder’’ male was placed in the home cage of the test mouse, whose bedding had not been changed for 4 days. Aggressive behavior was defined as biting, chasing, or wrestling. Cumulative

attack duration, and number of attacks were video recorded, then quantitated by a blinded assessment. This experiment was performed as described previously (16,72).

Testosterone replacement assay. Male mice were gonadectomized, given a testosterone pellet, and left to recover for 1 week before any behavioral tests were conducted. Pellets made of tubing with an inner diameter of 1.02 mm and an outer diameter of 2.16 mm filled for 1.2 cm with testosterone (Sigma T1500-1G) and inserted into the gonadectomy incision site of *Six3* HET and WT mice. These implants have been shown previously to produce elevated physiological levels of T (11.1 ± 0.8 ng/mL) (73) .

Volatile and non-volatile odor detection. To assess the ability of *Six3* HET mice to detect volatile and non-volatile odors, and to discern these odors from each other, we used a home-cage habituation-dishabituation test, as described previously (69,71). In these tests, the mice become habituated to a urinary scent after three trials, and are then dishabituated when a new odorant is presented.

Six3 HET and WT males were tested in three different paradigms. First males were presented with (1) volatile/non-contact stimuli, (2) non-volatile and volatile/contact stimuli, and (3) non-volatile (MUPs)/contact stimuli. *Six3* HET and WT males were presented with 20 µL of an odorant sample (either water or urine) pipetted onto a piece of Whatman paper taped to a plastic weigh boat. In tests (1) and (2), mice were presented with deionized water for two minutes three times in a row with one-minute intervals in between, followed by three 2-minute presentations of male urine and finally by three 2-minute presentations of a female estrus urine. In test (3), mice were presented with deionized water for two minutes three times in a row with one-minute intervals in between, followed by three 2-minute presentations of MUPs. Tests were videotaped and quantitated by an experimenter blinded to treatment group. The number of seconds that the mice stretched upwards to smell the filter paper containing the stimulus and the number of

seconds mice touched their nose to the odorant stimulus were recorded. If the mouse does not increase their interest in the new urinary stimulus, they cannot differentiate between the two stimuli. If the interest in the odorant is similar to baseline water, then the mouse cannot detect the stimulus.

For each day of testing, one-half of the subjects in the *Six3* HET and WT groups were presented with the male urinary stimulus followed by the estrus female urinary stimulus, and the other half were presented with the same urinary odors but in the reverse order. Subsequently, on a second day of testing, all of the subjects were re-exposed to the same odors but in the opposite order from their first day of exposure. The order of presentation of urine had no effect on the results of these trials; thus, we analyze and present here data from the trials where male urine was presented first followed by female urine. Tests were videotaped and behavior quantitated in a blind manner. Within groups, statistical analysis compared (1) the difference between the number of seconds that subjects spent investigating the third water stimulus versus the male urinary odorant presented, and (2) the difference between the number of seconds spent investigating the third male urinary stimulus versus the first presentation of the estrus female urinary stimulus.

In experiment (1), male *Six3* HET mice were tested for their ability to detect and distinguish exclusively volatile odors. Volatile odors are airborne and do not need to be directly contacted to be sensed, as opposed to non-volatile odor components. Thus, to separate the volatile odors from the non-volatile, a cage lid with holes to let volatile odors pass through was placed on top of the cage, and the weigh boat was placed on this cage top such that only volatile odorants were available at body level, with subjects having no physical access to the stimulus. As the mice could not contact the stimulus, they could not detect non-volatile odorant components. The number of seconds spent investigating the stimulus by stretching up to reach the weigh boat on top of the

cage was quantitated. In experiment (3), mice were tested for their ability to detect non-volatile odorants exclusively by presenting mice with MUPs.

Female odor detection was assessed with four separate odor presentations given consecutively for two minutes separated by one-minute intervals. First, water was given on Whatman paper taped to a weigh boat placed inside of the cage, to record a baseline for interest in an odorless presentation. Then male urine was presented inside of the cage where mice could contact the stimulus. The third presentation was water once more presented outside of the cage where the mice could not physically touch the stimulus but could stretch up and smell it, to record a baseline for investigation of odors presented in this new location. The final stimulus given was male urine on top of the cage, to test for volatile odor detection.

Collection of MUPs. Experiment was conducted as previously described (72). In brief, urine was collected fresh from group-housed adult C57BL/6J male mice, from multiple cages and combined. To fractionate the MUPs, urine was applied to Amicon Ultra Centrifugal Filters (10,000 MWCO regenerated cellulose, Millipore) and centrifuged at 6000 X g, in a table-top centrifuge at room temperature for 15 min. The first effluent collected was considered the LMW fraction. The HMW fraction was washed by adding sterile 1X PBS (equal to starting urine volume), and centrifuged five times at 6000 X g at room temperature for 15 min. The washed protein fraction was then diluted to starting urine volume with 1X PBS.

Statistical analysis. All the statistical analysis was performed using R data analysis software. A P-value of <0.05 was considered statistically significant. For all experiments, data are expressed as the mean ± SEM. Unpaired two-tailed t-tests are used in all cases, except in cases where data was abnormal, or the variances were unequal, where the Wilcoxon rank sum tests were used. Additionally, in several cases, Two-way ANOVA with Bonferroni post-hoc was used to analyze data. Power analyses were performed before experiments to determine n values. Experimental

groups were defined by genotype and thus no sorting mechanism was used. n values stated for each experiment report the number of mice in each group.

Results

Loss of one allele of *Six3* is sufficient to cause subfertility

To test the hypothesis that *Six3* heterozygosity affects reproductive competence, a 120-day fertility assay was performed. We found that both *Six3* HET males and females took longer to generate their first litter when paired with wild-type (WT) mates (Fig. 1.1a). This subfertility was amplified when *Six3* HET males and females were paired together, in which no litters were sired over the 120-day test period (Fig. 1.1a, b). Furthermore, *Six3* HET males fathered significantly fewer litters than controls (Fig. 1.1b). Litter size was not significantly different between genotypes in either sex (WT: males 8.3 ± 2.4, HET: males 7.0 ± 1.0 pups/litter; WT: females 8.3 ± 2.4, HET: females 6.9 ± 2.3 pups/litter; Students t-test, $p>0.05$). As reproductive competence relies on successful completion of puberty, we determined whether the subfertility was due to delayed pubertal onset. Both *Six3* HET males and females had normal pubertal onset as determined by preputial separation in the male and vaginal opening in the female, two external markers of pubertal onset in males and females, respectively (preputial separation WT: 26.7 ± 0.7 days, HET: 26.8 ± 0.8; vaginal opening WT: 27 ± 0.7, HET: 26.7 ± 1.0 days; Students t-test, $p>0.05$). Thus, the subfertility was not due to a delay in pubertal onset. Instead, the female delay to first litter was associated with significantly increased time to vaginal plug by a WT male (Fig. 1.1c), although all of these females plugged before the end of the 10-day assay, suggesting prolonged estrous cycles. Indeed, *Six3* HET females had prolonged estrous cycles (Fig. 1.1d-g). Interestingly, we noted a heterogeneous impact of *Six3* haploinsufficiency on estrous cyclicity wherein five *Six3* HET females had prolonged estrous cycles (Fig. 1.1f), one was in persistent estrus (data not shown), and one spent 80% of the time in persistent metestrus (Fig. 1.1g). As expected, based

on the normal litter size, *Six3* HET females had a similar number of ovarian corpora lutea, a marker of successful ovulation, compared to controls (Fig. 1.1h, i).

To discern whether the deficiency in *Six3* HET mating efficiency was due to a defect in spermatogenesis, sperm analysis was conducted. Examination in the *Six3* HET mice showed that total sperm count (Fig. 1.1j) and motility (Fig. 1k) were not significantly different between *Six3* HET and WT males, and that testis morphology was normal (Fig. 1.1l). To further ascertain the cause for the significantly reduced fertility of the *Six3* HET males, we evaluated their ability to produce a vaginal plug in female mice. *Six3* HET male mice plugged significantly fewer females compared to WT mice, with three of five pairs of mice never plugging over the 10-day assay (Fig. 1.1c). This effect was exacerbated in *Six3* HET/HET matings in which only one out of four pairs of mice provided a plug during the assay.

Defective GnRH neuron migration in *Six3* HET mice is associated with absence of olfactory fibers

Fertility depends on correct maturation, localization and function of GnRH neurons. Even a modest decrease in the number of GnRH neurons is sufficient to engender irregular or lengthened estrous cycles. To determine if the subfertility of *Six3* HET mice originated at the level of GnRH neurons, we performed GnRH immunohistochemistry and counted GnRH neurons. Adult male and female *Six3* HET mice had ~45% fewer GnRH-immunoreactive neurons in the hypothalamus with ~10% of the total GnRH neuronal population halted along their migratory route through the olfactory bulb, indicating a defect in migration (Fig. 1.2a, b). The total number of GnRH neurons in *Six3* HET brains was equivalent between sexes. To determine if the abnormal GnRH neuron migration arose during development, we counted GnRH neurons at e13.5 and e17.5. Despite the total number of GnRH neurons in the entire head being normal at both ages (Fig. 1.2c-f), the number of GnRH neurons was significantly higher in the nose and lower in the

hypothalamus in *Six3* HET than WT (Fig. 1.2c-f). At e13.5, a time point when we were also able to collect *Six3* KO embryos, we found that KO heads were misshapen and most brain structures (including the MOB) unrecognizable, as has been shown previously (59). In these embryos, all the GnRH neurons were found in one large tangled group in the region normally occupied by the MOE (Fig. 1.2e, f). This remarkable mass of GnRH neurons was observed in each of the KO mouse heads. The immunostaining was very specific, with no off-target staining observed (Fig. 1.2g), as has been previously reported (57). Thus, in *Six3* HET and KO embryos, GnRH neurons are inhibited in their migration from the nasal region. In addition, the migration of GnRH neurons is more severely disrupted in *Six3* KO than in *Six3* HET mice indicating a dose-dependence of *Six3*.

In embryos late in development, at e17.5, GnRH neurons were found delayed in anterior portions of the migratory pathway. Additionally, in the adult *Six3* HET mouse, GnRH neurons were found delayed in their migratory pathway, and more GnRH neurons were seen in the olfactory bulb. However, it is possible that there is a population of GnRH neurons in the brain that stop expressing GnRH in late development, and therefore is undetectable using anti-GnRH antibody IHC. To exclude this possibility, we created a *Six3*^{HET}:*Rosa*^{tdTomato}:GnRHcre mouse in which GnRH neurons are labeled with tdTomato for the life of the neuron regardless of the expression of GnRH. Therefore, if there are GnRH neurons in the brain, that are no longer expressing GnRH, they will be detectable using IHC for tdTomato. Six3 HET brains were assessed for tdTomato-positive neurons. In counting the anti-tdTomato IHC, a ~40% reduction in the number of GnRH neurons was observed in the HET mice as compared to WT mice (the same result that was found using the GnRH antibody) (Fig. 1.2h, i). Therefore, there was no detection of GnRH neurons that were no longer expressing GnRH. Thus, the source for the loss of hypothalamic GnRH neurons seen previously is solely due to mis-migration.

To investigate whether the abnormal GnRH neuron migration was due to effects within the GnRH neuron, a separate mouse model was used, termed *Six3*$^{flox/flox}$*:GnRH*^{cre}, where *Six3* is deleted within GnRH neurons. GnRH neuron numbers were assessed in this model and surprisingly GnRH neurons migrated normally, but the total numbers were increased by ~30% in both the adult mouse (Fig. 1.3a) and in e17.5 embryos (Fig. 1.3b). This indicates that *Six3* does not act within the GnRH neuron to inhibit the migration of this neuronal population. As expected, the increased number of GnRH neurons did not affect male or female gonadal function as evidenced by normal total amount of sperm and sperm motility in the male (Fig. 1.3c, d), and comparable number of corpora lutea and estrous cycle length of females (Fig. 1.3e, f). Thus, the source of impaired GnRH neuron migration stems from the role of *Six3* outside of the GnRH neuron along the migratory pathway.

While gonadal function was unaffected by the loss of *Six3*, we next sought to determine whether pituitary function was altered by the loss of *Six3*. Since GnRH numbers were strongly reduced in *Six3* HET animals, we sought to determine whether pituitary function was intact, as the secretion of GnRH can impact pituitary development and function. Fertility depends on sufficient GnRH stimulation of pituitary gonadotropes to secrete luteinizing hormone (LH) and follicle-stimulating hormone (FSH), which are required for normal gonadal function. Given the decrease in hypothalamic GnRH neurons in *Six3* HET mice, we measured the extent to which the reduction of hypothalamic GnRH neurons affects the reproductive physiology of the severely subfertile male mice. First, we analyzed the ability of the pituitary to respond to endogenous GnRH by measuring the basal level of LH in *Six3* HET males. There was no significant difference in basal LH levels (WT: 2015 ± 793, HET: 1568 ± 612 pg/ml; n= 5, Students t-test, $p>0.05$), or in the capacity of the pituitary to respond to a GnRH challenge, as evaluated by the fold change in LH (Fold change WT: 1.78 ± 0.3, HET: 2.10 ± 0.25; n= 5, Students t-test, $p>0.05$) between *Six3* WT and HET mice. Male fertility, particularly the secretion of LH, is very sensitive to appropriate GnRH

levels. To test whether the number of GnRH neurons in *Six3* HET mice is sufficient to generate a LH response, *Six3* HET and WT males were injected with Kisspeptin, a stimulator of GnRH neurons, and the fold change of LH from baseline was determined. Again, no significant difference between genotypes was observed (Fold change WT: 1.16 ± 0.24, HET: 1.80 ± 0.37, n=5, Students t-test, $p>0.05$).

***Six3* HET males lack normal mating behavior due to anosmia**

Given intact spermatogenesis, the presence of corpora lutea, and normal hormone levels in *Six3* HET mice, it does not appear that the loss of GnRH neurons is sufficient to produce the subfertility observed in these male mice. Therefore, we sought to investigate mating behavior. Male mouse sexual behavior relies on a functional olfactory system and the capacity to detect pheromones (21,71,74-77). To determine whether the deficit in plugging was due to altered sexual behavior, we determined whether a WT female could elicit sexual behavior in *Six3* HET males. When male mice were presented with an estrogen primed female (ovariectomized and primed with progesterone and estrogen injections), WT males mounted 9 times more frequently than *Six3* HETs (Fig. 1.4a). Mounting behavior is preceded by chemoinvestigation, wherein males detect female pheromones. Interestingly, *Six3* HET males spent significantly less time chemoinvestigating females than WT males, suggesting a defect in the odor processing in the *Six3* HET males (Fig. 1.4b). In consideration of the clear alteration of reproductive behavior, pheromone driven aggressive behavior was assessed. Interestingly, *Six3* HET males responded normally to the pheromones of WT male intruders as evidenced by their number of attacks toward the intruder male (Fig. 1.4c) and the total duration of the attacks (Fig. 4d). Mating behavior follows cues detected primarily by the MOE, while male-male aggressive behavior is driven by detection of pheromones in the VNO (77). To further assess the functionality of the VNO, territorial countermarking behavior against a strange male's urine was tested. This VNO-mediated behavior was tested by counting urine marking in response to the presentation of male urine. The number

of urine marks made was not significantly different between *Six3* HET and WT mice (Fig. 1.4e, f). These data indicate that the VNO is functional in the *Six3* HET male, while the MOE is impaired. In addition to pheromones, mating behavior is also driven by neural circuits that regulate sexual motivation (77). To determine if the lack of mounting behavior was due to a defect in motivation-regulated behavior, mice were tested for their preference of sugar versus water, a test that is an indicator of anhedonia. Anhedonia is the inability to find pleasure in in an activity that would carry hedonic value in a normal situation (78). Both WT and *Six3* HET mice displayed a preference for the sugar water over unsweetened water, showing that the neuronal motivation circuitry is intact (Fig. 1.4g), as is the sense of taste. This test also demonstrates that the sweet taste receptors of mice are intact, as identified by the preference towards the sweetened drink. In line with this, we found that *Six3* HET males had normal levels of running wheel activity (Fig. 1.4h), a rewarding behavior, which also requires normal locomotor function (79). Additionally, as expected, activity onset of wheel running in normal light:dark conditions (12h light: 12h dark) was normal for *Six3* HET male mice, indicating normal eye development and sensitivity to light (WT: 23.9 ± 0.11, HET: 24.03 ± 0.014; n=5, Student's t-test, t(8)=1.16, p= 0.279)

To further determine whether the deficiency in normal reproductive behavior of *Six3* HET males was due to altered testosterone, we gonadectomized *Six3* HET male mice and inserted a testosterone pellet. Sexual behavior was then reassessed with no change in the discrepancy in mounting behavior (WT: 130 ± 25, HET: 30 ± 18 mounts; n=3, Students t-test, t(4)=8.56, p=0.0001) and chemoinvestigation (WT: 30 ± 8, HET: 4 ± 7 seconds; n=3, Students t-test, t(4)=7.84, p=0.0007) seen between *Six3* HET and WT male mice. The impaired response of *Six3* HET male mice to estrus females was not altered when testosterone levels were equalized between the WT and HET mice; thus, the abnormal mating behavior of *Six3* HET is not due to a paucity of testosterone.

Abnormal MOE development leads to an inability of *Six3* HET males to detect and respond to volatile odors

The normal motivational behavior displayed in the sucrose preference test and running-wheel activity indicate that the absence of mounting behavior in *Six3* HET males is caused by a defect outside of the motivational circuit. To discern whether the altered mating behavior could be engendered by an olfactory deficit, we evaluated general olfaction using the buried food test (69). Indeed, the *Six3* HET males and females were unable to locate a buried food stimulus during the 15-minute assay (Fig. 1.5a, b). Odor processing occurs via two morphologically distinct circuits: the MOE and the VNO. The MOE neurons respond mainly to volatile odorants (including those that cue mating behavior) in the environment and VNO neurons respond mainly to non-volatile pheromones detected through direct contact with the odor; however, the VNO can also bind volatile odorants (16,72). To determine whether *Six3* HET mice can detect and discriminate volatile and non-volatile odors, habituation/dishabituation tests were performed using intact male and estrus female urinary odorants (Fig. 1.5c). To test the ability of *Six3* HET mice to detect and differentiate smells, we measured significant increases in investigation times (dishabituation) between (1) the third presentation of water and the initial presentation of male urinary stimulus and (2) the third presentation of male urine and the first presentation of estrus female urine in *Six3* WT and HET males. The first test conducted provided mice with both volatile and nonvolatile odorants with presentation of odors inside the cage. Both WT and *Six3* HET males could detect and differentiate between non-volatile/volatile urine components of male and estrus female urine (Fig. 1.5d). However, when the odor stimuli were moved outside of the cage (therefore only volatile odorants would be available to mice), *Six3* HET males were unable to detect the male urine or estrus female urine (Fig. 1.5e). This locates the olfactory deficit to the MOE. However, to provide further evidence that the VNO is functional, non-volatile odorants were exclusively presented to *Six3* HET and WT mice by using MUPs. MUPs are processed by the VNO and relay

information about the donor animal (49). To test VNO function, three presentations of MUPs were given to HET and WT mice following three presentations of water. Both *Six3* HET and WT mice detected these components, indicating proper VNO function (Fig. 1.5f).

The ability of *Six3* HET females to detect volatile odorants processed by the MOE was assessed in a similar experiment. The same result was obtained in this experiment as was seen in the *Six3* HET males, with *Six3* HET females being able to detect non-volatile male urine components, but not volatile male urine (Fig. 1.5g). Female *Six3* HET mice were not able to detect either male or female urine presentation (Fig. 1.5g). This test was similar in principle to the test conducted on male *Six3* HET mice (Fig. 1.5c-e), but the methodology was simplified as the mating defect observed in *Six3* HET females was not as severe as that observed in the *Six3* HET males.

Given the inability of *Six3* HET males to detect volatile female urine components, the response of *Six3* HET male mice to estrus female urine was assessed. When presented with estrus female urine, male *Six3* HET mice did not exhibit normal territorial marking, making significantly fewer urine spots around the estrus female urine than the WT mice (Fig. 1.6a, b). The abnormal response to female estrus cues in *Six3* HET males was confirmed in a separate experiment, where *Six3* HET males were presented with both estrus female and male urine simultaneously within the cage. *Six3* HET mice, unlike the WT mice, did not preferentially sniff estrus female urine over male urine (Fig. 1.6c).

To determine how *Six3* haploinsufficiency disrupted MOE-processed olfaction, we used immunohistochemistry for olfactory marker protein (OMP), which specifically localizes in the primary neurons of the olfactory system of vertebrates. A total loss of OMP staining of the MOE (Fig. 1.7a) and MOB (Fig. 1.7B) was observed in the *Six3* HET mice at e13.5, e17.5, and p56. In the e13.5 *Six3* KO embryos, morphologically recognizable olfactory structures were not detectable; however, a bundle of neurons and axonal fibers with OMP immunoreactive neurons was detected in the region where the MOE normally exists (Fig. 1.7a). In contrast, OMP staining

was preserved in the VNO of *Six3* HET and WT mice (Fig. 1.7c), supporting the normal non-volatile olfaction in these mice.

Olfaction requires olfactory fibers from the olfactory bulb projecting to the MOE. These olfactory fibers are also responsible for guiding GnRH neuron migration from the VNO into the forebrain during development. Peripherin, an intermediate filament protein can be used as a marker for these fibers (80). Alteration of these fibers, including mistargeting or absence of olfactory axons along the migratory path of GnRH neurons, could be causing the defects in GnRH neuron migration observed in the *Six3* KO and *Six3* HET mice (Fig. 1.2). To determine the destiny and localization of peripherin-expressing olfactory fibers, we stained for peripherin in *Six3* WT, HET and KO mice at e13.5. Whereas peripherin fibers appeared to be normal in the *Six3* WT, *Six3* KO mice displayed a complete absence of peripherin fibers in the upper olfactory system, and *Six3* HET mice displayed a decrease in the number of projections reaching the MOB (Fig. 1.7d, e). The only peripherin fibers of the *Six3* KO lead into the mass of neurons where GnRH- and OMP-immunopositive neurons were previously observed (Fig. 1.2b and 1.7d).

To confirm that odor processing fails to occur in *Six3* HET mice, immunostaining for c-Fos, a marker of neuronal activation, was conducted after exposure to female mouse urine or water. c-Fos activation was absent from the target region of MOE neurons, the mitral layer of the dorsal MOB (Fig. 1.8a, b). Thus, the neuronal circuits that process olfactory cues from female estrus urine are not activated in *Six3* HET males.

Discussion

Haploinsufficiency of Homeodomain Proteins Six3, Vax1, and Otx2, Causes Subfertility in Mice Via Distinct Mechanisms

Normosmic idiopathic hypogonadotropic hypogonadism (IHH) and its anosmic counterpart, Kallmann Syndrome, are two rare genetic disorders leading to various degrees of

subfertility, including complete infertility and absent puberty (81). This subfertility is often due to a reduction in the number of GnRH expressing neurons or impairment of the rhythmic release of GnRH. Over the last decade, numerous genes have been identified as responsible for these two conditions; however, more than 50% of IHH cases still have unknown origins (2,9). Genetic mutations known to cause IHH are frequently either autosomal recessive or dominant. Of note, it is becoming increasingly clear that a number of unidentified genetic causes of IHH are the result of compound heterozygosity (9). Compound heterozygosity is particularly hard to detect, as it requires identification of mutations in two distinct genes. Despite the difficulty in detecting polygenic IHH, haploinsufficiencies adversely affecting fertility have been reported in both rodents and humans (9,32,58,82-84).

In all mammals, including humans, GnRH neurons have a unique cellular origin in the nasal placode. In mice, GnRH neurons are first detected on embryonic day 11 (e11) in the olfactory placode, concurrent with the onset of GnRH expression (Fig. 1.9a). They then migrate from the vomeronasal organ (VNO) across the nasal septum into the developing basal forebrain, following the terminal nerve and the olfactory nerve (Fig. 1.9a) (7,53,85). The terminal nerve (cranial nerve zero or nervus terminalis) extends from the nasal submucosa, is located medially and in very close proximity to the olfactory tract, and projects to important limbic structures (e.g., amygdala, hypothalamic nuclei) (86). The olfactory nerve (cranial nerve I) contains axons from the olfactory neuroepithelium, travels up through the cribriform plate, and extends into the brain to innervate the olfactory bulb (87). At e14, a population of ~800 GnRH neurons (88) forms an arch from the olfactory placode through the developing forebrain into the hypothalamus, extending into the preoptic area. As the neurons migrate and mature, they increase their expression of GnRH (89,90). In adulthood, the same number of GnRH cell bodies is found scattered in the preoptic area, among the fibers of the diagonal band of Broca, and in the medial septum. GnRH fibers extend their axons not only to the medial eminence (ME), but also throughout the

hypothalamus and midbrain (19,91). Defects in this migration causing abnormal GnRH neuron location in the brain and incomplete maturation can result in infertility and IHH (92,93).

We have identified three homeodomain genes that, when heterozygous in mice, impair fertility. These genes first came to our attention as they were highly expressed in the mature immortalized mouse GnRH neuronal cell line, GT1-7 (94) as compared to the immature GnRH neuronal cell line, GN11 (95), and NIH-3T3 fibroblasts (Fig. 1.9b). Using RNA-seq comparing transcript levels in GT1-7, GN11, and NIH-3T3 cells to screen for candidates that may act in GnRH neuron maturation, we found a set of homeodomain transcription factors strongly expressed in GT1-7 cells (Fig. 1.9b). We have focused on Otx2, Vax1, Six3, and Six6. All of these homeodomain transcription factors directly bind to and regulate the Gnrh1 gene at conserved ATTA sites in the proximal promoter and/or the conserved enhancer (33,56,57,96-98). Although Otx2, Vax1, and Six3 homozygous deletions (null mice) are all neonatal or perinatal lethal, the heterozygous (Het) mice are viable, overall healthy, and born in Mendelian ratios. This review will address the contrasting mechanisms and sex-specificity of the subfertility of the mice with heterozygous mutations in the Otx2, Vax1, and Six3 genes.

Otx2, the vertebrate homologue of Drosophila *orthodenticle*, is a transcription factor that has been shown to be critical for normal brain and eye development (99-102). During embryogenesis, Otx2 is expressed in both the developing GnRH neurons (103) and presumptive pituitary at e12.5 (100) indicating its role in development of the HPG axis. This hypothesis is supported by the identification of several heterozygous OTX2 loss-of-function mutations in patients with combined pituitary hormone deficiency (104-106). Several germline and conditional knockout mice have been generated which have emphasized a role for Otx2 in head formation, postnatal survival, and growth (99,107-109). However, as Otx2-null mice are embryonic lethal

due to a failure to develop the forebrain, midbrain and anterior hindbrain, analysis of the development and maintenance of the HPG axis in these mice has not been possible.

We studied the role of Otx2 in GnRH neurons in heterozygotes Otx2 ($Otx2^{Het}$) mice (19,107) to investigate Otx2 in GnRH neuron differentiation and migration *in vivo*. Male $Otx2^{Het}$ mice (58) exhibit a progressive loss of fertility. To determine the origin of subfertility, we investigated the number and location of GnRH neurons during development in $Otx2^{Het}$ mice. At e13.5, $Otx2^{Het}$ embryos of both sexes have a >50% reduction in the total number of GnRH neurons in the head (nasal area, cribriform plate and brain combined, Fig. 1.10). Furthermore, by e17.5, when the majority of GnRH neurons are normally in the hypothalamus (Fig. 1.10, Wildtype), in the $Otx2^{Het}$ mouse, GnRH neurons are still present in the nose and crossing the cribriform plate to a greater extent than controls. At e17.5, mutant males have a ~30% reduction in total GnRH neurons (Fig. 1.11). These data show that Otx2 is important for development and progression of migration of GnRH neurons, and for GnRH expression in mature neurons (58). The male $Otx2^{Het}$ mice display compromised fertility and, while the loss of Otx2 does not affect expression of pituitary gonadotropin genes, it produces a significant fall in luteinizing hormone (LH) serum levels (58). In contrast, the female $Otx2^{Het}$ mice did not survive to adulthood in our studies. Thus, correct gene dosage of Otx2 is critical for normal development of the GnRH neurons and expression of GnRH in adult, male mice. Diaczok *et al*. established that deletion of Otx2 specifically from GnRH neurons results in hypogonadotropic hypogonadism in mice (56), adding *in vivo* data to previously published reports demonstrating the important role Otx2 plays as a transcriptional regulator of GnRH expression (97,98,110).

Ventral Anterior Homeobox (Vax1) is expressed in the eye, olfactory placode and ventral hypothalamus and is known to have a role in neuronal fate determination (111-113). It directs the formation of the ventral and rostral forebrain and Vax1-null mice have altered migration of

olfactory placode neurons into the forebrain (114) and reduced neuronal proliferation (115). The developmental defects in Vax1-null mice are in part caused by abnormal Sonic hedgehog signal transduction (115,116). Vax1-null mice are neonatal lethal due to severe holoprosencephaly and cleft palate (112,114,117). Despite this severe phenotype, one report of a human child with a homozygous mutation in *VAX1* phenocopies the findings in the Vax1-null mouse model (118). Interestingly, in humans, heterozygote mutations of *VAX1* have been associated with cleft lip/palate (119-121) supporting a dosage effect of Vax1 (32).

While Vax1-null mice are neonatal lethal, male and female $Vax1^{Het}$ mice are subfertile indicating dosage sensitivity of the Vax1 allele on GnRH neuron development (32). $Vax1^{Het}$ females produced normal numbers of superovulated oocytes, but corpora lutea were reduced, along with a slight increase in basal LH and estrogen. The cause of the subfertility originated in the hypothalamus where Kiss1 and Gnrh1 mRNA were altered, along with a substantial reduction in GnRH neuron number (Fig. 1.10 and 1.11). Although the pituitary responded normally to a GnRH challenge, diestrus females had reduced circulating LHβ and FSHβ. Furthermore, $Vax1^{Het}$ males had reduced Gnrh1 mRNA and neurons, while the pituitary had normal transcript levels and responses to GnRH. Interestingly, $Vax1^{Het}$ males had an 88% reduction in motile sperm. Thus, our data showed that $Vax1^{Het}$ subfertility originates in the hypothalamus making it a candidate for haploinsufficient IHH. In addition to the critical role of Vax1 in establishing normal Kiss1 levels and a correct GnRH neuronal population, the $Vax1^{Het}$ male sub-fertility might be caused by a combined role of Vax1 in the brain and the testis. Indeed, we detected Vax1 expression in the testis, but not in the mature sperm (32). Thus, Vax1 haploinsufficiency might impact testis/sperm function and contribute to $Vax1^{Het}$ sub-fertility, although at this point the mechanism remains unknown.

To determine when Vax1 was required for GnRH neuron development, we counted GnRH expressing neurons in the developing wildtype, $Vax1^{Het}$, and Vax1-null embryo. We found that $Vax1^{Het}$ and Vax1-null embryos have normal numbers of GnRH expressing neurons at e13 (Fig. 10), but $Vax1^{Het}$ embryos have a ~50% reduction in GnRH neurons at e17 (Fig. 1.10 and 1.11), whereas no GnRH staining was observed in the Vax1-null embryo at this age (Fig. 1.11b). To identify the role of Vax1 specifically in GnRH neuron development, we generated $Vax1^{flox}$ mice. Lineage tracing in $Vax1^{flox}$:$GnRH^{cre}$:$Rosa^{LacZ}$ mice identified Vax1 as essential for maintaining expression of GnRH, since the neurons survive but fail to express GnRH. The absence of GnRH staining in adult $Vax1^{flox}$:$GnRH^{cre}$ mice results in delayed puberty, hypogonadism, and infertility (57).

Mammalian Six proteins are vertebrate homologues of *Drosophila optix* (41), and Six3 and Six6 are close homologs sharing partially overlapping expression patterns (41). Six3 and Six6 are expressed early in development and strongly in the postnatal suprachiasmatic nucleus (SCN) (122). However, despite their initial overlapping pattern, they become segregated in the postnatal brain (43), with Six6 confined to the adult hypothalamus, eye and pituitary. Six6-null mice survive but have a hypoplastic pituitary and variable retinal hypoplasia, often with no optic chiasm or optic nerve (40,42), traits that parallel defects associated with human chromosomal deletions that include the human *SIX6* locus (40,123). Homozygous Six6-null mice survive but are subfertile (33) and lack the structures of the SCN and circadian rhythms (42), while Six6 heterozygous mice are fertile (33). In contrast, Six3-null mice die at birth, lacking most head structures anterior to the midbrain including the SCN, though the rest of the body appears normal (59).

Mating behavior in males and females is dependent on olfactory cues processed through both the main olfactory epithelium (MOE) and the vomeronasal organ (VNO) (13,45-47). Signaling through the MOE is critical for male mating behavior. The development of olfactory neurons is

closely linked to the development of GnRH neurons (5,25,51-54), which originate in the primordial nasal placode, and migrate along olfactory nerves into the forebrain (5-7), and both are compromised in Kallmann syndrome (anosmic IHH) (2,8,124-127). We found that dosage of Six3 affects the development of MOE but not the VNO (84). Anomalous MOE development in $Six3^{Het}$ mice leads to hyposmia, specifically disrupting male mounting behavior by impairing detection of volatile female estrus pheromones. Six3 is highly expressed in the MOE, main olfactory bulb (MOB), and hypothalamus; all regions essential in the proper migration of the GnRH neurons. $Six3^{Het}$ mice have compromised development of the MOE and MOB, resulting in 45% loss of GnRH neurons due to improper olfactory axon targeting (Fig. 1.10 and 1.11). This leads to female subfertility, but does not impact male hormone levels or sperm, indicating male infertility is exclusively linked to abnormal olfaction. Olfactory marker protein (OMP) specifically localizes in the primary neurons of the olfactory system. Remarkably, a total loss of OMP in MOE and MOB was observed in the $Six3^{Het}$ mice. In Six3-null e13.5 embryos (84), recognizable olfactory structures were not detectable. Instead, a bundle of neurons and axonal fibers with GnRH and OMP was detected in the region where the MOE normally exists. In contrast, OMP staining was preserved in the $Six3^{Het}$ VNO, explaining the normal non-volatile olfaction. Thus, we conclude that Six3 is haploinsufficient for MOE development, GnRH neuron migration, and fertility, and represents a novel candidate gene for Kallmann IHH. Remarkably, conditional deletion of Six3 using $GnRH^{cre}$, instead caused a 30% increase in the number of GnRH neurons as detected by immunohistochemistry (84).

Heterozygous deletion of Otx2, Vax1 or Six3 is sufficient to produce subfertility. All three homeodomain transcription factors bind to and regulate the Gnrh1 gene directly through ATTA and related elements but studies of their *in vivo* phenotypes are hampered by perinatal lethality of the null mice. We have studied the reproductive phenotypes of the heterozygous mice and

found that all three have reduced numbers of GnRH neurons and are subfertile. However, there is specificity to the subfertility by sex and by mechanisms of action. Our findings confirm the importance of considering haploinsufficiency as a contributor to human disease and IHH.

Disrupted volatile olfaction leads to infertility of *Six3* HET males

Loss of olfactory processing in the MOE has been shown to disrupt male sexual behavior in various studies (19,48,128). Here, we describe for the first time a role for the homeodomain protein *Six3* in MOE development. The impact of *Six3* loss on MOE development is dosage sensitive (haploinsufficient), in that the effect of *Six3* deficiency was significantly more dramatic in *Six3* KO than HET mice. In *Six3* KO embryos olfactory structures failed to develop into a morphologically recognizable form, and OMP-immunoreactive neurons were found in a cluster halted off their normal migratory pathway. This is markedly different from the *Six3* HET mice where all olfactory structures were morphologically recognizable, although developmentally impaired with loss of OSNs and loss of neuronal activation within the MOB. IHC for cFos was conducted, revealing that some error in main olfactory system (MOS) development leads to the loss of neuronal activity, which would normally produce male sexual behavior in response to estrus cues. Loss of this neuronal activation results in the reduction in fertility seen in the *Six3* Het males. To specifically determine which set of neurons in the olfactory system is resulting in this impairment, neuron activation would need to be tested.

The loss of olfactory processing due to developmental errors has been described in several mouse lines including *Pax*-6 *SeyNeu*/*SeyNeu* and *Dlx5* KO (52), showing that when cells from the olfactory epithelium do not migrate properly or innervate the brain, the olfactory bulb can still develop. To elicit appropriate sexual behavior in rodents, correct processing of olfactory cues, via two key olfactory circuits, the MOE/MOB and VNO/Accessory Olfactory Bulb (AOB), are required. The MOE is known to process volatile odors, while the VNO is responsible for

transmitting signals about water-soluble non-volatile compounds mediating innate behaviors (17). Volatile odorants processed in the MOE and the efferent signals that they cue have been strongly implicated in the initiation of male sexual behavior (14). The *Six3* HET males displayed a severe impairment in their ability to detect volatile odors, explaining their reproductive incompetence. The reduced mounting in response to estrus female cues offers an explanation for the finding that *Six3* HET males were unable to father litters during the fertility assay. Other mouse models with deficits in the MOE have shown similar sexual impairments, such as the *Cnga2* mice (128) and *Ac3* null male mice (21). Similar to the *Six3* HET mice, both the *Cnga2* and *Ac3* null males had an intact functional VNO but failed to mount female mice. The impaired preference for the scents of opposite-sex urine observed in *Six3* HET mice was also observed in the *Cnga1* and *Ac3* nulls, and MOE-ablated mice, supporting our conclusion that *Six3* HET males do not mount due to an incapacity to process volatile odors in the MOE (76). The presence of aggressive behavior, and countermarking behavior is further evidence of the proper functioning of the VNO. While aggressive behavior is thought to be regulated by both MOE and VNO circuits (128), there is evidence that under loss of MOE function, the VNO compensates to produce normal aggressive behavior. Thus, even under loss of MOE function, as is observed in the *Six3* HET mice, aggressive behavior can be mediated through the VNO to produce a normal response (14). Indeed, the VNO developed normally and was functional in *Six3* HET males, allowing the VNO to support normal aggressive response of *Six3* HET males towards WT intruders, and allowing the detection of MUPs. We speculate that deletion of *Six3* in adulthood might also impact function of the olfactory system, as *Six3* is a transcription factor and is expressed in the nose into adulthood. However, at this time, we have only identified the role of *Six3* in olfaction when heterozygous during development and in adulthood, not in adulthood alone. In conclusion, reduction in *Six3* expression in *Six3* heterozygote mice compromises development of the MOE and MOB, resulting in mismigration of GnRH neurons due to improper olfactory axon targeting. In addition, the

impairment in development leads to an incapacity of the males to smell estrous females, and thus impairs their normal male sexual behaviors.

Six3 haploinsufficiency impairs GnRH neuron migration

Fertility depends on correct generation and migration of GnRH neurons. Numerous genes have been jointly implicated in the migration of GnRH neurons and olfactory neurons, both of which migrate along axons of the terminal olfactory pathways (52). Mis-migration of GnRH neurons, in association with anosmia, gives rise to Kallmann syndrome, an infertility syndrome commonly due to the interruption of axonal guidance molecules that control development of the olfactory system (76). While there is a clear GnRH neuron migratory defect observed in the *Six3* HET mice, the reduction of hypothalamic GnRH neurons was not sufficient to produce either hypogonadism or hypogonadotropism. This is consistent with past findings stating that only 12% of GnRH neurons are required for pulsatile gonadotropin secretion and proper stimulation of the gonads (129). Therefore, the *Six3* HET males are subfertile due to defects in olfactory development producing altered mating behavior, rather than being due to insufficient GnRH secretion.

Our data support that the inability of a proportion of GnRH neurons to reach their appropriate destinations in the *Six3* HET mice is associated with the loss or mistargeting of olfactory peripherin fibers. *Six3* HET mice show a reduction in the peripherin fibers targeting the MOB, associated with a reduction in the number of GnRH neurons, while *Six3* KO mice show a complete absence of olfactory fibers extending from the MOE to the MOB, giving rise to a bundle of GnRH neurons mislocalized in the MOE. A similar tangled mass of olfactory and GnRH neurons was observed in *Sox10* KO mice (130), a gene identified as causing Kallmann syndrome (52). Indeed, defects in MOB formation, such as those seen in the *Six3* KO mouse, can directly affect the ability of the olfactory fibers to connect to the brain, which explains the loss of

olfactovomeronasal axons in this mouse, accompanied by a loss of GnRH neuron migration (52). Data from the *Six3*$^{flox/flox}$*:GnRH*^{cre} mouse indicate that the reduction in the number of GnRH neurons found in the adult hypothalamus is mediated through SIX3 actions external to the GnRH neurons themselves, and localized in cells along their migratory route. This is apparent because deletion of *Six3* exclusively within the GnRH neuron in the *Six3*$^{flox/flox}$*:GnRH*^{cre} mouse does not reduce the number of GnRH neurons found in the adult hypothalamus. Instead, the increase in the number of GnRH neurons observed in this mouse model is likely due either to improved survival of migrating neurons, increased GnRH neuron proliferation, maintained expression of GnRH in neurons which loose GnRH expression in late development, or reduced death of GnRH neurons. Interestingly, *Six3* is not the only protein that has been found to be a repressor GnRH. MSX1 has been shown to be a repressor of GnRH promoter expression through binding to homeodomain elements within the GnRH regulatory region (131). Therefore, MSX1 KO mice, like the *Six3*$^{flox/flox}$*:GnRH*^{cre} mice, show an increase in the number of GnRH expressing neurons within the hypothalamus (131).

Importantly, the *Six3* HET mouse is, to our knowledge, the first example of a gene that in the heterozygous state gives rise to a fully penetrant phenotype in reproduction. Thus, this may be a candidate gene for Kallmann's syndrome. While *Six3* haploinsufficiency alone is sufficient to cause subfertility, Kallmann syndrome can arise from haploinsufficiency of several genes cumulatively producing complete infertility. Other genetic mutations affecting central components of the olfactory system, such as *Prokr2, Pax6, Chd7, Fgf8/Fgfr1, Prok2, Sox10,* and *Sema3A*, have been identified as causes of Kallmann Syndrome or idiopathic hypogonadal hypogonadism in various mouse models (52,132-134). Cases of haploinsufficiencies resulting in compromised fertility and hyposmia/anosmia have thus far been identified in both rodents and humans (32,58,71,82,83).

Sex differences in subfertility/infertility of *Six3* HET mice

Despite comparable neuroanatomy in *Six3* HET males and females, males were more severely subfertile than females. Extended fertility assays revealed that the *Six3* HET males could plug a few WT females, albeit at a very reduced rate compared to WT mice. A potential explanation for the rare ability of the *Six3* HET males to mount and produce litters despite their loss of MOE input, is that it is possible that some of the *Six3* HET males were able to use tactile, visual, or auditory cues to trigger mating behavior; however, it does not necessary follow that *Six3* HET males can discern ovulating females (21). Our data support that the more severe reproductive impairment of the *Six3* HET males is caused by impaired MOE development and function, a structure demonstrated to be key in male, but not female sexual behavior (14). In contrast, female sexual behavior relies on the accessory olfactory system, regulating female sexual receptivity in the form of lordosis behavior (18,48). Although there are some cases in which MOE lesions produced alterations in female mating behavior (18,135), in the majority of cases, female mating behavior is markedly less disrupted than male mating behavior.

A similar differential impact on male and female fertility by gene deletions affecting anosmia and the number of GnRH neurons was observed in studies of the *B3gnt1* KO mice, a gene involved in the formation of axonal connections. *B3gnt1* KO females were fertile, whereas the *B3gnt1* KO males were unable to sire litters at a normal rate despite having normal reproductive organs (21). Additionally, they displayed impaired sexual response to females, and olfactory neuron loss (21). While fertility in *Six3* HET females was not as severely disrupted as it was in the males, they remained subfertile as evidenced by a delay in being plugged, a reduced number of litters and a delay to the first litter during the fertility assay. The decrease in litters mothered correlated with increased estrous cycle length. This agrees with other studies, in which it has been shown that a decreased number of GnRH neurons in the hypothalamus can impact female fertility more severely than male fertility and often is associated with longer and irregular

estrous cycles (32,33,129). We believe the prolonged and irregular estrous cycles to be the cause of reduced fertility, as opposed to a behavioral deficit in mating behavior (32). Mating behavior in females has repeatedly shown to be more strongly regulated by the VNO (a structure that was unaltered in the *Six3* HET mice) than the MOE (14). While the reason behind the subfertility/infertility of *Six3* HET males and females differs, both sexes lose their ability to smell, and have a reduction in the number of GnRH neurons.

The findings presented here reveal that SIX3 dosage is essential in the proper development of the MOE and MOB olfactory structures. Furthermore, both alleles of *Six3* are necessary for the proper migration of GnRH neurons and the detection of volatile odors. It is possible that SIX3 functions within the nose, in similar capacity to its role in the eye, by regulating the balance in proliferation and differentiation of olfactory structures (136). These findings have broader implications for human health, as expanding the knowledge basis of the mechanism through which *Six3* regulates neuronal development will provide insight into the diseases engendered by mutations in *Six3*, such as schizencephaly and holoprosencephaly (136). In conclusion, our study is the first to address the impact of *Six3* haploinsufficiency in adulthood and demonstrates *Six3* to be a key transcription factor in the development of the MOE, olfaction, GnRH neuron migration, and normal fertility, remarkably producing anosmia and subfertility/infertility in the heterozygous state.

Acknowledgements

The authors thank Lauren D. Sitts and Jason D. Meadows for technical assistance on this project. This work was supported by National Institutes of Health grants R01 HD082567 and R01 HD072754 (to P.L.M.) and by National Institute of Child Health and Human Development/National Institutes of Health P50 HD012303 as part of the National Centers for Translational Research in Reproduction and Infertility (P.L.M.). P.L.M. was partially supported by P30 DK063491, P42

ES101337, and P30 CA023100. E.C.P. was partially supported by National Institutes of Health R25 GM083275 and National Institutes of Health F31 HD098652. H.M.H. was partially supported by K99 HD084759. E.L.S. was partially supported by T32 HD007203, The Lalor Foundation, P42 ES101337, and T32 DK007044.

Chapter 1 has been published in *Molecular Neurobiology* (Pandolfi, Erica C.; Hoffmann, Hanne M.; Schoeller, Erica L.; Gorman, Michael R.; Mellon, Pamela L. 2018.) Haploinsufficiency of Six3 abolishes male reproductive behavior through disrupted olfactory development, and impairs female reproductive behavior through disrupted GnRH neuron migration. 2018. Dr. Hanne Hoffmann assisted with the experimental design, wheel-running experiments, and paper composition. Dr. Erica Schoeller assisted with the behavioral experiments. Dr. Michael Gorman assisted with the wheel-running experiments. The dissertation author was the primary investigator and author of this material. Pamela Mellon supervised the project and provided advice. Chapter 1 also contains a review article published in *Neuroendocrinology* (Hoffmann, Hanne M.; Pandolfi, Erica C.; Larder, Rachel; Mellon, Pamela L. 2018), and a manuscript published in *The Journal of Neuroscience* (Hoffmann, Hanne M.; Trang, Crystal; Gong P.; Kimura, Ikuo; Pandolfi, Erica C.; and Mellon, Pamela L. 2016).

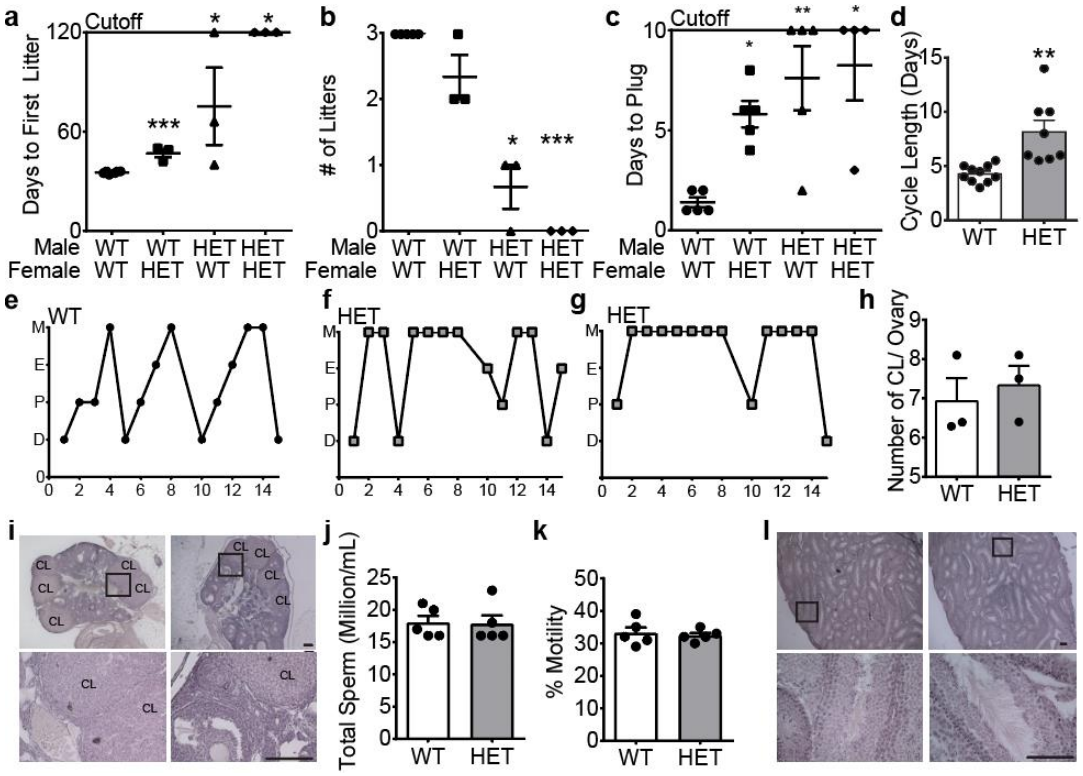

Figure 1.1. *Six3* HET mice are subfertile. **a,** Days until first litter (Mann Whitney test as compared to WTxWT, n=3-5) (WTxHET, p=0.0003), (HETxWT, p= 0.024), (HETxHET, p= 0.024). **b,** Average number of litters in a 120-day mating assay (Mann-Whitney test as compared to WTxWT, n=3-5) (WTxHET, p= 1.07), (HETxWT, p=0.018), (HETxHET, p= 0.018). **c,** Days until WT or HET males create a vaginal plug in WT or HET females during a 10-day assay (Mann-Whitney test as compared to WTxWT, n=4-5), (WTxHET, p=0.008), (HETxWT, p=0.024), (HETxHET, p=0.008). **d,** Length of estrous cycles monitored daily in *Six3* HET and WT females over 15 days (Student's t-test, p=0.001, t(16)=3.93, n=8-10). M, metestrus; E, estrus; P, proestrus; D, diestrus. Representative cycles are shown for **e,** WT female, **f,** and **g,** *Six3* HET females. **h,** Number of corpora lutea (Student's t-test, p= 0.574, t(4)= 0.529, n=3) and **i,** pictures of corpora lutea (CL) in *Six3* HET and WT ovaries, n=3. **j,** Total number (Student's t-test, p=0.910, t(8)= 0.117, n=5), and **k,** percent motile sperm (Student's t-test, p=0.688, t(8)= 0.416, n=5) in *Six3* HET and WT mice. **l,** Representative images of testes from *Six3* HET and WT mice, n=3. Boxes on images indicate where the higher magnification images were taken. *p<0.05, **p<0.005, ***p<0.001. Scale bars, 2 mm, 20 µm.

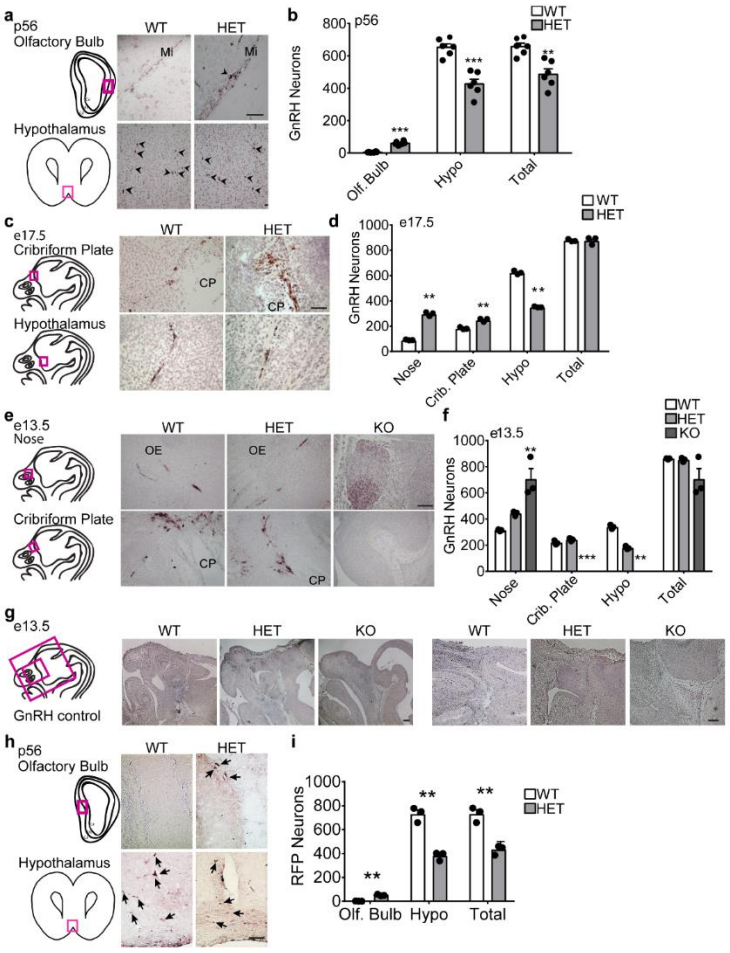

Figure 1.2. *Six3* HET and KO mice showed delayed migration of GnRH neurons. *Six3* HET and WT mice were processed for IHC staining for GnRH. **a, c,** and **e,** Representative images of staining in *Six3* WT and HET mice are shown with boxed areas on the drawings of the sagittal mouse head sections to the left of the panels indicating where the (*a*, *c*, and *e*) images were taken. **b,** GnRH neurons at p56 (Student's t-test, n=6 (3 females, 3 males)). Counting was conducted throughout the adult brain beginning with the front of the olfactory bulb to bregma –2.80. (olf. bulb, p= 0.00004, t(6)=11.1), (crib. plate, p=0.0001, t(9)=-6.17), (total, p=0.002, t(8)=-4.34). **d,** GnRH neurons at e17.5 (Student's t-test, n=3). Counting was conducted throughout the entire embryonic head (nose, p=0.001, t(2)=-22.4; crib. plate, p=0.003, t(4)=-7.40; hypo, p=0.0004, t(2)=31.1; total, p=0.973, t(2)=-0.03). **f,** GnRH neurons at e13.5 (Student's t-test, n=3; nose, p=0.002, t(3)=-12.2; crib. plate, p=0.116 t(4)=-2.06; hypo, p=0.0002, t(4)=13.6; total, p=0.488, t(2)=0.821). **g,** Controls for GnRH staining specificity, images are from e13.5 mice processes for anti-GnRH IHC. **h** and **i,** lineage tracing, IHC for tdTomato in *Six3*^{HET}:*Rosa*^{tdTomato}:*GnRH*^{cre} adult mice. tdTomato marks all GnRH neurons for the duration of the life of the neuron regardless of GnRH expression, to determine presence of GnRH neurons lacking GnRH expression. **i**, Number of tdTomatao-labelled GnRH neurons in *Six3*^{HET}:*Rosa*^{tdTomato}:*GnRH*^{cre} adult mice. (Student's t-test, n=3 ; olf. bulb, p=0.004, t(2)=-14.0 ; hypo, p=0.003, t(3)=8.41 ; total, p=0.004, t(3)=6.87). Arrows indicate tdTomato-positive neurons. Mi, mitral layer; CP, cribriform plate; OE, olfactory epithelium. **p<0.005, ***p<0.001. Scale bars, 100 µm (a, c, e, h), 2 mm (g left), 200 µm (g right).

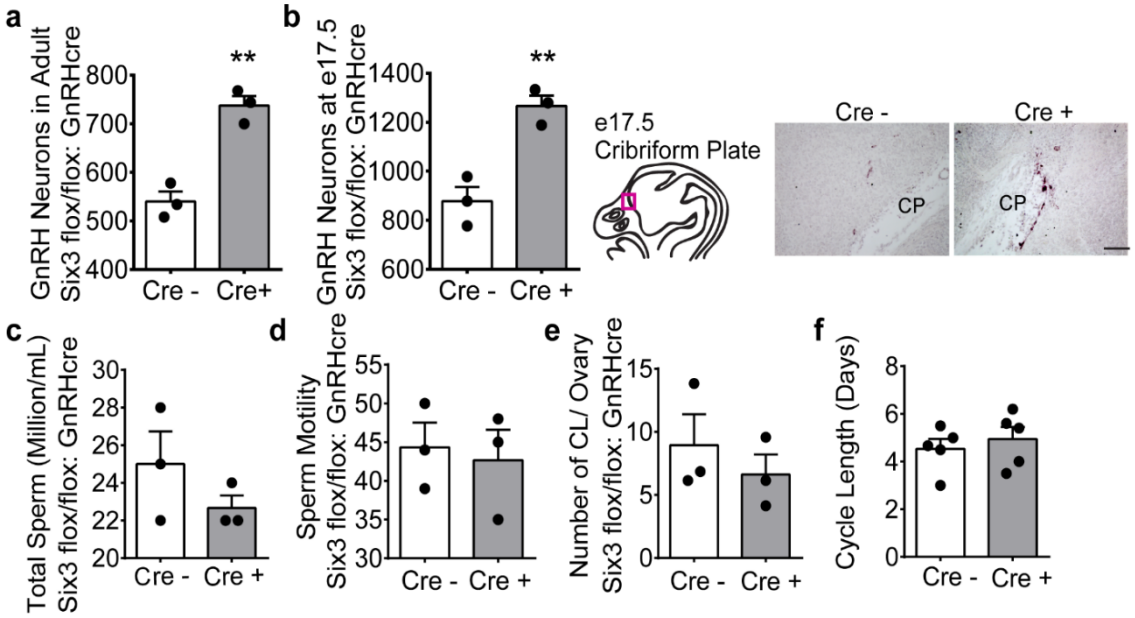

Figure 1.3. *Six3*$^{flox/flox}$*:GnRH*^{cre} mice have increased numbers of GnRH neurons and normal gonadal function. **a,** and **b** and In the *Six3*$^{flox/flox}$*: GnRH*^{cre} mice, the number of GnRH neurons at (*a*) p56 (Students t-test, p=0.0023, t(4)=6.91, n=3) and (*b*) at e17.5 (Students t-test, p= 0.006, t(4)=5.42, n=3) with representative images from e17.5 of anti-GnRH IHC antibody staining. **d,** Total number (Student's t-test, p=0.277, t(4) =1.26, n=3) and **e,** percent motility (Student's t-test, p=0.758, t(4)=0.330, n=3) of sperm. **f,** Number of corpora lutea in control and *Six3*$^{flox/flox}$*:GnRH*^{cre} mouse ovaries (Student's t-test, p=0.471, t(4)=0.796, n=3). **g,** Length of estrous cycles monitored daily in control and *Six3*$^{flox/flox}$*:GnRH*^{cre} mice (Student's t-test, p=0.471, t(8)=0.616, n=5). CP, cribriform plate. **p<0.005. Scale bars, 100 µm.

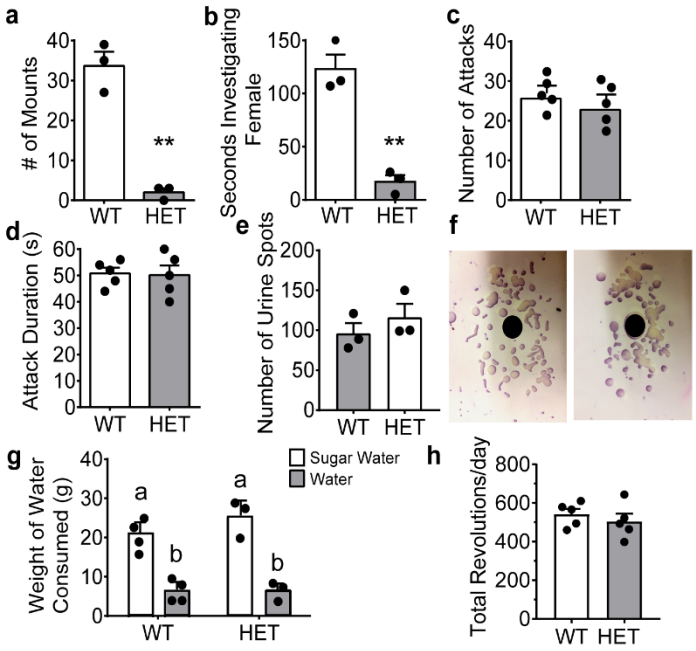

Figure 1.4. *Six3* HET males do not respond normally to estrus female cues, but maintain normal aggression patterns towards male intruders. **a,** *Six3* HET males mounting of estrus females, assay was 15 min (Student's t-test, p=0.001, t(4)=8.64, n=3). **b,** Male chemoinvestigation of estrus females, assay was five min (Student's t-test, p=0.002, t(4)=7.09, n=3). **c,** and **d,** Male aggression towards WT intruder males over 15 min as measured in (*c*) number of attacks (Student's t-test, p=0.387, t(8)=0.918, n=5) and (*d*) duration of attacks (Student's t-test, p=0.890, t(8)=0.143, n=5). **e**, Quantification of Territorial marking on Whatman paper **f**, in response to 60 µL pooled male urine (Student's t-test, p=0.392, t(4)=0.959, n=3). **g,** Anhedonia of *Six3* HET and WT mice measured by their intake of sugar water versus unsweetened water (different letters indicate statistical difference by Two-way ANOVA followed by Tukey post hoc, n= 3-4). **h**, Running wheel activity in 12h light:12h dark conditions for 1 week of *Six3* WT and HET male mice. **p<0.01.

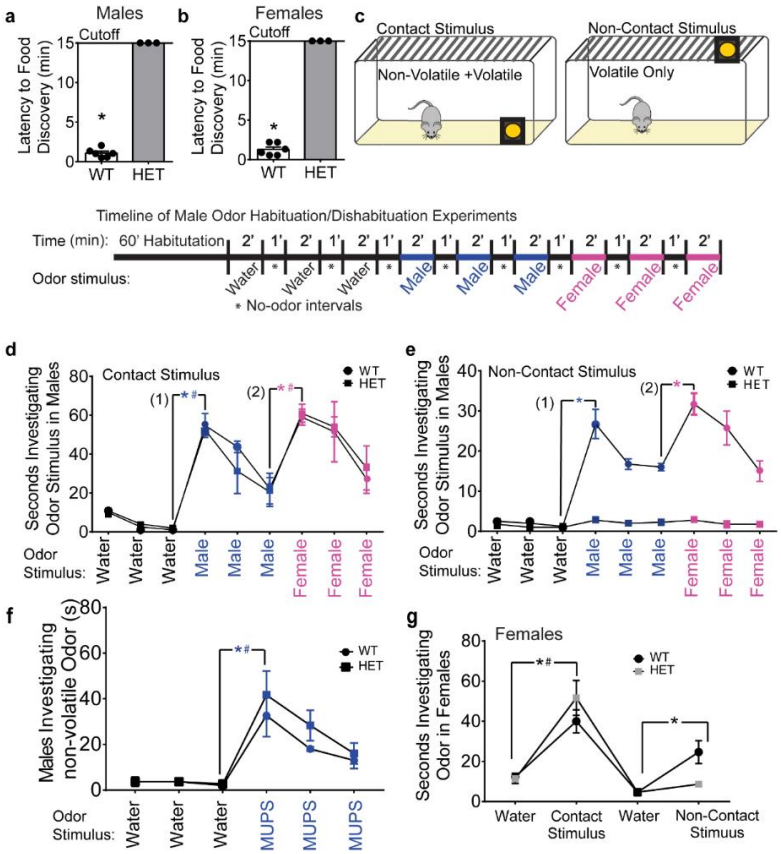

Figure 1.5. *Six3* HET mice are unable to detect volatile odors. **a** and **b,** Identification of anosmia using a buried food test (*a*) male (Mann-Whitney, p=0.024, n=3-6) and (b) female (Mann Whitney, p=0.025, n=3-6). **c,** Schematic and time line for the habituation/dishabituation tests conducted to discern the ability to detect and discriminate odors. **d, e,** and **f,** Habituation/dishabituation tests were conducted to discern the ability to detect and discriminate odors. Results from males (*e* and *f*) and females (*g*). Odor placement was used to separate volatile and non-volatile odor components. Mice must be able to physically contact the odor stimulus to detect non-volatile odor components. Thus, when the odor was placed outside of the cage (*f* and *g*), only volatile odors were detectable. We compared the difference between (1) the number of seconds that subjects spent investigating the third water stimulus versus the first urinary odorant presented and (2) the difference between the number of seconds spent investigating the third presentation of the first urinary stimulus versus the first presentation of the second urinary stimulus. **d,** Contact stimulus detection in male mice (Mann-Whitney, n=4; water/male urine: WT, p=0.006; HET, p=0.009; male urine/female urine: WT, p=0.013; HET, p=0.024). **e,** Non-contact stimulus detection in male mice (Mann-Whitney, n=4; water/male urine: WT, p=0.005; HET, p=0.523; male urine/female urine: WT, p=0.015; HET, p=0.264). **f**, VNO function was tested more directly using three odor presentations of MUPs after three presentations of water (Student's t-test, n=3; WT: p=0.028, t(2)=-5.61; HET: p=0.023, t(2)=-6.41). **g,** Odor investigation in female mice. Comparison of water to non-volatile/volatile odor (contact odor stimulus) (Two-way ANOVA followed by Tukey post hoc, n=3). In graphs with overlapping lines, * indicates WT mice and # indicates HET. $^{*,\#}p<0.05$.

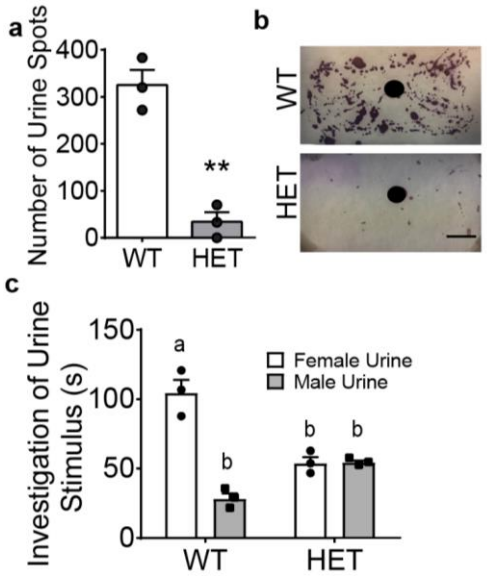

Figure 1.6. *Six3* HET mice respond abnormally to estrus female cues. **a,** Territorial marking in response to female estrus urine assessed by placing 60 µL of estrus female urine in the center of Whatman paper (black circle) and quantifying the number of urine spots made by *Six3* WT and HET mice after imaging these pieces of paper **b,** and subtracting a baseline sample with no odor exposure (Student's t-test, p=0.002, t(4)= 7.66, n=3). **c,** Urine preference test with *Six3* HET and WT mice presented with male urine and female estrus urine simultaneously. The amount of time mice spent investigating each odorant was measured over 5 minutes (different letters indicate statistical difference by Two-way ANOVA followed by Tukey post hoc, n=3). **p<0.01. Scale bars, 2.54 cm.

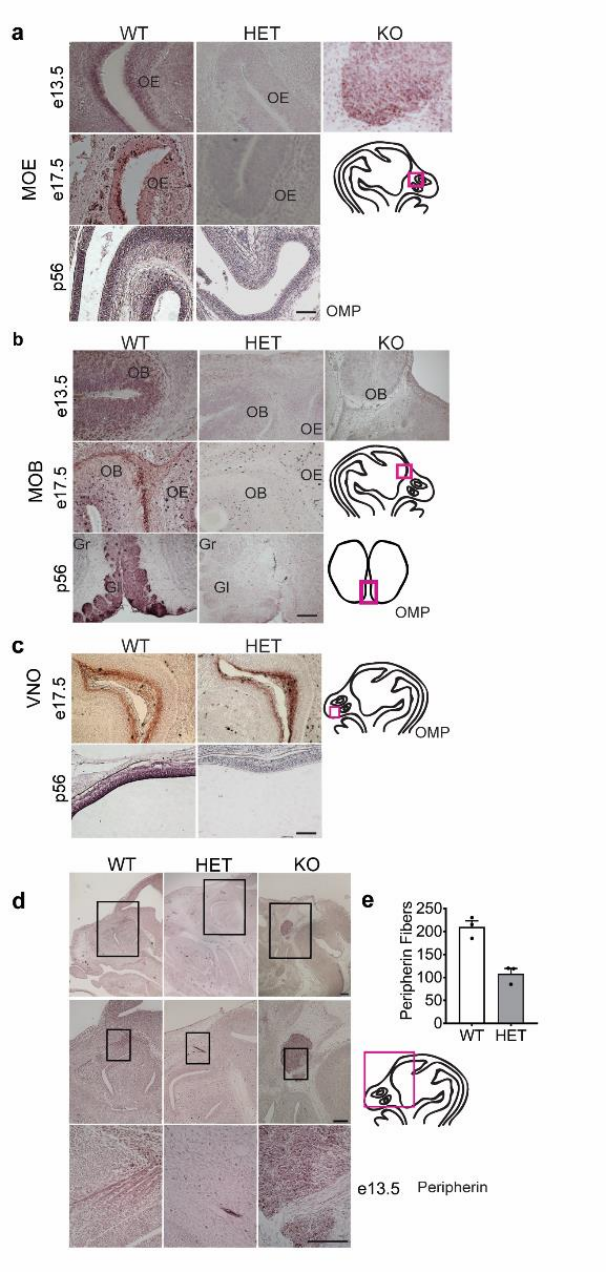

Figure 1.7. *Six3* HET mice lack olfactory neurons. **a, b,** and **c,** Olfactory Marker Protein (OMP) IHC to mark all mature olfactory sensory neurons (OSNs) of *Six3* WT, HET and KO mice at e13.5, 17.5, and p56 in (a) the MOE, (*b*) the MOB, and (*c*) the VNO, n=3. Boxes on drawings of the brain to the right of representative IHC images indicate where the pictures were taken. **d,** IHC for Peripherin-positive axons in the olfactory system at e13.5 in *Six3* WT, HET, and KO mice, n=3. **e,** quantification of peripherin fibers in *Six3* WT and HET embryos (Student's t-test, p=0.004, t(4)=5.82, n=3). Boxes on drawings of adult brain (*a*) or embryo head (*b, c*) indicate where the representative images were taken. OB, olfactory bulb; OE, olfactory epithelium; Gr, granular layer; Gl, glomerular layer. Scale bars, 100 µm (a, b, c), panel d, 2 mm, 10 µm, 100 µm.

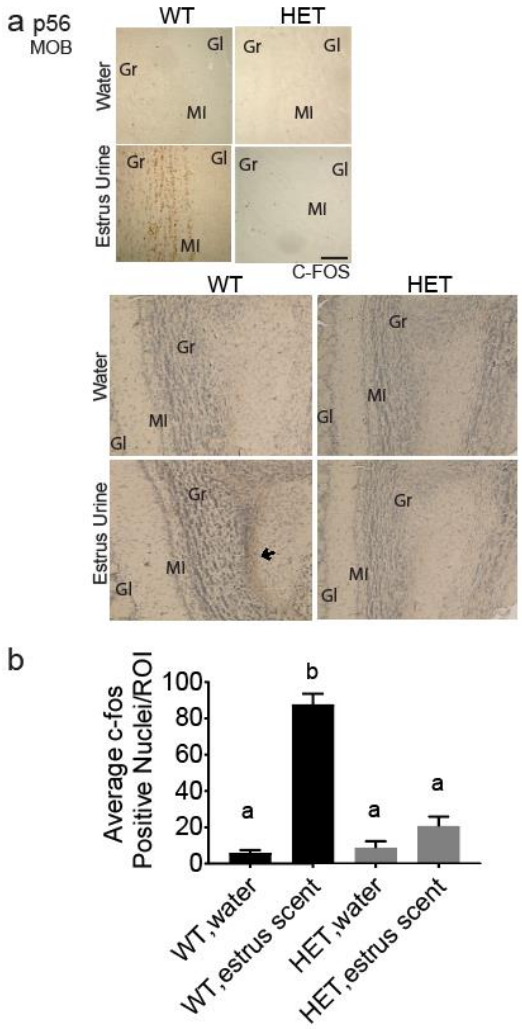

Figure 1.8. *Six3* HET mice lack MOB neuron activation in response to estrus scent. **a,** Dotted outline indicates quantified portion. Images obtained from the Allen Institute web site, Allen Mouse Brain Atlas, p56 coronal image 20, (http://mouse.brain-map.org). IHC for c-Fos performed to identify regions in the MOB activated by the female urinary volatile odors presented to *Six3* WT and HET male mice. Water was used as a negative control. Images are taken from the glomerular layer of the MOB, n=3. **c,** Quantification of ROI depicted in (b). Quantification was performed on biological replicates consisting of c-Fos positive nuclei within the defined region from a minimum of three unilateral sections. c-Fos-positive cells were quantified by an experimenter blinded to the treatment group. The numbers from each biological replicate were then averaged across all the animals in that group (different letters indicate statistical difference by two-way ANOVA followed by Tukey post hoc). Boxes on images of brains indicate where the higher magnification images below were taken. Gr, granular layer; Gl, glomerular layer; Mi, Mitral layer. Image reproduced with permission from the Allen Institute, Image credit: Allen Institute. Scale bar, 200 µm.

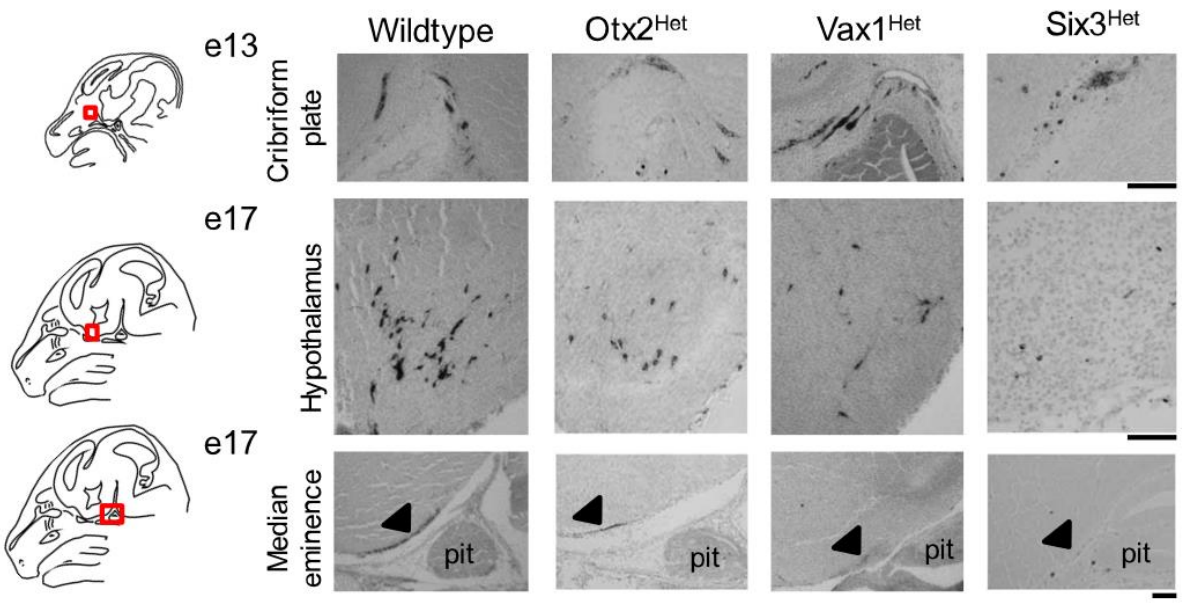

Figure 1.9. Developmental GnRH neuron migration and homeodomain gene expression. GnRH neuron maturation depends on internal and external factors to the GnRH neurons allowing developmental migration and maturation. Correct GnRH neuron migration and increased Gnrh1 expression is required for fertility. A) Schematic of a sagittal mouse head illustrating developmental GnRH neuron migration. GnRH neurons arise in the olfactory placode around embryonic day (e) 11 in the mouse. From there they migrate through the cribriform plate into the brain. Once within the brain, GnRH neurons follow a more ventral trajectory to finally localize scattered throughout the anterior hypothalamus. At completion of their migration, GnRH neurons send projections to the median eminence, where GnRH is released in a pulsatile fashion into the hypophyseal portal system. GnRH neurons require ~4 days to complete this migration. Blue dots illustrate the location of GnRH neurons at e13 and e17, and the blue arrows indicate the migration path. B) During GnRH neuron development a complex gene expression pattern is required for increased Gnrh1 expression in parallel with expression of receptors and other factors allowing GnRH neuron pathfinding. We used RNA-Seq comparison of homeodomain transcription factor gene expression in immortalized mature non-migratory GnRH neurons (GT1-7), immature migratory GnRH neurons (GN11), and fibroblasts (NIH-3T3) to identify novel transcription factors potentially involved in GnRH neuron maturation. RNA-Seq data are shown as the average of two biological replicates, and expressed as RPKM (reads per kilobase million). These data support quantitative RT-PCR analyses previously published for these genes (33,57,96,97).

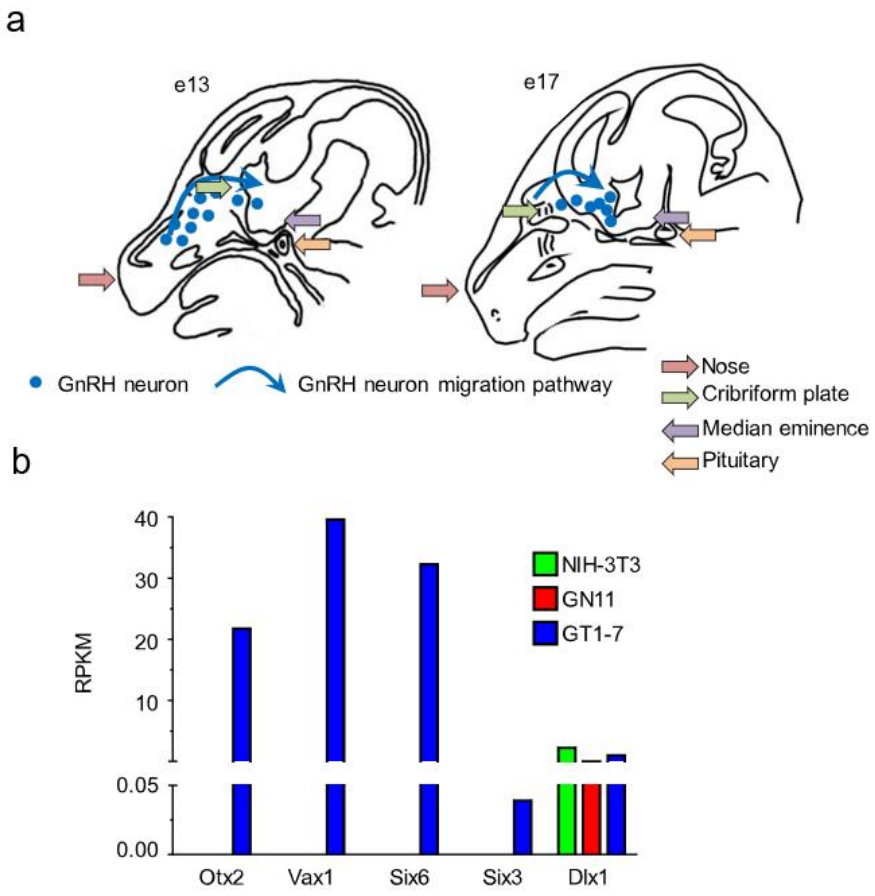

Figure 1.10. Reduced number of GnRH expressing neurons in the hypothalamus in 17 day-old mouse embryos heterozygous for Otx2, Vax1, or Six3. To determine how haploinsufficiency of Otx2, Vax1, and Six3 impacted GnRH neuron development, we performed immunohistochemistry for GnRH in mouse embryo heads from control, $Otx2^{Het}$, $Vax1^{Het}$, and $Six3^{Het}$ mice at e13 and e17. The red squares on the schematic illustrate the area imaged. GnRH IHC at e13 shows normal location and numbers of GnRH neurons at the cribriform plate in $Otx2^{Het}$, $Vax1^{Het}$, and $Six3^{Het}$ embryos as compared to wildtype. In contrast, at e17, $Otx2^{Het}$, $Vax1^{Het}$, and $Six3^{Het}$ embryos have fewer detectable hypothalamic GnRH neurons, causing a reduction of GnRH terminals at the median eminence (black arrow). Follow up studies found that reduced release of GnRH caused subfertility in these heterozygote mouse lines. Scale bar represents 100 µM. Abbreviation: pit: pituitary.

a

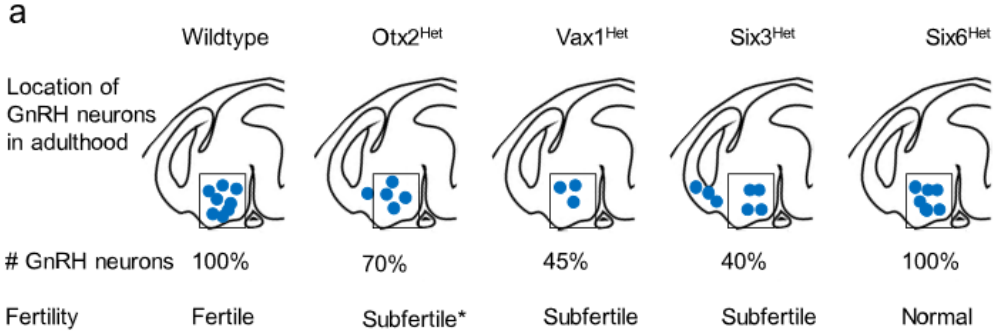

b

Allele	Genotype	Adult viability of mouse	Number of GnRH neurons at e17	Male fertility	Female fertility
Otx2	Het	Yes*	70%	Subfertile	N/A
	Null	No	N/A	N/A	N/A
Vax1	Het	Yes	40%	Subfertile	Subfertile
	Null	No	0%	N/A	N/A
Six3	Het	Yes	55%	Sub-infertile	Subfertile
	Null	No	0%	N/A	N/A
Six6	Het	Yes	100%	Normal	Yes
	Null	Yes	10%	Subfertile	Subfertile

Figure 1.11. Summary of role of Otx2, Vax1, Six3, and Six6 in GnRH neuron development and fertility. A) Sagittal illustration of GnRH neuron location after termination of migration in the adult brains of control and heterozygote animals and the correlation with fertility. Box indicates normal location of neurons that are most likely to project to the median eminence allowing GnRH release into the hypophysial portal system promoting LH and FSH release from the pituitary to promote gonadal function and fertility. B) Summary of findings in the Otx2, Vax1, Six3, and Six6 heterozygote (Het) and knock-out (null) mice. *Studies only performed in males due to inability to generate adult $Otx2^{Het}$ females. N/A: not applicable.

Chapter 2: Homeodomain Protein SIX3 is required for Development of the Main Olfactory Epithelium and Normal Olfaction

Abstract

Previous research has shown that dosage of the homeodomain gene *Six3* affects the degree of development of the main olfactory epithelium. Anomalous MOE development in *Six3* heterozygote (HET) mice leads to hyposmia, specifically disrupting male mounting behavior by impairing detection of volatile female estrus odors. Disruption of olfactory development in *Six3HET* mice is associated with a loss of olfactory sensory neurons (OSNs), and gonadotropin-releasing hormone (GnRH) neurons. Here, we study populations of OSN precursors in the *Six3HET* mouse and demonstrate that the trajectory of neuronal development is halted at the level of the immediate neuronal precursor. We then investigated the actions of SIX3 within OMP-expressing cells; and determined the contribution of SIX3 within this neuronal population to maintaining fertility. We created a $Six3^{OMP}$ mouse that has deletion of *Six3* using OMP-Cre. The $Six3^{OMP}$ mice displayed disrupted olfaction, with the loss of olfactory ability being sourced to the MOE. The loss of olfaction was not as severe as was observed previously using *Six3HET* mice, and there was no effect on overall fertility. There was a moderate reduction in the mature OSN population and a delay in GnRH neuron migration to the hypothalamus early in development. These findings show that SIX3 has direct actions within the olfactory epithelium that are necessary for development of the main olfactory epithelium, and that SIX3 functions within the environment of the olfactory neuron to regulate nasal development and ensure proper GnRH neuron migration.

Introduction

Mammalian behaviors such as aggression, mating, and fear all depend on signaling within the olfactory system (12). In particular, reproductive behavior in mice is dependent upon olfactory signaling to convey information about the sex, social, and reproductive status of conspecifics (13). This olfactory communication stimulates the necessary neuroendocrine responses that drive reproductive behavior (14,15). Rodents have two anatomically and functionally separate neuronal populations in the nose termed the main olfactory epithelium (MOE) and the vomeronasal organ (VNO) (16). Complex chemosignals are received and processed by sensory neurons in the MOE that project to glomeruli in the main olfactory bulb (MOB), while the sensory neurons in the VNO project to the accessory olfactory bulb (16). Although there is overlap between the functions of these two anatomically distinct organs systems, it is generally believed that neurons within the MOE respond mainly to volatile odorants in the environment, whereas VNO neurons mainly process signals about non-volatile pheromones (14,16-18). The odorants that cue mating behavior in male mice are volatile odorants processed by the MOE (14,19,20). Previous research demonstrates that exclusive impairment of the MOE results in disrupted male reproductive behavior due to the inability to recognize estrus females (18,20-22). These experiments have bolstered the conclusion that the MOE is mainly responsible for the processing of mating odorants. While human mating behavior is not largely driven by olfaction as it is in rodents and other mammals, olfaction is an essential part of our everyday lives, and therefore understanding the genetics of development of the olfactory system is essential (23). Furthermore, improper development of the olfactory system has been linked to abnormal sexual maturation in humans (23).

Development of the olfactory system is closely linked to the development of gonadotropin-releasing hormone (GnRH) neurons, a key neuronal regulator of fertility (5,25,51-54). GnRH neurons are an essential component of the hypothalamic, pituitary, gonadal axis, in which they

cue the pituitary to release luteinizing hormone and follicle-stimulating hormone that in turn stimulate the ovaries and testes to release estrogen, testosterone, and progesterone (3). GnRH neurons originate in the olfactory placode and migrate along olfactory axonal projections and the terminal nerve to reach the forebrain (5-7). Due to the topographical and migratory link between the GnRH neuronal population and the neurons of the MOE, it is not surprising that their fates are tied together and that both are compromised in the human developmental disorder termed Kallmann syndrome (4,8). Kallmann syndrome is a rare genetic disorder of complex and heterogeneous genetic etiology, characterized by the loss of fertility, absent or delayed puberty, and anosmia/hyposmia due to developmental errors in nasal structures and GnRH neurons (1,4). Previous genetic analyses studying familial cases of Kallmann syndrome have revealed that there are multiple genes involved in the regulation of GnRH neuron migration, and olfactory system development (9-11). Some cases of Kallmann syndrome have been linked to compound heterozygosity in patients (11). Despite the focus on identifying genetic factors in the etiology of this disease, over 68% of cases of Kallmann syndrome are of an unknown genetic origin, thus identification of new genes of interest in this condition is critical.

One gene that has been identified as important for olfactory development is the homeodomain gene *Six3*, which is highly expressed in the MOE, MOB, and hypothalamus, areas essential for maintaining reproduction and olfaction (www.brain-map.org, consulted Feb 2017) (84). We have shown that *Six3* is haploinsufficient for olfactory development and the proper migration of GnRH neurons in mice, resulting in subfertility (84). Utilizing *Six3* heterozygous mice, we showed that a decreased level of *Six3* results in the loss of mature OSNs (mOSN) in the main olfactory system (MOS) and reduces the number of olfactory projections associated with a disruption in the migration of GnRH neurons. It is not yet known where in the brain or nose *Six3* acts to mediate these effects. Our goal was to determine the roles of *Six3* specifically within the olfactory system. To achieve this, we used a mouse model with specific deletion of *Six3* within

the olfactory epithelium (OMP-cre), to determine whether targeted deletion within this neuronal population is sufficient to recapitulate the subfertility and migratory defects observed in the *Six3* heterozygous mouse model.

Methods

Mouse lines and animal housing. All animal procedures were performed in accordance with the University of California, San Diego, Institutional Animal Care and Use Committee regulations.

Mice were group-housed as previously described (84). All mice were on a C57BL/6J mouse background. *Six3-flox* mice were provided by Dr. Guillermo Oliver (59). *Six3-flox* mice were crossed with *OMP*-Cre (20,75) mice to create mice homozygous for the *Six3* deletion within OMP (mature and differentiated) olfactory neurons, termed $Six3^{OMP}$. The mice were killed by a CO_2 or isoflurane (Vet One) overdose. Unless specified, all animals used were ~3 months of age.

Behavioral experiments. All behavioral tests were performed during the first three hours of the dark phase using red light illumination. The experimenter was blind to the genotype of the subjects. Before each assay, the mice were habituated for 1 hour in a new cage with fresh bedding and no food or water. All females presented to males in behavioral tests were virgin ovariectomized and primed with 1 µg estradiol benzoate diluted in sesame oil at 9 A.M. the day before testing and 500 µg progesterone diluted in sesame oil at 2 P.M. on the day of testing.

Collection of tissue and histology. Brains, olfactory bulbs, and embryos were fixed overnight (~16 h) at 4°C in freshly made mixture of 6:3:1 absolute alcohol: 37% formaldehyde (Fisher F79-4): glacial acetic acid. Tissues were paraffin embedded and serially sectioned at 10 µm.

Immunohistochemistry. Immunohistochemistry (IHC) was performed as described previously (42). Sections were immunostained with rabbit anti-GnRH (1:1000; Novus Biologicals, catalog number: NB300-506, RRID:AB_2110266), anti-peripherin (1:200; Abcam, catalog number:

ab4573, RRID:AB_2171346), or rabbit anti-OMP (1:100; Santa Cruz Biotechnology, catalog number: sc-67219, RRID:AB_2158005). Peripherin and Mash quantification were conducted by counting all fibers or mash-positive neurons within the MOE/MOB region in the *Six3*^{OMP} and control. GnRH neuron counting and OMP staining were conducted as previously described (84). To increase the visibility of immunostained neurons, adjustments of brightness, contrast, and color balance were done with Image J (National Institutes of Health, Health, Bethesda) and applied to the entire image.

GnRH neuron counting and OMP staining were conducted throughout the entire embryonic head, and throughout the adult brain beginning with the front of the olfactory bulb (bregma 4.46) to bregma –2.80 (67). Each slide was collected and evaluated for GnRH and Olfactory Marker Protein (OMP) staining in a blinded manner using a Nikon Eclipse E400 microscope. Although all collected sections were assessed for staining, neuroanatomical landmarks were used to identify the regions of interest as depicted in the corresponding figures. Slides were coded to blind the researcher to treatment group during analysis. Adult brains analyzed for GnRH include equal numbers of both male and female subjects, although a sex difference in GnRH neurons has not been recorded to our knowledge. Embryos were not sexed.

Vaginal plug formation, mating assay, and generation of timed embryos. To monitor plug formation, a *Six3*^{OMP} or control female mouse was housed with either a *Six3*^{OMP} or control male mouse at 12 weeks of age and plug formation was monitored for ten consecutive days. Embryos were obtained using timed matings in which one male and one female mouse were housed together, and vaginal plug formation was monitored. If a plug was present, the day was noted as day 0.5 of pregnancy and used to collect embryos for timed mating at embryonic day e13.5 or e17.5. Control and *Six3*^{OMP} mice were housed in pairs, and the number of litters born and the number of pups per litter were recorded over a period of 14 weeks.

Mounting assay. Male mice were habituated to new cages for 1 hour. Ovariectomized and estrogen primed female mice were then introduced to WT, or *Six3*^{OMP} male mice of 16 weeks of age. This test was conducted three times with only the third trial quantified and reported. Trials were conducted one week apart from each other, and the same estrogen primed females were used in all assays. Pairs were videotaped and behavior quantitated in a blind manner with incidences of mounting being recorded over a period of 15 minutes.

Buried food test. A buried food test was conducted to check for gross malfunction of the main olfactory system as described previously (69). All mice were food-deprived overnight (18 hrs). A small piece of mouse chow was buried (~3 cm deep) at a random location in a clean mouse cage containing fresh bedding. One mouse was placed in the cage and timed for the latency to find the mouse chow during a period of up to 15 minutes. Mice were videotaped and behavior quantitated in a blind manner.

Urine collection. Urine was collected from stimulator estrus female mice by holding mice by the scruff of the neck over a piece of clean parafilm. Female stimulator mice were prepared by ovariectomizing female mice and inserting a low-dose estrogen pellet of 0.05 cm diameter subcutaneously. On the day of urine collection, stimulator females were injected with 1 µg of estradiol benzoate diluted in sesame oil 24 hours before collection, followed by 500 µg of progesterone diluted in sesame oil at 2 P.M. Urine was collected at 6 P.M. Urine from 5 different mice of each sex was pooled into separate male and female urine collections on the day of testing.

Volatile and non-volatile odor detection. To assess the ability of *Six3*^{OMP} mice to detect volatile and non-volatile odors, odor detection was assessed with three separate odor presentations given consecutively for two minutes separated by one-minute intervals. First, water was given on Whatman paper taped to a weigh boat to record a baseline for interest in an odorless presentation. After a break of 1 minute, male urine was presented on Whatman paper taped to a weight boat

and after another 1 minute break, female urine was presented in the same manner. To isolate the region of the olfactory system that was disrupted, the detection of volatile and non-volatile odorants were separated by changing the location of the urine stimulus as previously described (71). The number of seconds that the mice stretched upwards to smell the filter paper containing the stimulus and the number of seconds mice touched their nose to the odorant stimulus were recorded.

Six3 and Omp scRNA-seq expression profiling of mouse OE. Dissociated olfactory epithelial cells from three wild type 5-6 weeks old male C57BL/6J wild-type mice were used as input for Chromium Single Cell 3' Solution (10X Genomics) library preparation and sequencing on a HiSeq4000 (Illumina). Epithelial cells were isolated as previously described with the addition of a filtration step through 70 μM mesh and removal of dead cells using ClioCell nanoparticle debris removal (Amsbio) (137). Sequencing reads were processed and mapped to the mouse genome (mm10) using CellRanger software (version 2.1.0). Filtered count matrices for each library were tagged by an associated library batch ID, and count matrices combined across independent experiments using the Seurat software package (v2.1.0; https://github.com/satijalab/seurat) in R (v3.4.3). Cells with fewer than 200 or greater than 5000 genes or greater than 15% mitochondrial content were omitted for subsequent analyses and expression values were scaled by total UMI counts, multiplied by 10,000 and transformed to log space. Technical effects of batch and UMI coverage were regressed from scaled data using the RegressOut function and variable genes identified from a mean variability plot (138). Clustering was performed using the Pagoda2 software package (v0.0.0; https://github.com/hms-dbmi/pagoda2) in R (v3.4.3) (k = 10 and using the top 500 variable genes) (139). Cluster identities and t-SNE coordinates were imported into Seurat from Pagoda2 and differentially expressed genes (DEGs, adjusted p value < 0.05) between clusters were calculated using a Wilcoxon rank sum test (138) on genes detected in at least 25% of cells within a cluster. DEGs were used to assign identities to cell clusters based on

well-established markers. Immune cells were removed from this analysis and the remaining olfactory cell types were re-clustered. Gene expression tSNE plots for *Six3* and *Omp* were generated using the Seurat FeaturePlot function. Violin plots were generated from the normalized count data using the ggplot2 (v3.0.0; https://github.com/tidyverse/ggplot2) R (v3.4.3) software package (140).

Statistical analysis. All the statistical analysis except for the single cell expression profiling was performed using R data analysis software. A P-value of <0.05 was considered statistically significant. For all experiments, data are expressed as the mean ± SEM. Unpaired two-tailed t-tests are used in all cases, except in cases where data was abnormal, or the variances were unequal, in which case the Wilcoxon rank sum tests were used. For experiments containing ordinal data results, chi-squared analysis was used. Power analyses were performed before experiments to determine n values. Experimental groups were defined by genotype and thus no sorting mechanism was used. n values stated for each experiment report the number of mice in each group.

Results

The neuronal population of the main olfactory epithelium requires *Six3* to fully differentiate into OSNs

Previous research identified a role of *Six3* in the development of OSNs, as *Six3HET* mice were shown to have a loss of these mature olfactory sensory neurons in the MOS (84). To determine the stage of olfactory neuron development, IHC was conducted to assess the presence of olfactory progenitor cells in the MOS. Olfactory neurons are born as stem cells and at this stage do not have a specific marker to identify them in the nose. Stem cells proliferate to become olfactory progenitor cells that can be specifically identified by the presence of MASH1 protein. To determine whether olfactory progenitor cells were present in the MOE, IHC with anti-MASH1

antibody was performed on *Six3HET* and control mice at embryonic day 17.5 (e17.5). Staining revealed that there was no difference in the size of the population of MASH1-positive progenitor cells (Fig. 2.1a). The next stage of development for the olfactory neuron is the immature olfactory receptor neuron (iORN). These neurons can be specifically marked for neurogenin1 (NGN1), and thus IHC was conducted using an anti-NGN1 antibody in *Six3HET* and control mice. Assessment of staining in these mice at e17.5 revealed that NGN1-positive cells are similarly represented between genotypes (Fig. 2.1b). The progenitor cell populations are both intact, and therefore we explored the role of *Six3* within the mOSNs- the olfactory population that was absent in *Six3HET* mice (84).

Six3 is necessary for development of OSNs to complete differentiation of the olfactory epithelium

To explore the role of *Six3* in cells that express OMP, a conditional knock-out mouse model, *Six3-flox/OMPcre* mice was generated ($Six3^{OMP}$). Past research has shown *Six3* to be necessary in maintaining olfaction. To assess the contribution of *Six3* from OMP-expressing cells in olfaction, a buried cookie test was conducted. In this paradigm, $Six3^{OMP}$ and control mice were placed in a cage with a food pellet buried under the cage bedding, and the time until the mouse located this buried food was recorded. Male and female $Six3^{OMP}$ mice took significantly longer to locate their piece of buried food, with a ~70% delay compared to control mice. (Fig. 2.2a, b). Odor processing occurs via two morphologically distinct circuits: the MOE and the VNO. The MOE neurons respond mainly to volatile odorants (including those that cue mating behavior) in the environment and VNO neurons respond mainly to non-volatile pheromones detected through direct contact with the odor (16,48,71). As loss of *Six3* from OMP-expressing cells results in compromised olfaction, we sought to determine whether the MOE or the VNO was affected in $Six3^{OMP}$ mice. To experimentally test olfaction within each of these circuits, odors were presented

to *Six3*^{OMP} mice within their cage, wherein they could directly contact the odor stimulus and thus detect both the volatile and non-volatile odorants; and, in a similar experiment the same odorants were also presented outside of the cage where the experimental mice could not contact the stimulus and therefore only volatile odorants were available (Fig. 2.2c,d). In the first paradigm, *Six3*^{OMP} mice displayed no difference in their olfactory investigations of water, female urine, or male urine (Fig. 2.2e). However, when these odor stimuli were placed outside of the cage (therefore only volatile odorants would be available to mice), *Six3*^{OMP} males were less able to detect the male urine or estrus female urine (Fig. 2.2f). This locates the olfactory deficit to the MOE.

Loss of Six3 within OMP-expressing cells results in a reduction in OMP-positive ORNs but does not alter the migration of GnRH neurons

Given the impairment in olfactory capability seen in *Six3*^{OMP} mice, we sought to determine whether there was a loss of mature, differentiated olfactory neurons. Using IHC with anti-OMP antibody, we assessed the presence of ORNs within the MOE and MOB at e17.5 (Fig. 2.3a), and in the MOB in adulthood (Fig. 2.3b). In these regions, but not in the VNO, we observed a moderate decrease in the presence of OMP-positive mORNs (Fig. 2.3c). While there is a marked decrease, some OMP-positive ORNs were still present within the MOB at e17.5 and P56 (Fig. 2.3a,b). At P56, there was variation in the presence of OMP-positive neurons found in the epithelium, with 1/5 mice showing presence of OMP comparable to control mice, 2 showing great loss of OMP and 1 showing a modest presence of OMP. As GnRH neurons migrate along the olfactory projections of ORNs and the terminal nerve, we investigated whether the loss of ORNs resulted in a reduction in these axonal projections that are necessary for GnRH neurons to arrive in the hypothalamus (80). Axonal projections of ORNs were identified using IHC with anti-peripherin antibody, as peripherin marks these projections (141). No difference by genotype was observed

in the peripherin-positive fibers within the MOS, nor was there a difference in the morphology of these projections (Fig. 2.3d).

Past research has shown that *Six3* and mORNs play a role in preserving proper GnRH migration (21,84,142); therefore, we decided to determine whether actions of SIX3 within OMP-expressing neurons are necessary to preserve GnRH neuronal migration and survival. Using $Six3^{OMP}$ mice, we assessed the migratory ability of GnRH neurons early in embryogenesis, at e13.5. At this early stage of development, we did observe a delay in the migration of neurons, with a greater portion of GnRH neurons located in anterior portions of the migratory pathway, and conversely fewer GnRH neurons being found in latter portions of the migratory pathway. However, the total number of GnRH neurons did not differ between genotypes (Fig. 2.4a). In contrast, later in development, at e17.5, no differences were observed in the number of GnRH neurons found in the nose, olfactory bulb, or hypothalamus as compared to control mice (Fig. 2.4b). Additionally, the total number of GnRH neurons at this age was similar between $Six3^{OMP}$ and control mice (Fig. 2.4b). $Six3^{OMP}$ mice were assessed into adulthood as well to determine whether the GnRH neurons successfully migrated to their final destination within the medial preoptic area in $Six3^{OMP}$ mice. IHC with anti-GnRH antibody at p56 revealed that there was no difference in the number of GnRH neurons located within the hypothalamus (Fig. 2.4c). In addition, GnRH projections to the median eminence can be seen in both the control and $Six3^{OMP}$ mouse (Fig. 2.4c). In conclusion, although there was an impairment in the presence of ORNs, which has been shown to be associated with a loss of GnRH neurons (143), only an early delay in GnRH migration was observed.

Despite olfactory impairment, $Six3^{OMP}$ mice are fertile

It is well studied that olfaction drives reproductive behavior (14). Ablation of olfactory ability and numerous genetic mouse models of olfactory impairments have demonstrated an influence

of intact MOS odorant processing on mating ability in male mice (14,20). More specifically, it has been shown that haploinsufficiency of *Six3* in a whole-body knock-out mouse model resulted in a loss of male mating behavior (84). Therefore, although GnRH neurons are intact in the *Six3*^{OMP} mice, we decided to investigate mating behavior. We first conducted a plugging assay with control and *Six3*^{OMP} mice to determine whether there was an impairment in copulation, as male mice will leave a "plug" in the female vagina after coitus has occurred. The ability of males to produce this plug in WT females was affected by a loss of *Six3* within the OMP-expressing cells (Fig. 2.5a). The ability of mice to produce litters was also assessed, as a plug is indicative of coitus but not reproductive potential. Although males plugged at a reduced rate, there was no difference between the number of litters produced by *Six3*^{OMP} mice as compared to control male or female mice in a 90-day mating assay (Fig. 2.5b). The time that it took for cKO mice to produce their first litter in this assay was also not altered by the conditional deletion of *Six3* within the mOSNs (Fig. 2.5c). Finally, the number of pups produced in each litter did not differ by genotype (Fig. 2.5d). Thus, while olfaction is impaired in *Six3*^{OMP} mice and the reduced ability to detect volatile odorants decreases the mating behavior of male and female *Six3*^{OMP} mice, it does not affect fertility overall. To test this hypothesis, we conducted a mounting assay, in which the number of times male mice mounted estrus female mice was recorded over fifteen minutes. In this assay, while there was a delay in the time to the first mount, the number of mounts during the duration of this assay was not different between genotypes (Fig. 2.5e).

There is clearly an effect of the loss of *Six3* within OMP neurons on olfactory ability; however, this impairment is dampened compared to previous experiments conducted with *Six3KO* mice. Thus, our next goal was to ascertain the expression level of *Six3* within mOSNs, and also within other populations within the olfactory system. We conducted single cell sequencing of wild-type nasal epithelial cells and found that while some mOSNs did show expression of *Six3*, many did not (Fig. 2.6a). Analysis reveals two separate populations with many

neurons exhibiting little to no expression of *Six3*, and a smaller number exhibiting high expression of *Six3*. Interestingly, the cell types with the highest expression of *Six3* were sustentacular cells (SUSs) and horizontal basal cells (HBCs) (Fig. 2.6a). SUS cells are analogous to neuronal glial cells and are essential in the regulation of ORN homeostasis and proliferation (144). In contrast, the HBCs are a relatively quiescent candidate stem cell population whose function is not entirely known. We next analyzed our single-cell sequencing data to determine whether OMP is expressed within these populations highly expressing *Six3*; and therefore, whether the OMP-cre may target these cells as well. Indeed, we did see expression of *Omp* within this neuronal population, indicating that SIX3 may be acting within the SUS cells or HBCs to produce the aforementioned phenotypes (Fig. 2.6b). OMP and Six3 co-localized to the mOSN, SUS, and HBC populations (Fig. 2.6c).

Discussion

The role of *Six3* within the olfactory lineage in the formation of OSNs

We have shown here that in the *Six3HET* mouse, olfactory neuronal precursors are intact, however mature OSNs are lost. It was previously determined that the *Six3HET* mouse had complete loss of olfactory capability originating in the MOS, causing eradication of mating behavior in males (84). Therefore, we next sought to determine whether this loss of olfactory capability and alteration of mating behavior was a result of actions of *Six3* during differentiation of the ORNs of the MOS. Here, we use a conditional deletion mouse model that expresses cre recombinase in mOSNs to genetically dissociate the role of SIX3 within OMP-expressing cells from the actions of SIX3 in the environment of the nose (20). Using this $Six3^{OMP}$ mouse, we isolated the effect of SIX3 within the olfactory epithelium and found that SIX3 is essential in developing olfactory capability and OSNs.

The goal of this project was to determine whether actions specifically within OMP-expressing cells were driving previously observed defects in GnRH neuron migration and olfactory capability; however only one of these phenotypes was recapitulated when *Six3* was removed specifically within the OMP-expressing population. The population of ORNs was ablated in *Six3HET* mice, however it was merely decreased in *Six3*^{OMP} mice. Therefore, it is possible that SIX3 has a role within the precursor populations in ensuring the propagation of mORNs. Production of ORNs requires the tight regulation of proliferation, differentiation, and survival of progenitor neurons (145,146). The balance between the proliferation of progenitor cells, and the production of OSNs is regulated by a variety of positive and negative feedback signals in the MOE (144,145). The scenario of the precursor population being intact, while mature differentiated neurons are lost, has been seen before given reduction in SIX3. For example, mice with a specific deletion of *Six3* within the neuroretinal lineage lost some differentiated forms of neuroretinal progenitors (147). A similar loss of differentiated cells was seen given the loss of SIX6, a very closely related protein to SIX3 and a member of the SIX homeodomain protein family (147,148). In Drosophila, *Six6KO* retinas displayed a presence of retinal progenitor cells, however these cells demonstrated decreased proliferation and did not generate retinal ganglion cells (40). Therefore, it seems possible that SIX3 has actions within the differentiating epithelium that maintain the ORN population.

SIX3 is possibly exerting its effects on the differentiating mOSNs at one of the precursor stages. Previous work demonstrates that SIX3 is necessary within the Ngn1-positive iORNs to generate OMP-positive mORNs (149). This possibility, however, is dampened by the fact that iORNS produce low levels of *Six3*. Interestingly, another member of the SIX family, *Six1*, is implicated in the proliferation of olfactory progenitors into mORNs, by regulating the transition from Mash1-positive progenitors to Ngn1-positive intermediate precursor cells in the MOE (150,151). Previous studies have shown that the MOE of *Six1KO* mice was thinner than WT

counterparts, due to a loss of Ngn1-positive iORNs. Furthermore, these mice exhibit a loss of OMP-positive ORNs, similarly to the *Six3HET* mice and the *Six3*^{OMP} mice (149). Another *Six3* mouse model, Six3$^{neo/neo}$ (in which Six3 is reduced by more than 50%) demonstrated increased expression of Neurogenin2 and decrease expression of Mash1 (152). Further studies will need to be conducted to determine whether the lineage of olfactory neurons is abrogated in *Six3HET* mice due to actions within the iORN, and whether loss of *Six3* within olfactory progenitor or stem cell populations could be responsible for the loss of GnRH neurons and olfactory axonal projections previously observed in a *Six3HET* mouse (84).

Additionally, it is possible that OSNs in *Six3*^{OMP} mice are generated but apoptose when SIX3 is absent from the small proportion of OSNs that expresses *Six3*. It has been observed previously in mice with conditional deletion of *Six3* within neuroretinal cells that *Six3*-deficiency resulted in educed proliferation and apoptosis (153). Additional evidence of the essential role of SIX3 in the survival of cells, has been seen in medeka fish, wherein loss of *Six3* by morpholino knock-down resulted in the apoptosis of cells that normally express *Six3* (153). Apoptosis after removal of SIX3 has also been observed in mice and Drosophila, wherein the result was the massive cell death and loss of various morphologic structures (153,154). Closely related gene *Six6* has also been associated with apoptosis of terminally differentiated retinal cells when lost in a Six6KO mouse (40,155). Further studies will need to be conducted to determine the mechanism of loss of ORNs in *Six3*^{OMP} mice.

The role of SIX3 in the supporting cells of the olfactory epithelium

Given the differences between the severity of the phenotypes in *Six3HET* mice and *Six3*^{OMP} mice, other olfactory cell types were assessed. Interestingly, strong *Six3* and *Omp* co-expression were detected in two other nasal cell types: SUS cells and HBCs. HBCs are relatively quiescent and are thought to divide only occasionally to give rise to GBCs, which are assumed to

then give rise to ORNs and SUS cells (156). While this lineage is uncertain, it is known that HBCs rarely divide except in response to severe damage (144). Alternatively, it has been proposed that HBCs are responsible for maintaining the stem cell niche of GBCs, and are not part of the neuronal lineage of the olfactory epithelium (146,157). Furthermore, there is evidence that HBCs are only activated to multipotency and proliferation when SUS cells are ablated, and not when mOSNs alone are lost (156). Therefore, there are several possibilities as to why, in our *Six3*^{OMP} model where many mOSNs are absent, HBCs do not regenerate this population. One possibility is that while the mOSNs are absent, the SUS cells are intact, and thus the HBCs are not prompted to regenerate lost tissue. However, this cannot be easily confirmed as there is no reliable marker for SUS cells. Another possibility is that HBCs do regenerate the olfactory lineage in response to absence of mOSNs. However, the resurgence of the neurons is altered by the loss of *Six3* within HBCs, and therefore the proper differentiation of these neurons is altered and the iOSNs are defective in their production of mOSNs.

In addition to HBCs, our single cell sequencing illuminated a potential roll of SUS cells in our *Six3*^{OMP} model. SUS cells are supporting cells analogous to glial cells that lie within the neuroepithelium (157). SUS cells were identified in our single-cell sequencing as expressing high levels of both *Six3* and *Omp*, thus these cells were targeted by the *Six3*^{OMP} allele. It is possible that the loss of *Six3* within this cellular population altered the ability of these cells to support the growth, division, and sustenance of the olfactory epithelium, thus resulting in the loss of mOSNs and defective olfaction. In the future, it will be advantageous to determine what role Six3 has within the SUS cells.

Reduction of mature OSNs results in impaired olfactory capability

Six3^{OMP} mice were less capable of using odorant cues to locate food and were less responsive to the urinary cues of their conspecifics. While this is interesting as it sources a role

for SIX3 in olfactory capability to the olfactory epithelium, the loss of olfactory capability was not as severe as seen in the full-body *Six3HET* mouse; and, it only reduced mating behavior without affecting overall fertility (84). The loss of olfactory processing due to developmental errors has been described in several mouse lines including Pax-6 SeyNeu/SeyNeu and Dlx5 KO (52). The display of normal mating behavior in rodents is dependent upon correct processing of olfactory cues, via two key olfactory circuits, the MOE/MOB and VNO/Accessory Olfactory Bulb (14). The MOE is known to process volatile odors, while the VNO is responsible for transmitting signals about water-soluble non-volatile compounds mediating innate behaviors (17). Volatile odorants processed in the MOE and the efferent signals that they cue have been strongly implicated in the initiation of male sexual behavior (14). Thus, we investigated whether *Six3*^{OMP} mice could detect the urinary odorants of male and female mice. Interestingly, *Six3*^{OMP} male mice did not respond as strongly to the volatile odorants of male and female urine, indicating an impairment in the odor processing of the MOE. The persistence of fertility despite the drastic loss of olfactory capability within the MOE is likely because olfaction was not completely eradicated as demonstrated in the buried food assay. In this assay, mice were delayed in finding buried food but were eventually capable of locating the olfactory stimulus. Similarly, it seems they can detect estrous females. Although there was a substantial deficit in the plugging assay fertility was unaffected, indicating that coitus was only delayed by the olfactory handicap. The coitus that occurred was deemed to be successful as there was no difference in the number of pups produced by cKO mice compared to controls, and these mice were not delayed in the time it took them to produce their first litter. The association of the loss of olfaction and the loss of fertility has been described numerous times in mice (19,21); however, olfaction impairments only affect fertility if they alter the response of mice to mating cues (158). As seen in the mounting assay conducted here, while *Six3*^{OMP} mice took longer to initiate sexual behavior in response to estrous female mice, the number of mounts performed in the assay was not significantly lessened by this delay.

It is clear that the olfactory impairment in the *Six3*^{OMP} mice is not as severe as that seen previously in *Six3HET* mice (84). One possible explanation is that the OMP-cre does not begin expressing cre recombinase until e13.5 (75), at which point Mash1-positive olfactory progenitors are already present in the nasal epithelium, and Ngn1-positive INPs are beginning to form (146). Therefore, if loss of olfaction in the *Six3HET* mouse was due to effects within these populations, it is reasonable that those effects would not be seen in a conditional OMP-cre mouse. Furthermore, since GnRH neurons are already born and migrating at e13.5, and axonal projections are present within the olfactory system to guide their migratory journey, alterations to this system at e13.5 using the OMP-cre may not produce effects (159,160). This may explain why a delay in GnRH neuron migration was only observed in these mice early in embryogenesis.

The moderate deficit in olfactory capability seen in the food finding assay is likely due to the fact that mOSNs were still visible within the olfactory regions throughout development and into adulthood. The persistence of some of the mOSN population may have arisen because there appears to be two distinct mOSN populations in terms of their *Six3* expression. A large proportion of mOSNs were not identified as expressing *Six3*, however, a small sub-population expressed high levels of *Six3*. The olfactory deficit is, however, more drastic than would be expected from disrupting only this small population of OSNs. It is possible that the *Six3/Omp* expressing SUS cells play a role in the maintenance of this population and that Six3 removal from these neurons is largely mediating the observed phenotypes.

Conclusions

Together, these findings provide insight into an organ-specific strategy for the regulation of cellular progression by SIX3, a strategy that has been explored in other organ systems and likely exists in still more. These findings show that SIX3 has direct actions within OMP-expressing

neurons that are necessary to maintain olfaction, and that SIX3 functions within the environment of the olfactory neuron to regulate nasal development and ensure proper GnRH neuron migration. In conclusion, *Six3* is an important neurogenic regulator that plays a role in the generation of ORNs. These findings have broader implications for human health, as expanding the knowledge basis of the mechanism through which *Six3* regulates neuronal development will provide insight into the diseases engendered by mutations in *Six3*, such as schizencephaly and holoprosencephaly (63,64,161,162).

Acknowledgements

The authors thank Jason D. Meadows for technical assistance on this project. This work was supported by National Institutes of Health grants R01 HD082567 and R01 HD072754 (to P.L.M.) and by National Institute of Child Health and Human Development/National Institutes of Health P50 HD012303 as part of the National Centers for Translational Research in Reproduction and Infertility (P.L.M.). P.L.M. was partially supported by P30 DK063491, P42 ES101337, and P30 CA023100. E.C.P. was partially supported by National Institutes of Health R25 GM083275 and National Institutes of Health F31 HD098652.

Chapter 2 is currently being prepared for submission for publication of this material. Pandolfi, Erica C.; Burow; Dr. Jones, Samantha A.; Mellon, Pamela L. The dissertation author is the primary investigator and author of this material. Dr. Samantha Jones, Dr. Dana Burow, and Dr. Miles Wilkinson contributed the single-cell sequencing data. Pamela Mellon supervised the project and provided advice.

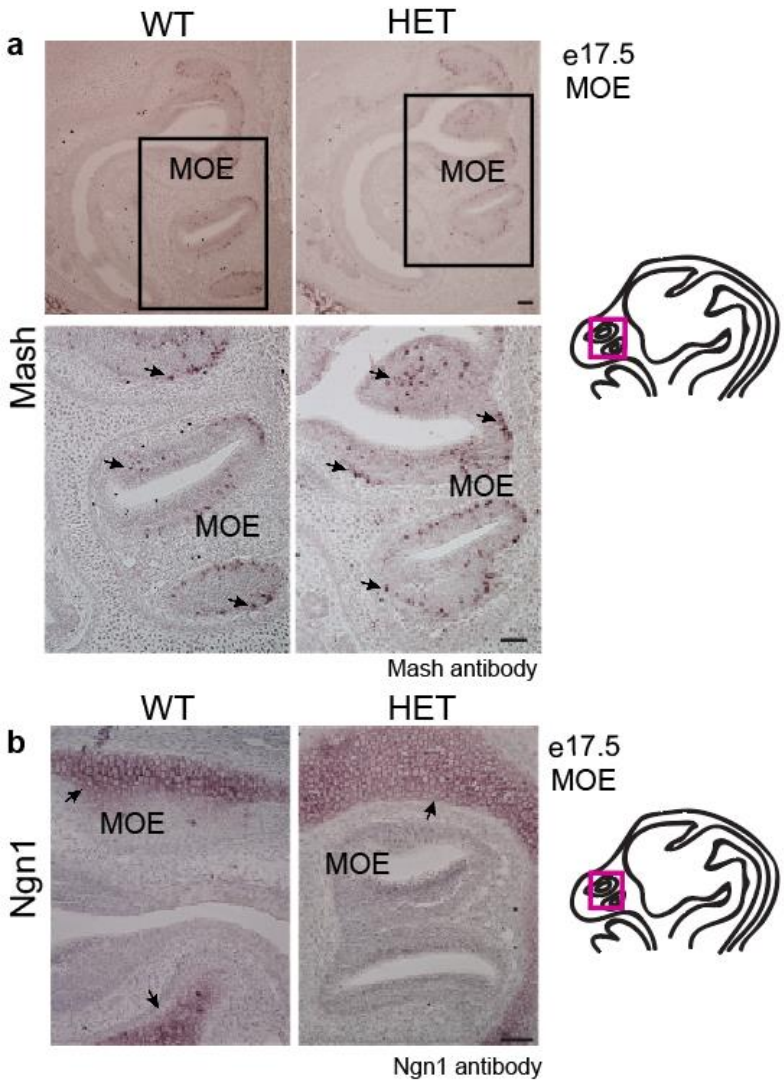

Figure 2.1. Olfactory Progenitor Cells are intact in Six3HET mice. **a,** IHC of Mash-positive progenitor cells with anti-MASH shows no difference in the number of progenitor cells. **b,** IHC of iOSNs with anti-NGN1 antibody shows no difference in the presence of immature olfactory neurons. MOE, main olfactory epithelium. Scale bar, 100 µm.

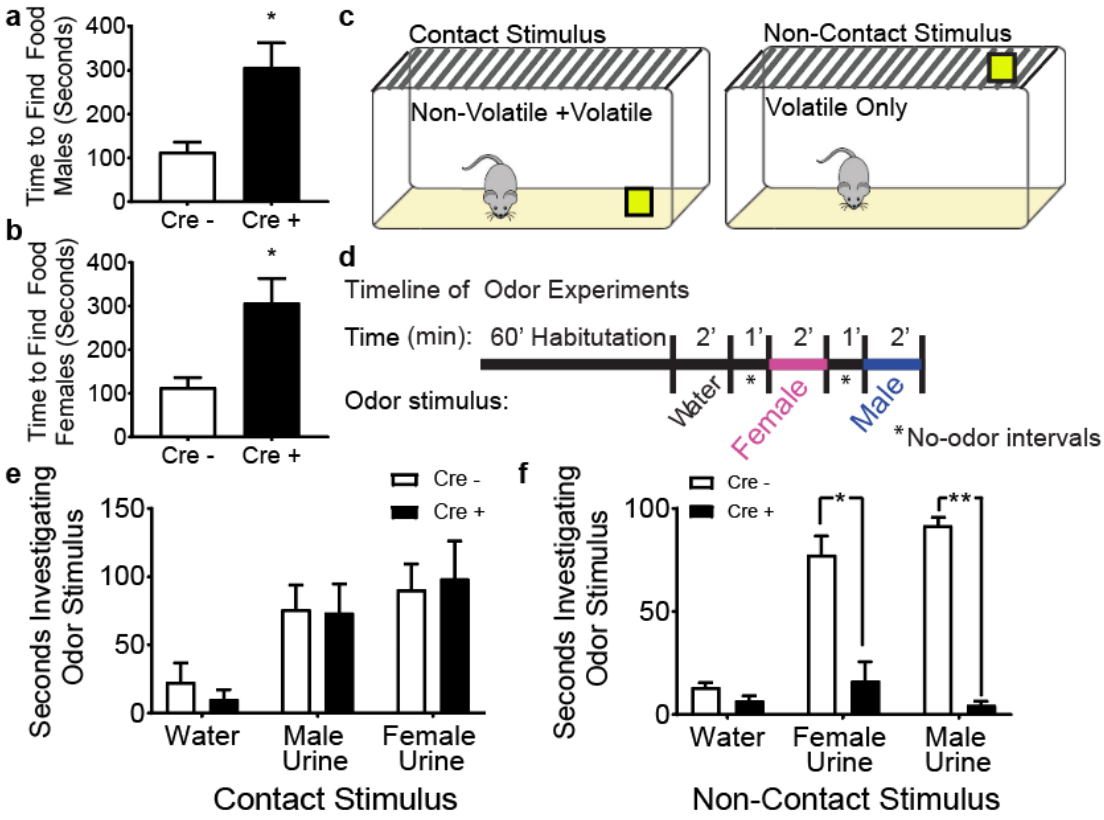

Figure 2.2. Six3^{OMP} mice have impaired olfaction and loss of OSNs. **a,** Six3^{OMP} male mice take ~70% longer to locate the buried food in their cage compared to control mice. **b,** Female Six3^{OMP} mice are also delayed in finding their buried food compared to control mice by ~70%. **c,** Tests were conducted to discern the ability to detect and male and female urinary odors. Odor placement was used to separate volatile and non-volatile odor components. Mice must be able to physically contact the odor stimulus to detect non-volatile odor components. Thus, when the odor was placed outside of the cage **(e)**, only volatile odors were detectable. **d,** Contact stimulus detection in male mice (water: student's t-test, n=3-4, p=0.480, t(3)= -0.806); (female urine: student's t-test, n=3-4, p=0.932, t(5)= 0.251); (male urine: student's t-test, n=3-4, t(5)= 0.252, p=0.812). **e,** Non-contact stimulus detection in male mice showed a significant decrease in the interest of (water: student's t-test, n=3-4, p=0.095, t(5)= -2.079); (female urine: student's t-test, n=3-4, p=0.007, t(5)= -4.534); (male urine: student's t-test, n=3-4, t(3)= -19.4, p=0.0002).

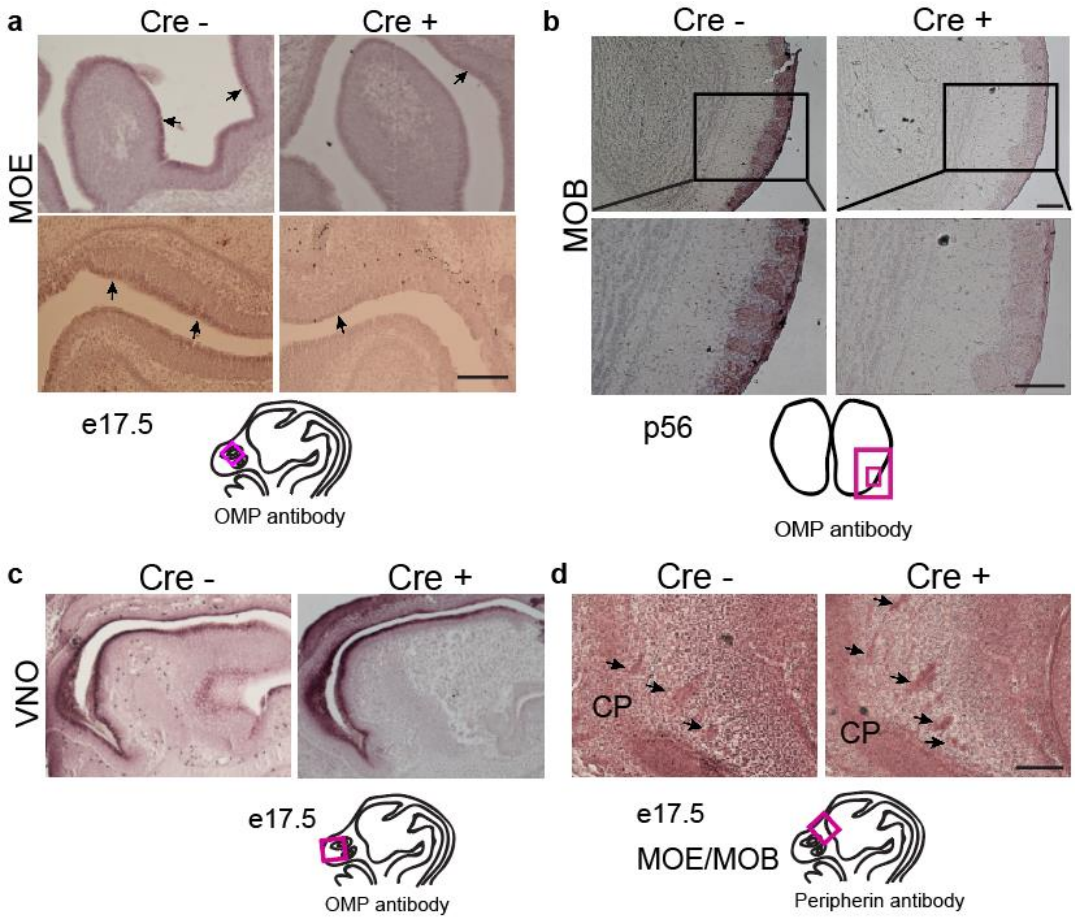

Figure 2.3. Six3^{OMP} mice show decreased OMP expression but have intact axonal projections. **a,** Using IHC with anti-OMP, there is a decrease in the presence of ORNs in Six3^{OMP} mice compared to control mice at e17.5 **(b)** and at P56. **c,** Using IHC with anti-OMP, there is presence of OMP within the VNO. **d,** IHC to assess olfactory projections with anti-peripherin shows no difference was observed in the number or morphology of olfactory axonal projections as compared to control mice. CP, cribriform plate. Scale bar, 100 µm.

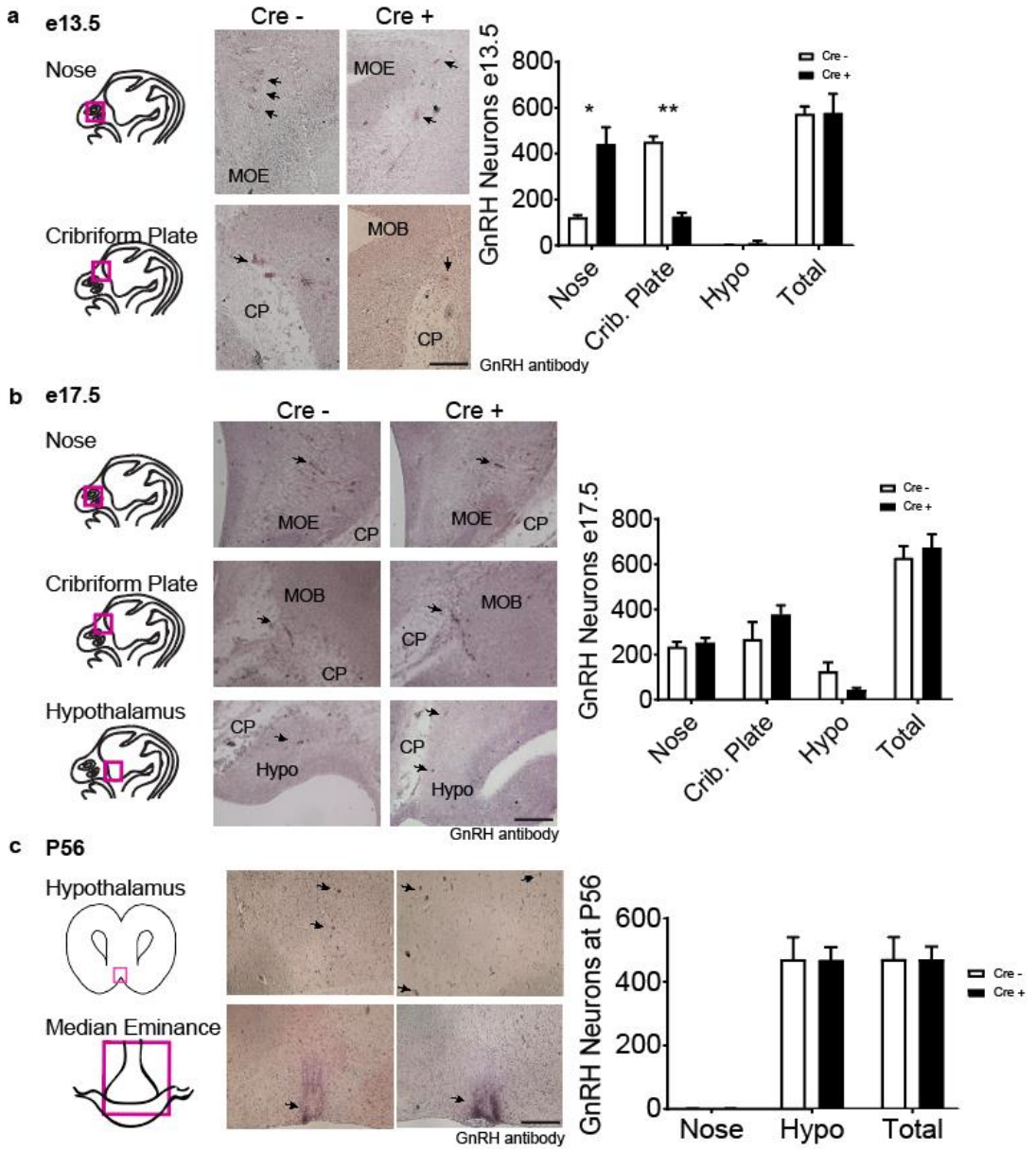

Figure 2.4. GnRH neuron migration is delayed early in embryogenesis, but unaffected later in embryogenesis and in the adult. **a,** GnRH neurons at e13.5 (nose: student's t-test, n=3, p=0.046, t(2)= -4.35); (cribriform plate: student's t-test, n=3, p=0.0006, t(4)=11.405); (hypothalamus: student's t-test, n=3, p=0.463, t(2)= - 0.896) (total: student's t-test, n=3, p=0.970 t(3)= -0.041). **b,** No difference was observed in the migration of GnRH neurons e17.5, (nose: student's t-test, n=3, p=0.586, t(4)= -0.591); (cribriform plate: student's t-test, n=3, p=0.290, t(3)= -1.27); (hypothalamus: student's t-test, n=3, p=0.463, t(3)= - 0.896) (total: student's t-test, n=3, p=0.180 t(2)= 1.944). **c,** Equivalent numbers of GnRH neurons were located in the hypothalamus and in the olfactory bulb in male and female mice at p56, (nose: student's t-test, n=3, p= 0.881, t(4)= 0.036); (hypothalamus: student's t-test, n=3, p= 0.981, t(4)= 0.025) (total: student's t-test, n=3, p=0.996, t(4)= 0.056). MOE, main olfactory epithelium. CP, cribriform plate. HYPO, hypothalamus.

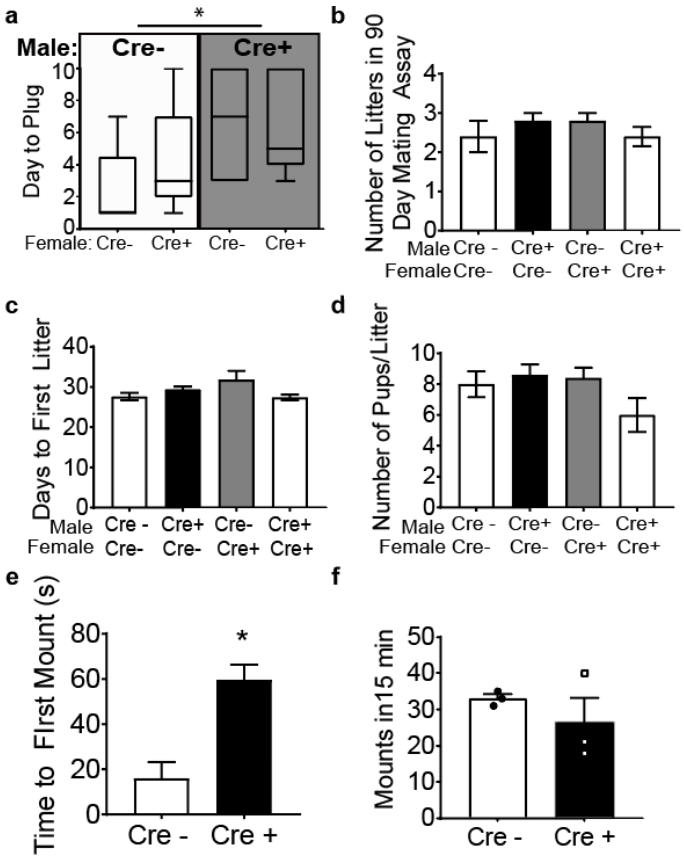

Figure 2.5. Six3^{OMP} mice have intact fertility but delayed mating and deficient plugging. **a,** Male and female mice displayed defective plugging activity in a 10-day plugging assay as compared to cre- x cre- matings. The ability of each sex to either create or receive a plug was determined (male cre- compared with male cre+: X2 (2, N = 5) = 6.86, p =0.009; female cre- compared with female cre+: X2 (1, N = 5) = 1.34, p =0.25. **b,** There is a no difference in the number of litters that Six3^{OMP} mice can produce as observed in a 90-day mating assay (cre- x cre+: student's t-test, n=5, p=0.397, t(8)= 0.894); (cre+ x cre-: student's t-test, n=5, p=0.397, t(8)=0.894); (cre+ x cre+: student's t-test, n=5, p= 1.01, t(8)=0). **c,** There was no delay to the first litter produced in this assay (cre- x cre+: student's t-test, n=5, p=0.159, t(8)= 1.57); (cre+ x cre-: student's t-test, n=5, p=0.118, t(8)=1.78); (cre+ x cre+: student's t-test, n=5, p= 0.866, t(8)=0.174). **d,** There was also no difference in the number of pups produced per litter in this assay (cre- x cre+: student's t-test, n=5, p=0.593, t(8)=0.557); (cre+ x cre-: student's t-test, n=5, p=0.720, t(8)=0.371); (cre+ x cre+: student's t-test, n=5, p= 0.185, t(8)=145). **e,** In a fifteen minute mounting assay, Six3^{OMP} mice were delayed in their first mount of an ovariectomized estrous primed female (student's t-test, n=3, p= 0.011, t(4)=4.45), however the number of mounts **(f)** during the duration of this assay was not significantly different (student's t-test, n=3, p= 0.394, t(4)= 0.955).

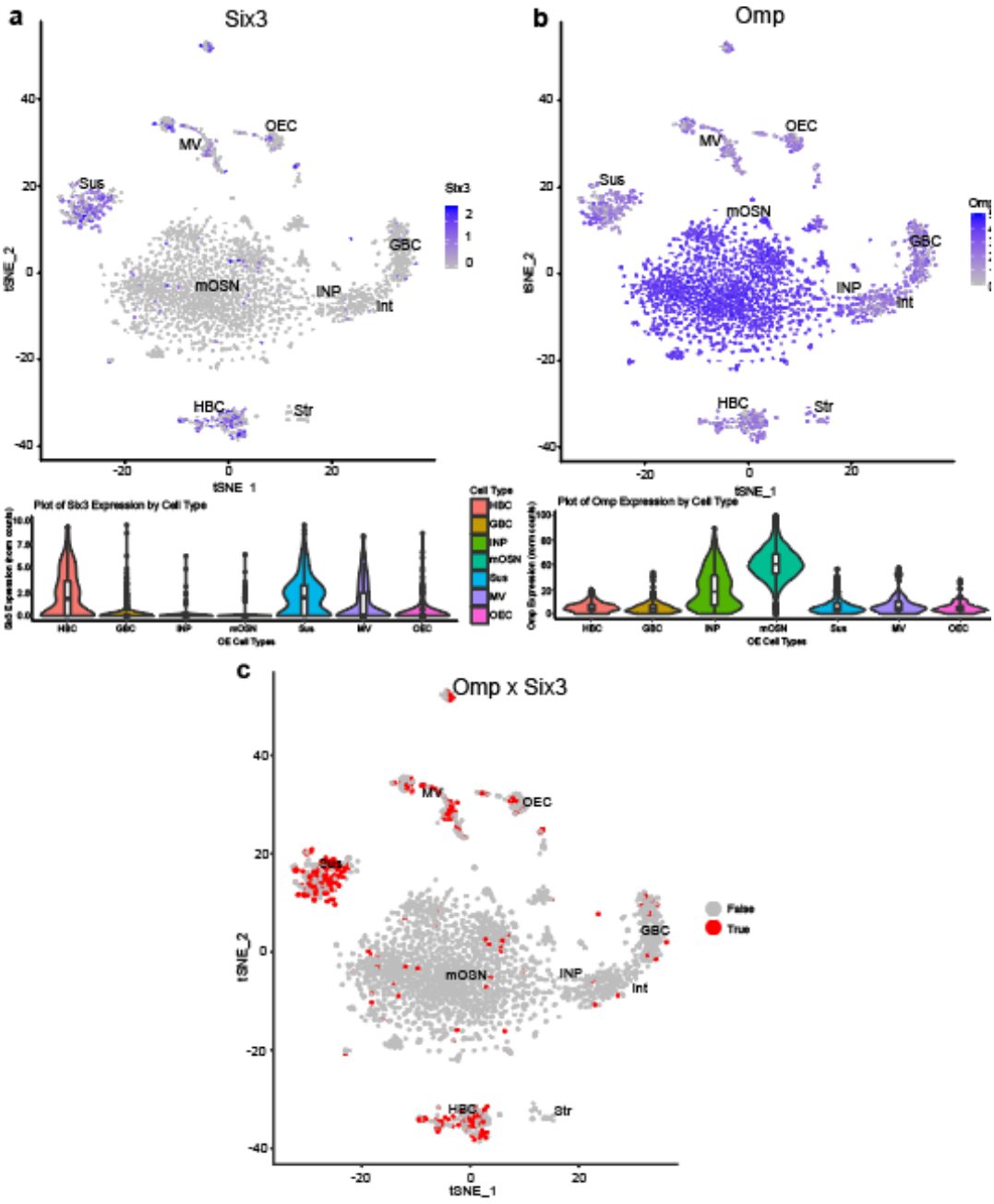

Figure 2.6. *Six3 and Omp scRNA-seq expression profiling of mouse OE.* **a,** Single cell sequencing of nasal cells for expression of *Six3*. **b,** Single cell sequencing of nasal cells for expression of *Omp*. **c,** Identification of cells co-expressing high levels of *Six3* and *Omp*.

Chapter 3: Deletion of Six6 from Gonadotropin-Releasing Hormone (GnRH) Neurons Decreases GnRH Gene Expression Resulting in Hypogonadism and Infertility

Abstract

Hypothalamic gonadotropin-releasing hormone (GnRH) neurons are at the apex of the hypothalamic-pituitary-gonadal (HPG) axis that regulates mammalian fertility. Insufficient GnRH disrupts the HPG axis and is often associated with the genetic condition idiopathic hypogonadotropic hypogonadism (IHH). The homeodomain protein sine oculis-related homeobox 6 (*Six6*) is known to be an essential factor in the development of GnRH neurons. While it is known that *Six6* is dramatically increased during GnRH neuronal maturation and that overexpression of *Six6* induces GnRH transcription in neuronal cells, the direct role of *Six6* within the GnRH neuron is unknown. Here we find that global *Six6* knock-out (KO) embryos show apoptosis of GnRH neurons beginning at embryonic day 14.5 with 90% loss of GnRH neurons by postnatal day one. We sought to determine whether the hypogonadism and infertility reported in the *Six6KO* mice are generated via actions within the GnRH neuron by generating a *Six6-flox* mouse. To determine the specific role of *Six6* in GnRH neurons and its relation to IHH, we crossed *Six6*$^{flox/flox}$ mice with *LHRHcre* mice allowing us to identify the specific role of *Six6* in GnRH neurons *in vivo*. Using male and female *Six6-flox/LHRHCre* mice, we see that loss of *Six6* within the GnRH neuron abolishes GnRH expression in ~90% of GnRH neurons. We further demonstrate that the deletion of *Six6* within the GnRH neuron leads to infertility, hypogonadism, hypogonadotropism, and delayed puberty. We conclude that *Six6* plays distinct roles in maintaining fertility both within the GnRH neuron, and within the migratory environment of the GnRH neuron by maintaining expression of GnRH and survival of GnRH neurons respectively. These results increase knowledge of the role of *Six6* in the brain and may offer insight into the mechanism of IHH.

Introduction

Mammalian reproduction is mediated by the pulsatile release of gonadotropin-releasing hormone (GnRH) from GnRH neurons. GnRH neurons are located at the apex of a hormonal axis, the hypogonadal-pituitary-gonadal (HPG) axis, that controls a multitude of physiological functions including reproduction, menstruation, pregnancy, and menopause. As part of this axis, GnRH is synthesized in the hypothalamus and then stimulates the release of luteinizing hormone (LH) and follicle-stimulating hormone (FSH) from the anterior pituitary. These hormones, in turn, act on the gonads to produce testosterone, estrogen, and progesterone in the process of gametogenesis (163,164). During development, GnRH neurons complete a long migratory journey (25). GnRH neurons originate in the olfactory placode at embryonic day (e) 11.5, migrate across the cribriform plate, and through the basal forebrain before arriving in the presumptive hypothalamus. Once in the hypothalamus, GnRH neurons extend their axons to the median eminence (ME) where secreted GnRH enters the hypophyseal portal system and reaches the pituitary (143).

Errors in GnRH secretion from the GnRH neuron, migration of the GnRH neuron, or development of the GnRH neuron can result in levels of GnRH that are insufficient to properly cue the HPG axis. This can result in the condition idiopathic hypogonadotropic hypogonadism (IHH), which is characterized by varying degrees of impaired fertility (2). Additionally, insufficient GnRH can result in the subtype of IHH, Kallmann syndrome, that is characterized by impaired fertility paired with anosmia (165). These conditions have been linked to numerous genetic mutations; however, more than 50% of cases of IHH have unknown genetic origins (9).

Several genes responsible for ventral forebrain development have been associated with IHH. Developmental errors in the olfactory placode and ventral forebrain can produce IHH because their abnormal development and function is prone to disrupt the development of GnRH neurons and their migration from the olfactory placode to the hypothalamus (166). Studies conducted in global homozygous, heterozygous, and tissue-specific knock-out mouse models

have shown that loss of certain homeodomain proteins, including *Vax1, Otx2, Dlx1/2, and Six3* can result in loss of GnRH and therefore various degrees of subfertility and infertility have been recorded (33,56,58,131).

One homeodomain protein that has been shown to play an essential role in the development of GnRH neurons and regulation of fertility is sine oculis-related homeobox 6 (*Six6*) (33). Using a global knock-out model, *Six6* has been identified as a potential candidate in polygenic IHH (33). *Six6* is a highly conserved homeobox gene required for proper forebrain and eye development (41,167). The timing and spatial expression pattern of *Six6* overlaps with the emergence, migration, and development of GnRH neurons (43). Additionally, overexpression of *Six6* induces GnRH transcription in neuronal cells via binding to evolutionarily conserved ATTA sites located within the GnRH proximal promoter (33). The mouse model *Six6KO* showed that complete loss of *Six6* results in a 90% reduction in GnRH neurons as detected by GnRH immunohistochemistry, leading to both male and female infertility (33). Male *Six6KO* mice showed reduced FSH; however, LH, testosterone, and spermatogenesis were unaffected. Female reproductive physiology was more drastically affected by total loss of *Six6*, with female mice showing noncyclic estrous cycles, reduced ovary size, and fewer corpora lutea (33).

The specific mechanism engendering the hypogonadism and infertility reported for this *Six6KO* mouse however is unknown. *Six6* is expressed throughout the regions through which GnRH neurons develop, and within the GnRH neuron. Therefore, it is unclear whether GnRH is deficient due to actions of SIX6 within the GnRH neuron, or whether SIX6 is essential for the survival/migration of the GnRH neuron due to actions in the migratory environment of the GnRH neuron. We here describe that *Six6* plays an essential role within the GnRH neuron in maintaining expression of GnRH, where the loss of *Six6* solely from GnRH neurons results in infertility and reproductive impairment.

Methods

Mouse lines and animal housing. All animal procedures were performed in accordance with the University of California, San Diego, Institutional Animal Care and Use Committee regulations (IUCAC protocol S00261). Mice were group-housed with ~4 to a cage on a 12-hour light, 12-hour dark cycle (on 6:00 A.M., off 6:00 P.M.), with *ad libitum* chow and water. All mice were kept on a C57BL/6J mouse background. *Six6KO* mice were generated as previously described (40) and were kindly provided by Dr. Xue Li (Children's Hospital of Boston, Harvard Medical School, Boston, MA). *Six6^{flox}* mice were generated from a *Six6* Knock-out First KOMP (UC Davis, Knock-Out Mouse Project, www.komp.org) construct by electroporation into C57BL/6J mouse embryonic stem cells, selection using G418, and screening for homologously recombined cells. A homologously recombined clone of mouse embryonic stem cells was then injected into blastocysts to produce chimeric mice which were then outbred to C57BL/6J and crossed with a *flpase* mouse [(168); http://jaxmice.jax.org/strain/003800.html] to create the *Six6^{flox}* conditional KO allele. *Six6^{flox}* genotyping was performed with *Six6WT* forward: 5'GAAGCCCTTAACAAGAATGAGTCGG 3'; *Six6^{flox}* forward: 5'CTTCGGAATAGGAACTTCGGTT 3', reverse: 5'CTTTGAATTTGGGTCCCTGG 3'. Primers to test for germline recombination are forward: 5'aagacagactgcattcccagc 3'; reverse: 5'agactcactgcttcaaggagc 3'. These mice were then mated to *LHRH^{cre}* (66) mice for conditional removal of *Six6* within the GnRH neurons. For lineage tracing, *Rosa^{tdTomato}* (JAX #007909) (68) and Rosa^{Lacz} (JAX #003309) reporter mice were used and mated to *Six6^{flox}* and *LHRH^{cre}* mice to create the *Six6$^{flox/flox}$/Rosa^{LacZ}/LHRH^{cre}* and *Six6^{KO}/Rosa^{tdTomato}/GnRH^{cre}* lines. The same approach was used for lineage tracing in the *Six6KO* mouse model. Mice were killed by CO_2 or isoflurane (Vet One, Meridian) overdose. Controls used for the *Six6KO* line were *WT* mice; controls for the *Six6$^{flox/flox}$/LHRH^{cre}* line were *Six6$^{flox/flox}$*, controls for the *Six6$^{flox/flox}$/Rosa^{LacZ}/LHRH^{cre}* line were *Rosa^{LacZ}/LHRH^{cre+}* mice; controls for the *Six6^{KO}/Rosa^{tdTomato}/GnRH^{cre}* were *Rosa^{tdTomato}/LHRH^{cre+}.*

Collection of tissue and histology. Ovaries and uteri from diestrus females and testes from males were dissected and weighed from animals of 3 months of age. Diestrus ovaries, brains, olfactory bulbs, embryos, and testes were fixed for two days (~49 hr) at 4°C in freshly made mixture of 6:3:1 absolute alcohol: 37% formaldehyde (Fisher F79-4): Glacial Acetic Acid, then dehydrated in 70% ethanol before paraffin embedding. Sagittal sections (10 µm) were cut on a microtome and floated onto SuperFrost Plus slides (Thermo Fisher Scientific). Ovaries, testes, brains, and noses were stained with hematoxylin and eosin (H&E; Sigma-Aldrich). In ovaries, the number of corpora lutea in a single ovary per mouse was recorded by an investigator blinded to the treatment/genotype.

Determination of pubertal onset and estrus cyclicity. These procedures were described previously in detail (32). To assess estrous cyclicity, vaginal smears were performed daily between 9:00 and 11:00 A.M. on 3- to 5-month-old mice by vaginal lavage.

Timed mating. Each *Six6*$^{flox/flox}$*/LHRH*$^{cre+}$ or *Six6*$^{flox/flox}$ female mouse was housed with a *Six6* $^{flox/flox}$*/LHRH*$^{cre+}$ or *Six6* $^{flox/flox}$ male mouse, and vaginal plug formation was monitored. If a plug was present, the day was noted as day 0.5 of pregnancy. Embryos were then collected at day e12.5, e13.5, e15.5, e17.5.

Fertility assessment. At 12–15 weeks of age, virgin *Six6* $^{flox/flox}$*/LHRH*$^{cre+}$ and *Six6*$^{flox/flox}$ mice were housed in pairs. The number of litters and pups produced in 90 days was recorded. Control matings used were *Six6*$^{flox/flox}$ with *Six6*$^{flox/flox}$*.*

GnRH-pituitary stimulation tests. For two weeks prior to the hormonal challenge, mice were adapted to handling stress such that they would be unaffected by stress during serial sampling. Baseline tail blood was collected from male and female metestrus/diestrus littermates. Ten minutes after receiving an *ip* injection of 1 µg/kg GnRH (Sigma #L7134) diluted in physiological saline, tail blood was collected again. For kisspeptin challenge, 15 minutes after *ip* injection of 30

nM of kisspeptin (Tocris #4243) diluted in physiological saline, tail blood was collected again. The total volume of blood collected did not exceed 100 µL. Blood was collected between 11:00 AM and 12:00 PM and was allowed to clot for 1 hour at room temperature. Blood was then centrifuged for 15 min at 2600 g. Serum was collected and stored at -20°C before Luminex analysis was used to measure LH and FSH. The assay detection limit was 0.24 ng/mL, inter-assay CV was 15.2 and intra-assay CV was 11.5.

Testosterone Analysis. For serum hormone analysis, mice were killed by isoflurane overdose and blood collected from the abdominal aorta between 9:00 and 11:00 AM. Blood was allowed to clot for 1 hour at room temperature and then centrifuged (15 min, 2600 X g). Serum was collected and stored at -20°C before RIA analysis for testosterone at the Center for Research in Reproduction, Ligand Assay, and Analysis Core, University of Virginia (Richmond, Virginia). Samples were run in singlets. All intraassay coefficients of variance (ACOVs) are based on the variance of samples in the standard curve run in duplicate. Testosterone: lower detection limit: 9.6 ng/dL, intra-ACOV 5.4% and inter-ACOV 7.8%.

Immunohistochemistry (IHC). IHC was performed as previously described (32), with the only modification being antigen retrieval by boiling the samples for 15 min in 10 mM sodium citrate, pH 6. Briefly, the primary antibody used was rabbit anti-GnRH (1:1000; Thermo Fisher Scientific, PA1-121) or rabbit anti-GnRH (1:1000; Immunostar, 20075, Lot 1037001). All GnRH staining in *Six6*$^{flox/flox}$*/LHRH*^{cre} mice was conducted using the Immunostar antibody, as previous lots used on *Six6KO* mice were no longer functional. GnRH-positive neurons were counted throughout the brain in adults, and throughout the head in embryos. The whole head was counted in embryos, and whole brain was counted in the adult from bregma 1.70 to bregma –2.80 (67). All sections were counted by an investigator blinded to the treatment/genotype. For lineage tracing in the *Six6KO* mice, tdTomato expression was detected with a rabbit anti-rfp primary antibody (1:1000;

Abcam, ab62341, Table 1). For lineage tracing in the *Six6*$^{flox/flox}$*/LHRH*^{cre} mice, β-Galactosidase was detected using anti-β-Galactosidase antibody (1:300; Abcam, ab9361).

Cell death analysis. Assays for apoptosis in e14.5 *Six6KO* mice were performed using protocols specified in the DeadEnd terminal deoxynucleotidyl transferase-mediated biotinylated UTP nick end-labeling (TUNEL) system (Sigma-Aldrich, 11684795910). Relative levels of cell death between WT and *Six6KO* mice were determined by counting the number of TUNEL+, GnRH+ cells throughout the head.

Statistical analysis. Statistical analyses were performed using either Student's t test, Mann-Whitney, or two-way ANOVA, followed by post hoc analysis by Tukey as indicated in figure legends, with p=0.05 to indicate significance. Statistical Software GraphPad Prism was used for analysis. N values represent the number of samples included in each group.

Results

Six6KO leads to GnRH neuron death

Our previous work has shown that in the global *Six6KO* mice, GnRH neurons originate normally, with the average number of GnRH neurons at e13.5 being similar in WT and KO mice (33). We also showed that adult *Six6KO* mice were missing ~90% of GnRH neurons as detected by GnRH IHC (33). It has not yet been determined however at what embryonic stage GnRH expressing neurons in *Six6KO* mice begin to disappear. Determining when GnRH neurons are lost can provide insight into the developmental mechanisms of *Six6,* and may indicate which region of the migratory pathway of GnRH is altered. To determine this, we used IHC with an anti-GnRH antibody and counted the number of GnRH neurons in late embryogenesis of *Six6KO* mice. At e15.5, there is an ~89% reduction in the number of GnRH neurons, a drastic decrease from the amount present at e13.5, where GnRH neuron numbers were normal in *Six6KO* (33) (Fig.

3.1a). The whole head was systematically analyzed for GnRH neurons, and no ectopic localization of the neurons was observed.

Thus, *Six6* is exerting some effect on or within the GnRH neuron between e13.5 and e15.5, resulting in the loss of GnRH IHC. However, historically, difficulties have arisen in defining the mechanism of GnRH neuron loss. It is possible that loss of *Six6* abolishes the expression of GnRH from this neuronal population, making these neurons undetectable using IHC with an anti-GnRH antibody. Therefore, using IHC with an anti-GnRH antibody, it is not possible to distinguish whether GnRH neurons are absent or are failing to express GnRH (26,29,169-171). Here, we assessed the mechanism engendering this loss of GnRH neurons using a *Six6*^{KO}/*Rosa*^{tdTomato}/*GnRH*^{cre} mouse. Using this mouse, we conducted lineage tracing wherein GnRH neurons express tdTomato within all of the cells targeted by *GnRH*^{cre}, regardless of GnRH expression. We have previously characterized this *GnRH*^{cre} promoter, and have found that the *GnRH*^{cre} allows recombination at e13.5 (32). Assessing the *Six6*^{KO}/*Rosa*^{tdTomato}/*GnRH*^{cre} mouse with IHC at e13.5, we show that tdTomato neurons are generated normally compared to control mice (as was seen in the *Six6KO* mouse at e13.5) and are successfully labeled with tdTomato (Fig. 3.1b). The lineage tracing in the adult mouse showed the presence of tdTomato neurons in the *Rosa*^{tdTomato}/*GnRH*^{cre} mouse, but a loss of ~96% of GnRH neurons in the *Six6*^{KO}/*Rosa*^{tdTomato}/*GnRH*^{cre} mouse. Thus, the loss of GnRH neurons in the *Six6KO* mouse model is not due to a loss of GnRH expression when *Six6* is removed from the whole body, but rather to loss of GnRH cells themselves.

Using lineage tracing, we discovered that the GnRH neurons in the *Six6KO* model were in fact absent, and therefore we next asked whether their absence was the product of apoptosis. This was assessed using the TUNEL technique to test for DNA fragmentation in cells *ex vivo*. Analysis was conducted using double labeling with an antibody for GnRH neurons and the TUNEL assay. In e14.5 mice, only a few apoptotic cells were seen in the WT mice (9 ± 2), whereas a

significantly greater number (240 ± 33), were observed in the KO mice (Fig. 3.1c). Therefore, the actions of *Six6* in the global knock-out mouse model resulted in apoptosis of GnRH neurons, either through effects in the environment of the GnRH neuron, or within the GnRH neurons, or both. The specific role of *Six6* within the GnRH neuron cannot be discerned without creating a separate mouse model, the *Six6*$^{flox/flox}$*/LHRH*^{cre} mouse.

Removal of *Six6* specifically within the GnRH neuron decreases GnRH neuron number

It is possible that the loss of GnRH neurons in *Six6KO* mice at e15.5 was due to a lack of *Six6* expression within GnRH neurons, opposed to being due to the loss of *Six6* expression in the cellular environment through which GnRH neurons migrate. Thus, to determine this, we moved from using a global knockout, to a *Six6*^{flox} mouse generated in our laboratory (Fig. 3.2a). We crossed this mouse with *LHRH*^{cre} mice (Fig. 3.2a) (66), allowing for specific deletion of *Six6* in GnRH neurons (56,57,172,173). GnRH-expressing neurons were counted in adult *Six6*$^{flox/flox}$*/LHRH*^{cre} mice. In the *Six6*$^{flox/flox}$*/LHRH*^{cre} mouse, the number of GnRH neurons began declining in early embryogenesis, at e13.5, with significantly fewer GnRH neurons seen in the Cre+ mouse compared to control (90% reduction) (Fig. 3.2b). This trend continued into late embryogenesis (Fig. 3.2c) and adulthood (Fig. 3.2d), with Cre+ mice having 90% fewer GnRH neurons than control mice at e17.5 and P56.

Loss of *Six6* within the GnRH Neuron Causes Infertility

The propensity of *Six6*$^{flox/flox}$*/LHRH*^{cre} males and females to copulate was measured in a plugging assay. While all the control females were plugged by day three when paired with control males, it took significantly longer for male *Six6*$^{flox/flox}$*/LHRH*^{cre} mice to plug control females, and for *Six6*$^{flox/flox}$*/LHRH*^{cre} females to be plugged by control males (Fig. 3.3a). In this assay one Cre+ female was plugged by a control male, and one Cre+ male plugged a control female. The rest of the Cre+ mice did not plug during the duration of the assay, in contrast to the control matings

which all plugged by day 4 of the assay. The ability of *Six6*$^{flox/flox}$*/LHRH*^{cre} mice to reproduce was assessed via a 90-day fertility assay (Fig. 3.3b). In this assay, all of the control matings produced litters by the end of the 90-day assay, with most producing 3 litters during this period of time (Fig. 3.3b). Female *Six6*$^{flox/flox}$*/LHRH*^{cre} mice when mated with control mice did not produce any litters in the three-month period, and neither did male *Six6*$^{flox/flox}$*/LHRH*^{cre} mice when mated to control females (Fig. 3.3b). Thus, *Six6*$^{flox/flox}$*/LHRH*^{cre} mice are severely impaired in their ability to produce litters.

Decreased levels of GnRH can also result in delayed or absent puberty (a characteristic of IHH), therefore we assessed whether the *Six6*$^{flox/flox}$*/LHRH*^{cre} mice had altered onset of puberty, as assessed by determining preputial separation in the males and vaginal opening in the females. Control male mice underwent preputial separation at 29 ± 0.40 days, and control female mice underwent vaginal opening at 30 ± 0.32 days; the onset of puberty was significantly delayed in both sexes of *Six6*$^{flox/flox}$*/LHRH*^{cre} mice, with male mice undergoing preputial separation at 45 ± 6.4 days and females vaginal opening at 57 ± 6.0 days (Fig. 3.3c, d).

Loss of *Six6* within the GnRH neuron results in hypogonadism

We next sought to determine whether the deficiency in GnRH seen in the *Six6*$^{flox/flox}$*/LHRH*^{cre} would affect gonadal development. We observed a drastic effect on testicular development with Cre+ testicles being ~1/4 the size of control testicles (Fig. 3.4a). No sperm were present inside Cre+ testicles (Fig. 3.4b). Developmental impairment of Cre+ testes structures provides an explanation for the infertility seen in the *Six6*$^{flox/flox}$*/LHRH*^{cre} mice. Testicular development relies on LH and FSH release from the pituitary in response to GnRH (174). Thus, we measured LH and FSH levels, with lower LH and FSH serum levels observed in Cre+ mice compared to control mice (Fig. 3.4c, d). Testosterone was also measured with no statistically significant difference between genotypes. (Fig. 3.4e).

Female gonadal development was similarly affected by the loss of GnRH neurons, however, not as drastically as the males, with the size of *Six6*$^{flox/flox}$*/LHRH*^{cre} ovaries being significantly smaller at ~30% the size of control ovaries (Fig. 3.5a). Ovarian histology revealed a significant reduction in the number of corpora lutea in *Six6*$^{flox/flox}$*/LHRH*^{cre} mice (Fig. 3.5b). The absence of corpora lutea indicates abnormal progression through the estrous cycle and absence of an LH surge. To further assess the ability of *Six6*$^{flox/flox}$*/LHRH*^{cre} females to progress though the estrous cycle given their paucity of GnRH neurons, vaginal smears were collected from 3.5-month-old *Six6*$^{flox/flox}$*/LHRH*^{cre} females and littermates for 10 days. While all control females cycled at least twice during this time frame, only one Cre+ mouse completed a cycle during this period (Fig. 3.5c). *Six6*$^{flox/flox}$*/LHRH*^{cre} mice spent the duration of the sampling assay in diestrus, with only one mouse moving into estrous (Fig. 3.5c, d).

To better understand the hormonal milieu producing this non-cyclic phenotype in the *Six6*$^{flox/flox}$*/LHRH*^{cre} mice, we assessed the levels of gonadotropins. Indeed, circulating diestrus LH levels were reduced in Cre+ females compared with control females; however, no difference was seen in FSH (Fig. 3.6a and 3.6b). This reduction in LH is reflective of the deficiency in GnRH neurons in the *Six6*$^{flox/flox}$*/LHRH*^{cre} mice. Finally, to confirm that the lack of circulating LH and FSH is due to a lack of GnRH, and not a defect in LH/FSH release at the pituitary, we performed GnRH and Kisspeptin challenges. As expected, an increase from basal LH was induced in response to an injection of GnRH in both genotypes (Fig. 3.6c). A kisspeptin challenge was then conducted to determine whether the population of GnRH neurons in the *Six6*$^{flox/flox}$*/LHRH*^{cre} mice is sufficient to mount an LH response when stimulated by kisspeptin. We did see an increase in the release of LH in the control mice in response to kisspeptin, however, there was no statistical difference in the LH levels detected before and after kisspeptin injection in the *Six6*$^{flox/flox}$*/LHRH*^{cre} mice (Fig. 3.6d), although the fold change in LH release appeared comparable (Fig. 3.6d).

Loss of *Six6* in *Six6$^{flox/flox}$/LHRH^{cre}* neurons results in the loss of GnRH expression

In the *Six6$^{flox/flox}$/LHRH^{cre}* mice, ~90% of GnRH neurons are undetectable by GnRH IHC. When GnRH neuron counting was conducted, the entire head of embryos were collected and analyzed for off-path GnRH neurons. None were discovered, indicating that mis-migration does not appear to be the source of the missing GnRH neurons. To discern the mechanism for the absence of GnRH neurons seen in the *Six6$^{flox/flox}$/LHRH^{cre}*, lineage tracing was conducted using *Six6$^{flox/flox}$/Rosa^{LacZ}/LHRH^{cre} mice*. In these mice, the GnRH neurons are labeled with LacZ for the duration of the life of the neuron, regardless of GnRH expression due to the early onset of *LHRH^{cre}* expression recombining the *Rosa^{LacZ}* alelle. The number of GnRH neurons were counted at e12.5 and e17.5, with equivalent number of LacZ-positive neurons being seen between genotypes at both ages in the *Six6$^{flox/flox}$/Rosa^{LacZ}/LHRH^{cre}* and *Rosa^{LacZ}/LHRH^{cre}* mice (Fig. 3.7a, b). Therefore, GnRH neurons are present in the *Six6$^{flox/flox}$/LHRH^{cre}* mouse; but are not expressing GnRH.

Discussion

Six6 is essential in the maturation of GnRH neurons, and has separate functions within and outside of the GnRH neuron

Homeodomain transcription factors have been found to be modulators of GnRH neuron migration and development. Several factors such as *Six3*, *Vax1*, and *Otx2* have been associated with both GnRH neuron maturation, and infertility (32,33,56,58). *Six6* is a key homeodomain transcription factor that was shown to be essential in the maintenance of fertility and GnRH neuron development (33). Given the complex nature of reproduction, with multiple organs, hormones, and developmental mechanisms working together to maintain fertility, complications can arise at multiple levels (4,92,166,175,176). Infertility originating at the level of the GnRH neuron can be due to lack of gene expression, defects in development, or disruption in migration (28,177). In this

study, we determine the essential role of *Six6* in GnRH neurons, and therefore in the maintenance of fertility.

Our study reveals that *Six6* is essential within the GnRH neuron and externally to the GnRH neuron, in determining the fate of GnRH neurons. Using a whole body *Six6KO* mouse, we have found that the expression of *Six6* in early embryogenesis (e13.5) is not necessary for the generation of GnRH neurons but is essential in maintaining the survival of this population into adulthood. Additionally, we compared the fate of GnRH neurons in the *Six6KO* mouse, with the fate of GnRH neurons in a mouse with conditional deletion of *Six6* specifically within the GnRH neuron. In this $Six6^{flox/flox}/LHRH^{cre}$ mouse, we found that *Six6* is not needed within the GnRH neuron to generate this neuronal population or for its migration or survival, but it is needed to maintain GnRH expression. In comparing these two mouse models, we see differences in the mechanisms of loss of GnRH neurons. Interestingly, in the whole-body *Six6KO* model GnRH neurons are lost due to apoptosis, whereas in the $Six6^{flox/flox}/LHRH^{cre}$ mouse, GnRH neurons are present but lack GnRH expression. Therefore, *Six6* has separate and distinct roles within the GnRH neuron itself and within the environment of the GnRH neuronal migratory pathway. *Six6* is expressed along the entire migratory route of the GnRH neuron, from the olfactory placode to the olfactory bulb, and also in the hypothalamus. It is likely that in the Six6KO mouse, Six6 could be exerting its effects on the survival of GnRH neurons at some point along this route (41,43).

Six6 is essential for maintenance of the GnRH neuron population

Our goal in completing this study was to illuminate the role of Six6 in the maintenance of GnRH neurons, and therefore in the maintenance of fertility. GnRH neurons are essential in regulating fertility, pregnancy, puberty, and numerous other physiological life functions (1,92). GnRH neurons are a key regulator of the HPG axis, thus when this neuronal population is compromised, the entire HPG axis is disrupted and infertility ensues (1,93). GnRH neurons must properly originate, develop, mature, and migrate from the nose into the brain and down into the

hypothalamus (25). Mis-migration of GnRH neurons results in GnRH being released outside of the hypophyseal portal system and therefore it is never received by the pituitary to stimulate the HPG axis (93,177). Furthermore, either death of GnRH neurons or the loss of GnRH expression will similarly result in insufficient hormone production from the HPG axis (178). Here, we have identified the essential role that *Six6* plays in maintaining the integrity of the GnRH neuron population.

In the environment of the GnRH neuron, *Six6* is necessary for the survival of GnRH neurons, as determined in the *Six6KO* mouse model. The entire population of GnRH neurons can be seen in early embryogenesis at e13.5, but ~90% of this neuronal population is lost by e15.5. Therefore, *Six6* must play a role in maintaining the neuronal population between e13.5 and e15.5. Studies of the role of *Six6* in the eye have shown that the global loss of SIX6 results in early exit from the cell cycle of retinal progenitor cells resulting an absence of retinal ganglion cells, the terminally differentiated cell of this lineage (40). Six6 is known to be expressed in the hypothalamus at e11.5 and e15.5 and may be acting in this region to exert its effects on the survival of GnRH neurons (41). Further studies of *Six6* in development suggest its involvement in reduced proliferation, and increased apoptosis (40). It is believed that SIX family proteins may serve as a nexus point for the balance between proliferation and cell death in the development of tissues (148). Indeed, studies of *Six3*, a very closely related homeodomain transcription factor to *Six6*, demonstrate a role for *Six3* in the proliferation of olfactory tissues (84). The absence of *Six3* has also been associated with apoptosis in mice in the anterior neural plate and in neuroretinal cells (149,153). Additional evidence of the essential role of SIX3 in the survival of cells, has been seen in medeka fish and in drosophila, wherein mutations in the *Six3* homolog resulted in massive cell death (154). Thus, our work here bolsters the evidence that *Six6* is a key regulator in cell death.

The Role of Six6 in the Development of GnRH neurons

Previously, it was identified that *Six6* was essential in maintaining GnRH neurons in mice using a Six6KO mouse (33). Identifying this essential role of *Six6* led us to question what the actions of Six6 within the GnRH neuron are during development. To understand the role of *Six6* within GnRH neurons in development, we generated *Six6*^{flox} mice and crossed them with *LHRH*^{cre} mice. By comparing both of these mouse models, we can ascertain what contribution SIX6 has within the GnRH neuron, to previously identified hypogonadism and infertility. Deletion of *Six6* within GnRH neurons resulted in a reduction in the number of detectable GnRH neurons equivalent to that seen in the *Six6KO*. One notable difference is in the fate of GnRH neurons in these two mouse lines. In contrast to the death of GnRH neurons observed by lineage tracing in *Six6KO* mice, the *Six6*$^{flox/flox}$*/LHRH*^{cre} mice show that a loss of SIX6 abolishes GnRH expression. GnRH neurons in the *Six6*$^{flox/flox}$*/LHRH*^{cre} mice remain alive, and migrate correctly to the hypothalamus; however, they no longer express GnRH. Therefore, *Six6* is required for both the survival of GnRH neurons and for the maintenance of GnRH expression. Comparison of these two mice highlights the complexity of the transcription factor network regulating the GnRH neuron system.

The discrepancy in the fate of GnRH neurons in these two mouse models is interesting and adds to the growing knowledge of the roles transcription factors play in the development and fate of GnRH neurons. *Otx2* for example has been identified as an essential transcription factor in the maintenance of GnRH neurons, as removal of *Otx2* from within the GnRH neuron resulted in apoptosis of GnRH neurons (56). In contrast, *Six3* has been identified as mediating the proper migration of GnRH neurons but not within the neurons for GnRH gene expression (84). Furthermore, another transcription factor, *Vax1*, has been identified as essential within this neuronal population for maintained GnRH expression (57). The GnRH neuron system is redundant in that many neurons can be lost before a reproductive phenotype is observed (129).

Despite this redundancy, the GnRH neuron system can still be compromised as there are numerous mechanisms that may disrupt GnRH signaling (4,93,124,165,166). Our research adds to the current knowledge of GnRH neuron development and GnRH signaling by illuminating the necessity of *Six6* in the expression of GnRH and in the survival of GnRH neurons.

In addition to adding to our current knowledge of the transcription network that controls GnRH neurons, our work provides insight into the development of GnRH neurons. Gonadotropin-releasing hormone (GnRH) neurons originate in the nasal placode and migrate along a carefully orchestrated journey out of the placode and across the cribriform plate (36,54,92,177,179). They then turn caudally to move down into the hypothalamus during prenatal development (36,54,92,177,179). This route is delineated in part by the axonal projections that GnRH neurons attach to and migrate along, and in part by guidance and chemosensory cues (7,89,180). Disruptions in their guidance or movement result in IHH (4). When such a disruption is located in the nasal epithelium, the development of olfactory structures is disrupted, resulting in the IHH subtype Kallmann syndrome (4). Recent work has focus on the role of transcription factors (e.g. *Vax1, Otx2, Dlx1/2,* and *Six3*) in this journey and has utilized mouse models to illuminate the intricate mechanisms at play in the successful migration and development of GnRH neurons (32,57,58,84,97,110). Our work demonstrates the essential role of *Six6* in this process and illuminates the involvement of the *Six6* homeodomain transcription factor in the survival of GnRH neurons, and in the proper transcription of GnRH. Adding Six6 to the list of factors that influence GnRH neuron development and expression illuminates our understanding of the trajectory of GnRH neurons.

Removal of *Six6* from the GnRH neuron results in the loss of GnRH expression

Through lineage tracing of the *Six6KO* and *Six6*$^{flox/flox}$*/LHRH*^{cre} mice, we identified that SIX6 plays a crucial role in the expression of GnRH, and also in the survival of GnRH neuron.

Furthermore, it demonstrates that *Six6* is unique in that it a transcription factor that has been identified to be involved in both expression of GnRH and survival of GnRH neurons. Discrepancies in our global knock-out mouse model, and the GnRH-specific knock-out mouse model provide interesting insight into contribution of *Six6* to the proper signaling and development of GnRH neurons. We showed that *Six6$^{flox/flox}$/LHRH^{cre}* mice exhibited a loss of detectable GnRH neurons as early as e13.5, with ~ 70% of GnRH neurons lacking expression of GnRH at this early stage of embryogenesis. In contrast, in the *Six6KO* mouse, GnRH neurons were not lost until ~e14.5. As GnRH neurons die at this early stage in the *Six6KO* mouse, it is unknown whether GnRH expression is also inhibited in the whole-body KO after e13.5. However, given that GnRH neurons are present and expressing GnRH at e13.5 in the *Six6KO* mouse, it is clear that GnRH expression is not decreased at e13.5 as it is in the *Six6$^{flox/flox}$/LHRH^{cre}* mouse. Therefore, it is possible that GnRH expression is not lost in the global KO model because some extrinsic factor compensates for the reduction in SIX6. Additionally, Six6 may have additional actions within the environment of the neuron that modulate GnRH expression.

The loss of expression when *Six6* is removed from the GnRH neuron in the *Six6$^{flox/flox}$/LHRH^{cre}* mouse can be explained because *Six6* has been shown to bind to conserved ATTA sites within the rat GnRH enhancer and promoter (33). Additionally, *Six6* is known to regulate the expression of GnRH via binding to ATTA sites in the promoter (33). Past studies have shown that overexpression of *Six6* in GnRH neuronal cell lines correlated with increased expression of GnRH (33,57). Thus, the removal of *Six6* decreased the expression of GnRH.

Infertility in *Six6$^{flox/flox}$/LHRH^{cre}* mice originates at the GnRH neuron

To confirm that the reproductive deficiency of *Six6$^{flox/flox}$/LHRH^{cre}* mice arises at the level of GnRH neurons, we challenged females with injections of GnRH. The fact that *Six6$^{flox/flox}$/LHRH^{cre}* mice could elicit a response to an injection of GnRH indicates a functioning

and responsive pituitary. Additionally, this confirms that low gonadotropin levels in the *Six6*$^{flox/flox}$*/LHRH*^{cre} mice were not due to a lack of responsiveness of the pituitary to GnRH, but to insufficient GnRH input to the pituitary. Thus, we identified the source of infertility in the *Six6*$^{flox/flox}$*/LHRH*^{cre} mouse model to be the lack of GnRH expression at level of the hypothalamus. Although the fold change of LH in response to Kisspeptin in the *Six6*$^{flox/flox}$*/LHRH*^{cre} mice was similar to that of the control mice, there was no statistical difference between the LH levels before and after the kisspeptin injection in the *Six6*$^{flox/flox}$*/LHRH*^{cre} mice. It is important to note that in this experiment we are using extra-physiological levels of kisspeptin in the ip injection, and thus probably stimulated GnRH release from all the remaining terminals, allowing LH to be released despite the paltry number of GnRH neurons remaining in the *Six6*$^{flox/flox}$*/LHRH*^{cre} mice.

It has been demonstrated that there is great redundancy within the GnRH neuron system (129). Male mice have been found to be fertile with as few as 12% of their GnRH neurons (129). The requirement for females is decidedly higher with aspects of fertility being compromised when the number of GnRH neurons is reduced to 34% of the normal population (129). The *Six6*$^{flox/flox}$*/LHRH*^{cre} mice have ~50 GnRH neurons, and thus are left with less than 10% of the normal population of GnRH neurons. Thus, the fertility impairment in the *Six6*$^{flox/flox}$*/LHRH*^{cre} females is expected; however, in the case of the males, their deficit hovers around the precipice of the number of GnRH neurons required for fertility. In this case, the severe male infertility is somewhat surprising, although there was one male mouse that was fertile, with one male successfully plugging and impregnating a control female mouse. Therefore, our findings provide further knowledge of the GnRH neuron requirement for fertility, as we have demonstrated that *Six6*$^{flox/flox}$*/LHRH*^{cre} males reduced to only ~50 GnRH neurons are in most cases severely infertile.

IHH is engendered by GnRH deficiency, which can result from alterations in the migration, development, and/or survival of GnRH neurons (2,4,93). Such disruptions in the levels of GnRH can also impair a multitude of physiological functions including fetal development, pregnancy,

puberty, and menopause (1,2,93). It is likely that through identification and understanding of the rare genetic variants that underlie GnRH deficiency, we may be able to illuminate mechanisms behind precocious or delayed puberty. Despite the important ramifications of GnRH deficiency, there is much still to learn about the regulation of the GnRH neuron. The work presented here provides insight into the development and maturation of GnRH neurons, and the dependence of these neurons on the transcription factor *Six6*.

Acknowledgements

The authors thank Jason D. Meadows for technical assistance on this project. This work was supported by National Institutes of Health grants R01 HD082567 and R01 HD072754 (to P.L.M.) and by National Institute of Child Health and Human Development/National Institutes of Health P50 HD012303 as part of the National Centers for Translational Research in Reproduction and Infertility (P.L.M.). P.L.M. was partially supported by P30 DK063491, P42 ES101337, and P30 CA023100. E.C.P. was partially supported by National Institutes of Health R25 GM083275 and National Institutes of Health F31 HD098652.

Chapter 3 is currently being prepared for submission for publication of this material. Pandolfi, Erica C.; Hoffmann, Hanne M.; Mellon, Pamela L. The dissertation author is the primary investigator and author of this material. Dr. Hoffman created the *Six6flox* mouse helped with preparation of the manuscript. Pamela Mellon supervised the project and provided advice.

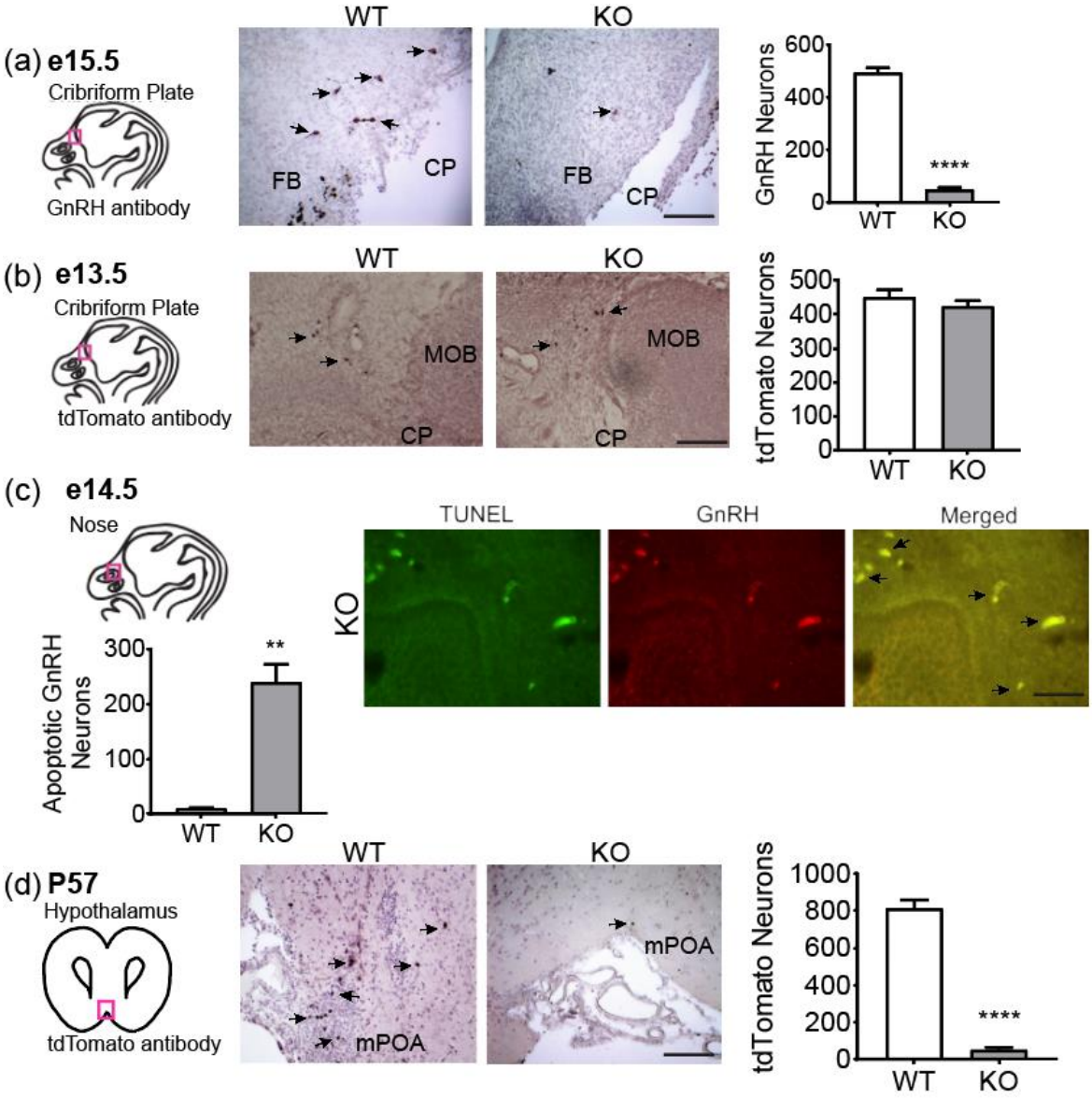

Figure 3.1. GnRH Neurons in *Six6KO* mice are lost to apoptosis at e14.5. **a,** IHC with anti-GnRH antibody at e15.5 in *Six6KO* mice (n = 3). **b,** Double-IHC with TUNEL and anti-GnRH antibody (n = 4). Scale bar, 20 µm. **c,** Number of tdTomato+ neurons quantified from IHC with anti-RFP antibody in *Six6*^{KO}/*Rosa*^{tdTomato}/*GnRH*^{cre} mice at e13.5 (n = 3). **d,** Number of tdTomato+ neurons quantified from IHC with anti-RFP antibody in *Six6*^{KO}/*Rosa*^{tdTomato}/*GnRH*^{cre} mice at P57 (n = 4). Arrowheads indicate tdTomato+ neurons. **(a)-(c)** Statistical analysis was by Student's t-test as compared with control mice. FB, forebrain. Scale bar, 100 µm. **, $p < .01$; ****, $p < .0001$.

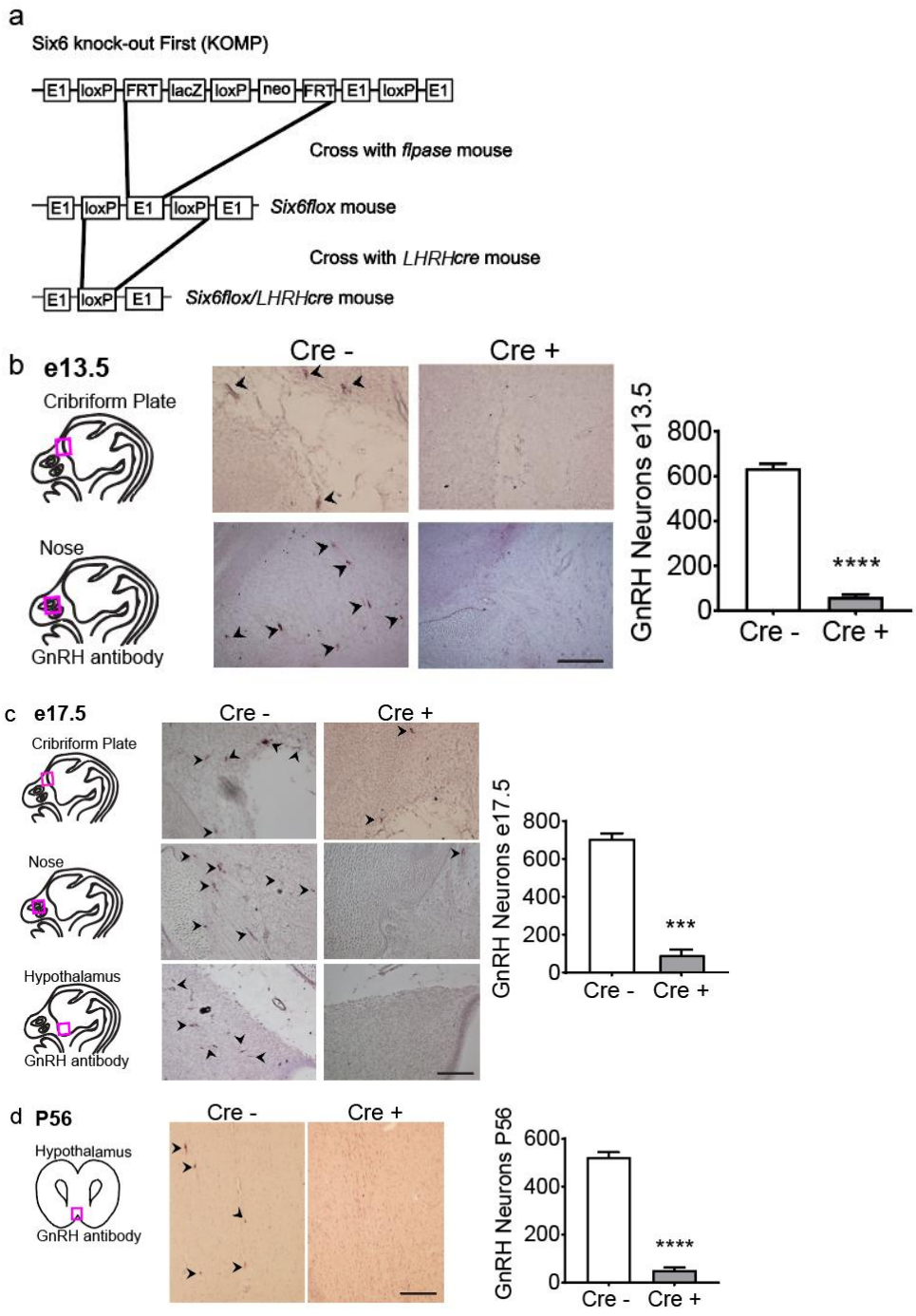

Figure 3.2. Loss of *Six6* specifically from the GnRH neuron results in a loss of ~90% of GnRH neurons. **a,** Creation of the *Six6*$^{flox/flox}$*/LHRH*^{cre} mouse. **b,** GnRH neurons at e13.5 in *Six6*$^{flox/flox}$*/LHRH*^{cre} mice (n = 3-4). **c,** Quantification of GnRH neurons at e17.5 from IHC with anti-GnRH antibody (n = 3-4). **d,** GnRH neurons in the adult at P56 *Six6*$^{flox/flox}$*/LHRH*^{cre} mouse (n = 3). **(b-d)** Drawings to the left of images represent locations in the head/brain where images were taken. Scale bar, 100 μm. Statistical analysis was by Student's t test as compared with control mice. CP, cribriform plate. ***, $p < .001$; ****, $p < .0001$.

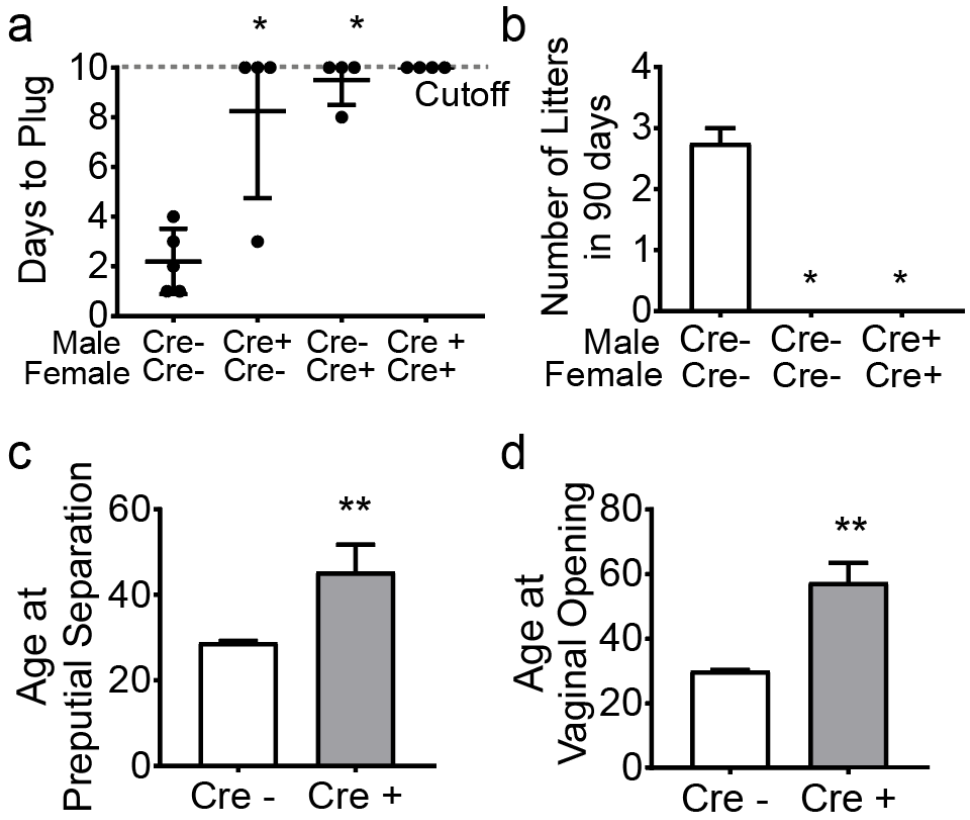

Figure 3.3. *Six6$^{flox/flox}$/LHRH^{cre}* mice have disrupted fertility and delayed puberty. **a,** Ten-day plugging assay of Cre+ and Cre- mice at 3 months of age, as compared to Cre- x Cre- mating (n = 3), statistical analysis by Mann-Whitney test. **b,** Number of litters produced in 90-day fertility assay between Cre+ and Cre- mice, as compared to Cre- x Cre- mating (n = 3-6). **c,** Onset of preputial separation in male mice was measured from day 20 until pubertal onset (n = 3). **d,** Onset of vaginal opening was measured from day 20 until pubertal onset (n = 3). **(b-d)** Data were analyzed by Student's t test as compared with control. *, $p < .05$; **, $p < .01$.

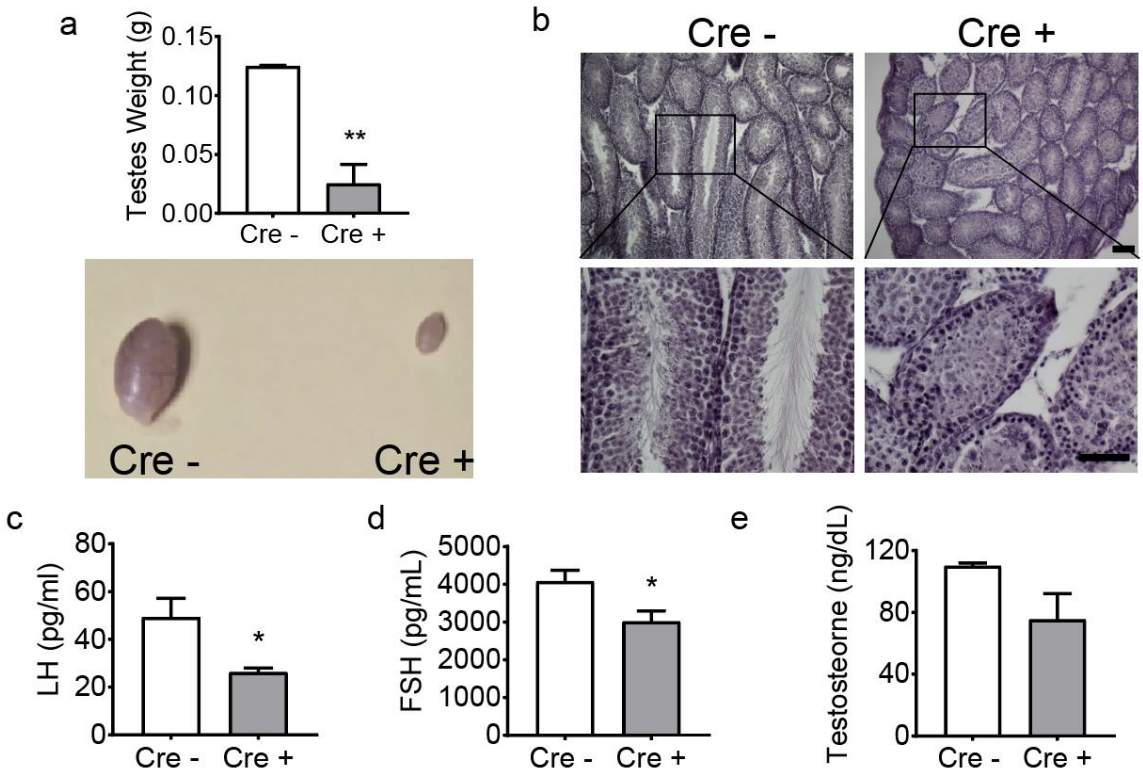

Figure 3.4. *Six6*$^{flox/flox}$*/LHRH*^{cre} male mice are hypogonadal and hypogonadotropic. **a,** Testicular weight of Cre- and Cre+ mice (n = 3). **b,** Images of H&E stained Cre- and Cre+ testicles. **c,** Serum was collected from adult male mice and assayed for LH (n = 5-6) and **(d)** FSH (n = 5-6), and **(e)** testosterone (n=4-7). **f,** Images of testicles from Cre- and Cre+ mice. Scale bar, 1cm. All data were analyzed by Student's t test as compared with control. Scale bar, 100 μm. **, $p < .01$.

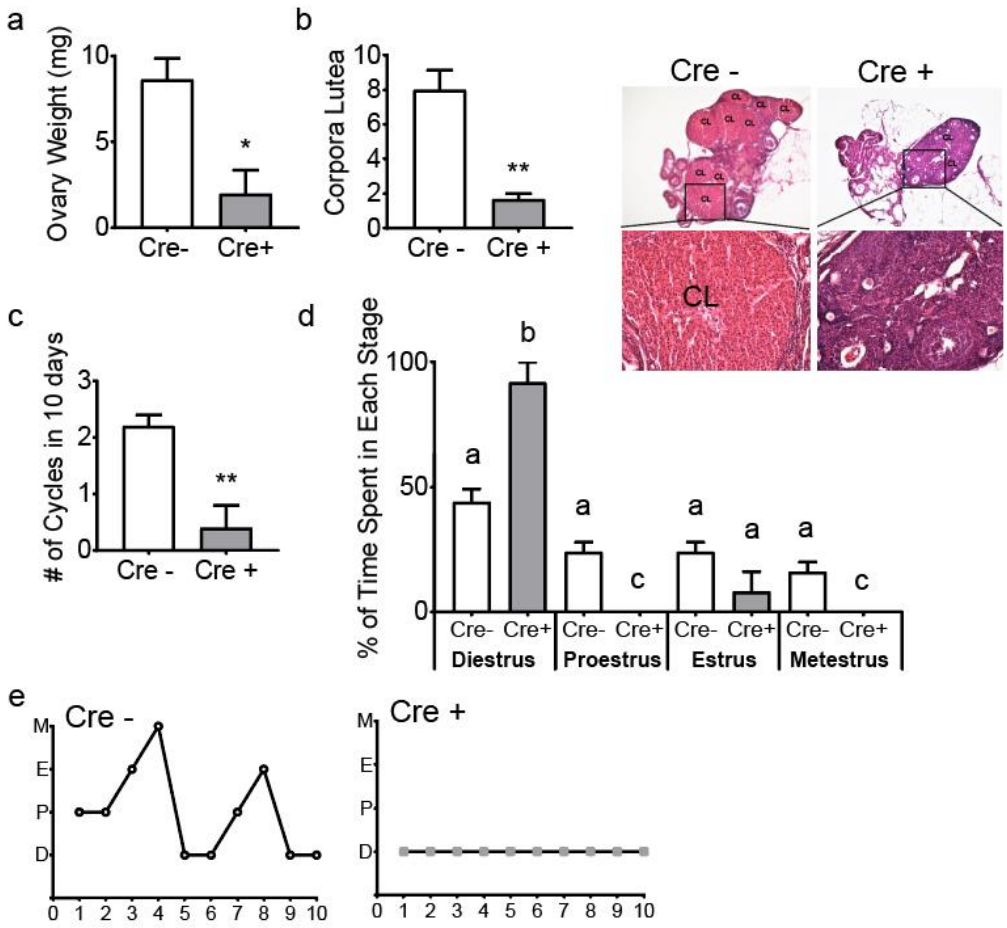

Figure 3.5. *Six6*$^{flox/flox}$*/LHRH*^{cre} female mice are hypogonadal and non-cyclic. **a,** Ovarian weights of Cre- and Cre+ mice (n = 3). **b,** Number of corpora lutea in Cre- and Cre+ mice (n=3). Images of H&E stained ovaries. **c,** Estrous cycle was monitored daily in Cre- and Cre+ mice. The number of complete cycles in 10 days was recorded (n=5). **(a-c)** Data were analyzed by Student's t test as compared with control. **d,** The number of days spent in each stage of the estrous cycle was recorded (n = 5). Different letters indicate statistical difference by two-way ANOVA followed by Tukey post hoc. **e,** Representative cycles from one Cre- and one Cre+ mouse. D, diestrus; P, proestrus; M, metestrus; E, estrus. Scale bar, 100 µm. *, $p < .05$; **, $p < .01$.

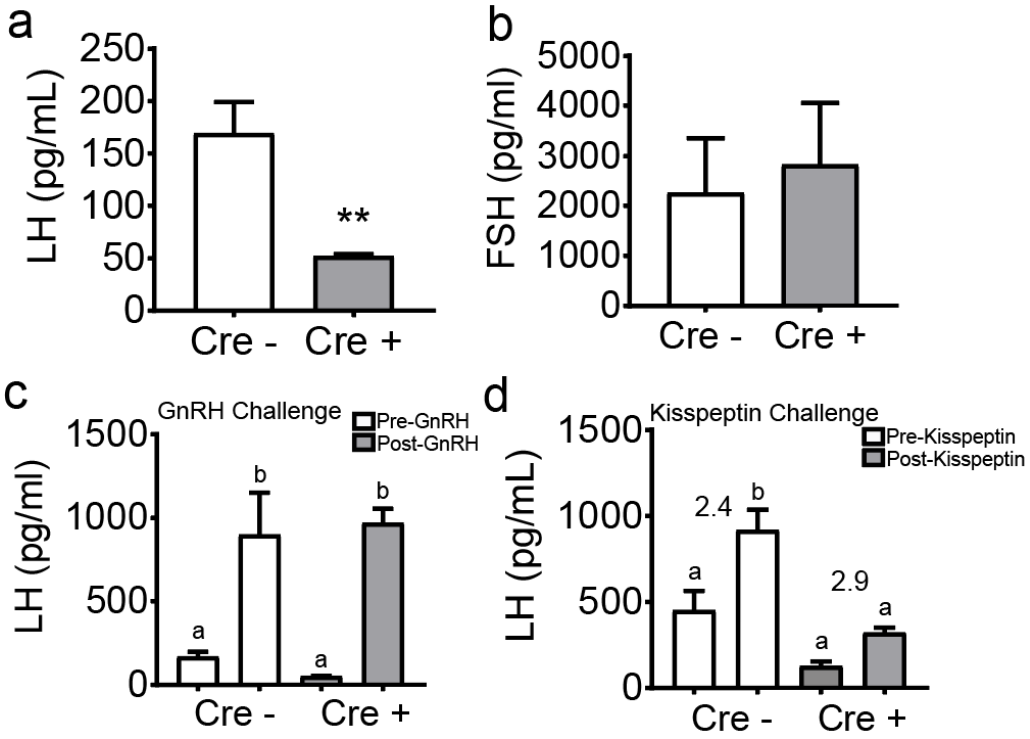

Figure 3.6. *Six6*$^{flox/flox}$*/LHRH*^{cre} females are hypogonadotropic due to deficient GnRH. **a,** Serum was collected from adult female diestrus mice and assayed for **(a)** LH (n = 5-6) and (B) FSH (n = 5-6). **(a, b)** Statistical analysis was by Student's t test as compared with Cre-. **c,** Serum LH was measured immediately prior to, and 10 minutes after a single GnRH challenge in Cre- and Cre+ diestrus females (n = 5-6). Numerical values included on the graphs indicate the average fold-change of Cre- and Cre+ mice LH in response to GnRH injections. **d,** Serum LH was measured prior to and 15 minutes after a single Kisspeptin challenge in Cre- and Cre+ diestrus females (n = 5-6). Numerical values included on the graphs indicate the average fold-change of Cre- and Cre+ mice LH in response to kisspeptin injections. **(c, d)** Different letters indicate statistical difference by two-way ANOVA followed by Tukey post hoc. **, P < .01.

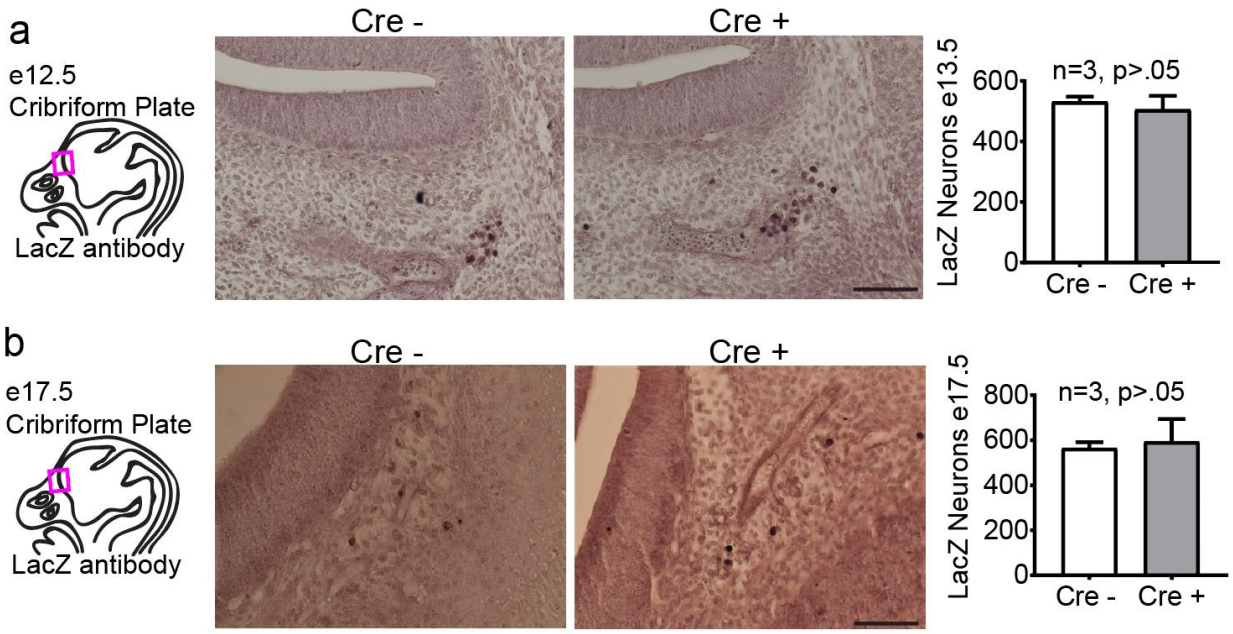

Figure 3.7. Lineage tracing in *Six6^{flox}/Rosa^{LacZ}/LHRH^{cre}* mice identify a lack of GnRH expression in GnRH neurons. **a,** Lineage tracing using LacZ to mark GnRH neurons regardless of GnRH expression show LacZ-positive GnRH neurons at e12.5. **b,** LacZ-positive neurons in the adult. OB, olfactory bulb; CP, cribriform plate; MPOA, medial preoptic area. Scale bar, 100 µm.

Chapter 4: Ectopic Expression of the *GnRHcre* Produces Phenotypes Not Mediated Through the GnRH Neuron when *Six6* is Exclusively Deleted Within the GnRH Neuronal Population

Abstract

Cre-lox technology has become widely utilized and the findings of this research continues to guide the course of scientific discovery. However, complications with cre recombinase can include off-target expression, the possible cytotoxicity of cre expression, germline recombination, inefficient gene deletion, or non-specific cre expression; all of which can result in the experimenter reaching erroneous conclusions. The pitfalls of this incredibly useful technology have been enumerated however individual cre recombinase mouse lines must be investigated to assess the extent of these pitfalls. Recent research has identified off-target expression of the frequently used gonadotropin-releasing hormone (GnRH) promoter driven cre expressing mouse line ($GnRH^{cre}$). In this project, we used $Six6^{flox}/GnRH^{cre}$ mice to assess the extent of off-target expression and to determine whether this expression could lead to erroneous conclusions. We accomplished this by comparing results from the $Six6^{flox}/GnRH^{cre}$ line with previously obtained results from $Six6^{flox}/LHRH^{cre}$ mice (a mouse line without known ectopic expression). We found that ectopic expression in the eye is severe enough to result in blindness, and that ectopic expression within the SCN results in erratic circadian rhythms. These results confirm the ectopic expression of the $GnRH^{cre}$ mouse and raise concerns for it use and the interpretation of previously published results.

Introduction

Conditional gene deletion in mice via the cre-lox system is a commonly used powerful tool that can identify the cell or tissue specific role of genes in certain diseases or physiological processes (181). These approaches can be used alone to determine a gene's function within a certain tissue or can be compared to a full-body "knock-out" (KO) mouse. The construction of a conditional knock-out mouse is achieved by breeding a "flox" strain containing two 34 bp loxP sequence elements flanking the gene region of interest, with a cre strain that expresses the bacteriophage-derived cre recombinase (181). While this system is advantageous for isolating the effects of a gene within a particular cell type, it has its drawbacks. Limitations of cre-lox technology include the possible cytotoxicity of cre expression (182), germline recombination (19,183), inefficient gene deletion, or non-specific cre expression (181,184,185); all of which can result in the experimenter reaching erroneous conclusions. Another potential weakness in the cre-lox system is that the precision of cre expression is variable depending on where the cre transgene inserts (186). Avoiding these limitations can be managed by identifying recombination using PCR, and by locating ectopic expression by identifying the expression of a reporter gene such as a ROSA26-driven reporter (57,187,188).

Recent studies have identified several of these deficiencies in a frequently used gonadotropin-releasing hormone (GnRH) promoter driven CRE expressing mouse line (66). This cre-expressing vector specifically targets GnRH neurons, a neuronal population located at the apex of the hypothalamic-pituitary-gonadal axis. GnRH neurons act through this axis to control a multitude of physiological functions including reproduction, menstruation, pregnancy, and menopause (179). As part of this axis, GnRH is synthesized in the hypothalamus and then stimulates the release of luteinizing hormone (LH) and follicle-stimulating hormone (FSH) from the anterior pituitary, these hormones in turn will act on the gonads to produce testosterone, estrogen, and progesterone in the process of gametogenesis (163,164). Before releasing GnRH

into the hypophyseal blood stream, GnRH neurons must complete a long migratory journey (25). GnRH neurons originate in the olfactory placode at embryonic day (e) 11.5, migrate across the cribriform plate, and through the basal forebrain before arriving in the presumptive hypothalamus (25). Once in the hypothalamus, GnRH neurons will extend their axons to the median eminence (ME) where GnRH will enter the hypophyseal portal system and reach the pituitary (143).

Using a *GnRH^{cre}* can determine the contribution of a gene to the functioning of the HPG axis, and also to the maintenance of fertility. The popularly utilized *GnRH^{cre}* mouse was generated by inserting the mouse 3.4 Kb promoter to drive Cre recombinase expression in all GnRH neurons (66). In addition to those intended GnRH neurons, some ectopic expression was identified (66). There is however, another Cre that targets the GnRH neuron, the *LHRH^{cre}* mouse. The *LHRH^{cre}* mouse is derived from a mouse bacterial artificial chromosome containing the Gnrh1 gene driving Cre expression being inserted into the genome (19). This results in only 96% of GnRH neurons expressing Cre; however, there is no identified off-target expression (19). These two cre-expressing vectors must be compared to determine whether the ectopic expression of the *GnRH^{cre}* may lead the experimenter to reach erroneous conclusion. Given the ectopic expression in the *GnRH^{cre}* mouse, we sought to investigate a gene that is essential both within and without the GnRH neuron.

Six6 has been identified as a key neuronal regulator in fertility through studies using a *Six6^{flox}/LHRH^{cre}* mouse. These experiments explored the role of *Six6* specifically within the GnRH neuronal population by using the GnRH targeting Cre, the *LHRH^{cre} (19)*. These studies revealed that *Six6* has an essential role within the GnRH neuron, wherein it acts to stimulate the release of GnRH. Evidence from *Six6^{flox}/LHRH^{Cre}* mice indicated that loss of SIX6 within the GnRH neuron abolishes GnRH expression in ~90% of GnRH neurons. It was further demonstrated that the deletion of *Six6* within the GnRH neuron leads to infertility, hypogonadism, hypogonadotropism, and delayed puberty. *Six6* was also identified as a key neuronal regulator in fertility through

studies using a Six6KO mouse (33). In findings similar to those using *Six6^{flox}/LHRH^{Cre}* mice, *Six6* was deemed necessary within GnRH neurons to sustain GnRH gene expression and preserve fertility in mice in the Six6KO whole-body model (33).

Six6 has also been implicated in the development of several other tissues. There is ample evidence that SIX6 is essential within the SCN to sustain circadian rhythms. *Six6KO* mice displayed aberrant circadian rhythms and lacked optic nerves (42). While these mice did show some circadian rhythmicity, it was severely hampered by the loss of *Six6* (42). The presence of SCN morphology was undetectable in *Six6KO* mice, and known markers of the SCN, vasoactive intestinal polypeptide (VIP) and arginine vasopressin (AVP) were similarly absent (42). Thus, SIX6 plays an essential role in the development of the SCN. SIX6 also has been identified as being necessary for the proper development of ocular structures (40,42,153,189). Studies of the role of *Six6* in the eye have shown that the eyes of *Six6KO* mice show increased early exit from the cell cycle (40). Studies in the human have associated SIX6 mutations with glaucoma (189). Loss of SIX6 in Xenopus results in early exit from the cell cycle of retinal progenitor cells resulting an absence of retinal ganglion cells, the terminally differentiated cell of this lineage (40). SIX6 clearly has important roles in the SCN and in the eye. Previous work has demonstrated that the *GnRH^{cre}* targets the SCN, however it is not yet known whether it targets the eye.

Here, we will investigate whether the *GnRH^{cre}* has expression within the eye, and determine whether this results in aberrant phenotypes when the *Six6* gene is targeted by *GnRH^{cre}*. As the *GnRH^{cre}* is widely used, and many papers have been published previously using this cre, it is imperative that we ascertain the extent of the ectopic expression and identify tissues that are targeted by the *GnRH^{cre}*. Through comparison of these results with previously obtained results using the *LHRH^{cre}*, we can determine whether ectopic expression with the *GnRH^{cre}* results in erroneous phenotypes.

Methods

Mouse lines and animal housing. All animal procedures were performed in accordance with the University of California, San Diego, Institutional Animal Care and Use Committee regulations (IUCAC protocol S00261). Mice were group-housed with ~4 to a cage on a 12-hour light, 12-hour dark cycle (on 6:00 A.M., off 6:00 P.M.), with *ad libitum* chow and water. All mice were kept on a C57BL/6J mouse background. *Six6KO* mice were generated as previously described (Li et al., 2002) and were kindly provided by Dr. Xue Li (Children's Hospital of Boston, Harvard Medical School, Boston, MA). *Six6^{flox}* mice were generated from a *Six6* Knock-out first KOMP (UC Davis, Knock-Out Mouse Project, www.komp.org) construct and crossed with a *flpase* mouse (Rodríguez et al., 2000; http://jaxmice.jax.org/strain/003800.html) to create the *Six6^{flox}* conditional KO allele. *Six6^{flox}* genotyping was performed with *Six6WT* forward: 5'GAAGCCCTTAACAAGAATGAGTCGG 3'; *Six6flox* forward: 5'CTTCGGAATAGGAACTTCGGTT 3', reverse: 5'CTTTGAATTTGGGTCCCTGG 3'. These mice were then mated to *GnRH^{cre}* (66) mice or *LHRH^{cre}* mice for conditional removal of *Six6* within the GnRH neurons. For lineage tracing, *Rosa^{tdTomato}* reporter mice (https://www.jax.org/strain/007908) were used (68) and mated to *Six6^{flox}* and *LHRH^{cre}* mice to create the *Six6^{flox}/Rosa^{RFP}/LHRH^{cre}* line. The same approach was used for lineage tracing in the *Six6KO* mouse model. Mice were killed by CO_2 or isoflurane (Vet One, Meridian) overdose. Controls used for *Six6KO* line were *Six6WT* mice; controls for the *Six6^{flox}/LHRH^{cre}* line were *Six6$^{flox/flox}$* and *LHRH^{cre-}*; controls used for *Six6^{flox}/Rosa^{LacZ}/LHRH^{cre}* line were *Six6^{wt}/Rosa^{LacZ}/LHRH^{cre+}.*

Collection of tissue and histology. Ovaries and uteri from diestrus females and testes from males were dissected and weighed from animals of 3 months of age. Diestrus ovaries, brains, olfactory bulbs, embryos, and testes were fixed for two days (~49 hr) at 4°C in freshly made mixture of 6:3:1 absolute alcohol: 37% formaldehyde (Fisher F79-4): Glacial Acetic Acid, then dehydrated in 70% ethanol before paraffin embedding. Sagittal sections (10 µm) were cut on a microtome and

floated onto SuperFrost Plus slides (Thermo Fisher Scientific). Ovaries, testes and brains were stained with hematoxylin and eosin (H&E; Sigma-Aldrich). In ovaries, the number of corpora lutea in a single ovary per mouse was recorded by an investigator blinded to the treatment/genotype. The brain was sectioned from Bregma 1.32 to Bregma -2.7 (67).

Determination of pubertal onset and estrus cyclicity. These procedures were described previously in detail (Hoffmann et al., 2014). To assess estrous cyclicity, vaginal smears were performed daily between 9:00 and 11:00 A.M. on 3- to 5-month-old mice by vaginal lavage.

Timed mating. Each *Six6^{flox}/GnRH^{cre+}* or *Six6^{flox}/GnRH^{cre-}* female mouse was housed with a *Six6^{flox}/GnRH^{cre+}* or *Six6^{flox}/GnRH^{cre-}* male mouse, and vaginal plug formation was monitored. If a plug was present, the day was noted as day 0.5 of pregnancy. Embryos were then collected at day e12.5, e13.5, e15.5, e17.5.

Fertility assessment. At 12–15 weeks of age, virgin *Six6^{flox}/GnRH^{cre+}* and *Six6^{flox}/GnRH^{cre-}* mice were housed in pairs. The number of litters and pups produced in 90 days was recorded. Control matings used were *Six6^{flox}/GnRH^{cre-}* with *Six6^{flox}/GnRH^{cre-}.*

GnRH-pituitary stimulation tests. For two weeks prior to the hormonal challenge, mice were adapted to handling stress such that they would be unaffected by stress during sampling. Baseline tail blood was collected from male and female metestrus/diestrus littermates. Ten minutes after receiving an *ip* injection of 1 µg/kg GnRH (Sigma #L7134) diluted in physiological saline, tail blood was collected again. For kisspeptin challenge, 15 minutes after *ip* injection of 30 nM of kisspeptin (Tocris #4243) diluted in physiological saline was injected, tail blood was collected again. The total volume of blood collected did not exceed 100 µL. Blood was collected between 11:00 AM and 12:00 PM and was allowed to clot for 1 hour at room temperature. Blood was then centrifuged for 15 min at 2600 g. Serum was collected and stored at -20°C before Luminex analysis was used

to measure LH and FSH. The assay detection limit was 0.24 ng/mL, inter-assay CV was 15.2 and intra-assay CV was 11.5.

Testosterone Analysis. For serum hormone analysis, mice were killed by isoflurane overdose and blood collected from the abdominal aorta between 9:00 and 11:00AM. Blood was allowed to clot for 1 hour at room temperature and then centrifuged (15 min, 2600 X g). Serum was collected and stored at -20°C before RIA analysis for T at the Center for Research in Reproduction, Ligand Assay, and Analysis Core, University of Virginia (Richmond, Virginia). Samples were run in singlets. All intraassay coefficients of variance (ACOVs) are based on the variance of samples in the standard curve run in duplicate. T: lower detection limit: 9.6 ng/dL, intra-ACOV 5.4% and inter-ACOV 7.8%.

Immunohistochemistry (IHC). IHC was performed as previously described (32), with the only modification being antigen retrieval by boiling the samples for 15 min in 10 mM sodium citrate, pH 6. Briefly, the primary antibody used was rabbit anti-GnRH (1:1000; Immunostar, 20075, Lot 1037001). GnRH-positive neurons were counted throughout the brain in adults, and throughout the head in embryos. The whole head was counted in embryos, and whole brain was counted in the adult from bregma 1.70 to bregma –2.80 (67). All sections were counted by an investigator blinded to the treatment/genotype. For lineage tracing, red fluorescent protein (RFP) expression was detected with a rabbit anti-rfp primary antibody (1:1000; Abcam, ab62341, Table 1). Assessment of the SCN marker vasoactive intestinal polypeptide (VIP) was done using a rabbit anti-VIP antibody (1:300; Santa-Cruz, sc-7841).

Wheel-running behavior. To determine if *Six6$^{flox/flox}$/GnRH^{cre}* mice had normal activity on running wheels, *Six6$^{flox/flox}$/GnRH^{cre} and control* mice were housed individually in cages with running wheels. Food and water were available *ad libitum* during the entire experiment. After 1-week acclimation to the polypropylene cages (17.8 × 25.4 × 15.2 cm) containing a metal running wheel

(11.4 cm diameter), locomotor activity rhythms were monitored with a Vitalview data collection system (Version 4.2, Minimitter, Bend OR) that compiled in 6 min bins the number of electrical closures triggered by half wheel rotations. Running wheel activity was monitored for 2 weeks on a 12h Light:12h Dark cycle. Cage changes were scheduled at 3-week intervals. Wheel-running activity was analyzed using ClockLab Analysis (ActiMetrics Software). Only female mice were included in these assays.

Statistical analysis. Statistical analyses were performed using either Student's t-test, Mann-Whitney, or two-way ANOVA, followed by post hoc analysis by Tukey or Bonferroni as indicated in figure legends, with p=0.05 to indicate significance. Statistical Software GraphPad Prism was used for analysis. N values represent the number of samples included in each group.

Results

Removal of Six6 using the GnRH^{cre} reduces GnRH neuron number

Our main goal was to compare results using the *GnRH^{cre}* that has known ectopic expression, with previously conducted experiments using the *LHRH^{cre}*. To execute this, we crossed a *Six6^{flox}* mouse with a *GnRH^{cre}* mouse. GnRH-expressing neurons were counted through development and into the adult in *Six6$^{flox/flox}$/GnRH^{cre}* mice. In the *Six6^{flox}/GnRH^{cre+}* (conditional KO, or cKO) mouse, the number of GnRH neurons began declining in early embryogenesis, at e13.5, with significantly fewer GnRH neurons seen in the cKO mouse compared to control (65% reduction) (Fig. 4.1a). Even fewer neurons were present in the cKO mouse later in development at e17.5, with ~90% fewer GnRH neurons than the control mice (Fig. 4.1b). The adult cKO mice showed a similar loss with both males and females having ~90% fewer GnRH neurons than control mice (Fig. 4.1c).

Loss of GnRH using GnRH^{cre} causes infertility

The propensity of cKO males and females to copulate was measured in a plugging assay. While all the control females were plugged by day three, it took significantly longer for male cKO mice to plug control females, and for cKO females to be plugged by control males (Fig. 4.2a). The ability of *Six6*$^{flox/flox}$*/GnRH*^{cre} mice to reproduce was assessed via a 90-day fertility assay. In this assay, control pairs of mice all produced 3 litters. Female cKO mice when mated with control mice did not produce any litters in the three-month period. Three male cKO mice were mated with control females and only one male mouse could produce a litter during the period of 90 days (Fig. 4.2b). Thus, cKO mice are impaired in their ability to produce litters. Decreased levels of GnRH can also result in delayed or absent puberty (a characteristic of IHH), therefore we assessed whether the *Six6*$^{flox/flox}$*/GnRH*^{cre} mice had altered onset of puberty. Pubertal onset in the female mouse can be determined by vaginal opening. Control female mice underwent puberty at 29 ± 0.34 days, and control male mice underwent puberty at 30 ± 0.26 days; the onset of puberty was significantly delayed in both sexes of *Six6*$^{flox/flox}$*/GnRH*^{cre} mice, with female mice undergoing puberty at 43 ± 2.1 days and male mice 47 ± 1.3 days (Fig. 4.2c, d). cKO mice were not smaller than their littermate counterparts.

Loss of Six6 within the GnRH neuron results in hypogonadism

We next sought to determine whether the deficiency in GnRH seen in the *Six6*$^{flox/flox}$*/GnRH*^{cre} mice would affect gonadal development. Males exhibited a drastic effect on testicular development with cKO testicles being ~ 1/4 the size of control testicles (Fig. 4.3a, c). No sperm were present inside cKO testicles (Fig. 4.3b). Developmental impairment of cKO testes structures provides an explanation for the infertility seen in the *Six6*$^{flox/flox}$*/GnRH*^{cre} mice. Testicular development relies on LH and FSH release from the pituitary in response to GnRH (174). Thus, we measured LH and FSH levels, with no difference observed in LH levels between control and cKO mice, but a decrease in FSH levels was observed in cKO mice (Fig. 4.3d, e). Testosterone

was also measured with a trend to lower T levels in cKO mice but no statistically significant difference (Fig. 4.3f).

Female gonadal development was similarly affected by the loss of GnRH neurons, however, not as drastically as the males, with the size of cKO ovaries being significantly smaller at ~2/3 the size of control ovaries (Fig. 4.4a). No difference was seen in the uterine weights of cKO and control mice (WT= 0.09 ± 0.01, cKO= 0.08 ± 0.01, n=3, Student's t-test). Ovarian histology revealed a significant reduction in the number of corpora lutea in cKO mice (Fig. 4.4b, c). The absence of corpora lutea indicates abnormal progression through the estrous cycle and absence of an LH surge. To further asses the ability of *Six6*$^{flox/flox}$*/GnRH*^{cre} females to cycle given their paucity of GnRH neurons, estrous smears were collected from 3.5-month-old cKO females and littermates for 12 days. While control females completed on average 3 cycles in the 12-day sampling period, cKO mice did not complete any cycles, with each mouse being in prolonged diestrus for the duration of the assay (Fig. 4.4d, e). Indeed, circulating diestrus LH levels were reduced in cKO females compared with control females; however, no difference was seen in FSH serum levels (Fig. 4.5a, b). This reduction in LH is reflective of the deficiency in GnRH in the cKO mice. Finally, to confirm that the lack of circulating LH and FSH is due to a lack of GnRH, and not an error with LH/FSH release at the pituitary, we performed GnRH and Kisspeptin challenges. As expected, LH release was induced in response to an injection of GnRH in both genotypes as indicated by fold change of LH in response to GnRH (Fig. 4.5c). Unexpectedly, we did not see reduced release of LH in the *Six6*$^{flox/flox}$*/GnRH*^{cre} mice in response to kisspeptin, as no difference between control and cKO mice was found in the fold change of LH from (Fig. 4.5d). This may be because the remaining GnRH neurons when stimulated in a synchronous manner are sufficient to allow a large LH release in the cKO mice.

Loss of Six6 in Six6^{floxflox}/GnRH^{cre} neurons results in the loss of GnRH expression

In the *Six6*$^{flox/flox}$*/GnRHcre* mice, ~90% of GnRH neurons are undetectable, which could be the result of three potential errors. First, GnRH neurons could be mis-migrating and therefore would be found somewhere off their migratory path or they could lack the ability to express GnRH and would thus be undetectable using a GnRH antibody. When GnRH neuron counting was conducted, the entire head of embryos were collected and analyzed for off-path GnRH neurons. None were discovered, indicating that mis-migration does not appear to be the source of the missing GnRH neurons. A second possibility is that GnRH neurons could be dead and therefore undetectable. A third possibility is that GnRH neurons may be present within the hypothalamus but lacking GnRH expression and are therefore undetectable using a GnRH antibody. To discern the mechanism for the absence of GnRH neurons seen in the *Six6*$^{flox/flox}$*/GnRH*^{cre}, lineage tracing was conducted using *Six6*^{flox}*/Rosa*^{tdTomato}*/GnRH*^{cre} *mice*. In these mice, the GnRH neurons are labeled with tdTomato for the duration of the life of the neuron, regardless of GnRH expression. The number of GnRH neurons was counted at e12.5 and in adulthood, with equivalent number of tdTomato-positive neurons being seen between genotypes at both ages in the *Six6*$^{flox/flox}$*/Rosa*^{tdTomato}*/GnRH*$^{cre+}$ and *Six6*^{wt}*/Rosa*^{tdTomato}*/GnRH*$^{cre+}$ mice (Fig. 4.6a, b). Therefore, GnRH neurons are present in the *Six6*$^{flox/flox}$*/GnRH*^{cre} mouse; but are not expressing GnRH.

GnRH^{cre} has ectopic expression in the eye and in the SCN

The suprachiasmatic nucleus is the main circadian pacemaker, and has been shown in a variety of publications to regulate reproductive function in mice, primates, and humans (190,191). Previous data demonstrates that GnRH^{cre}, in addition to targeting GnRH neurons, also targets the SCN. As *Six6* is expressed within the SCN, the extent to which the SCN is impaired in *Six6*$^{flox/flox}$*/GnRH*^{cre} mice was assessed. Activity onset of female mice wheel running in normal 12h-light:12h-dark conditions was assessed with normal onset in control mice (Fig. 4.7a). Control mice ran during the dark portion of the photoperiod, and exhibited almost no running during the light portion indicating normal eye development and sensitivity to light (Fig. 4.7a).

Six6$^{flox/flox}$*/GnRH*^{cre} female mice displayed a variety of running patterns with one mouse showing strong circadian periodicity, two showing weak periodicity, and one showing no periodicity (Fig. 4.7a). Subsequently, wheel activity was measured in 24h constant darkness, and cko mice displayed a range of activity patterns, with two mice showing weak periodicity and two mice showing strong periodicity; while control mice retained robustly rhythmic activity patterns (Fig. 4.7a).

As *Six6* is also known to be expressed in the eye, (40,43) the ability of *Six6*$^{flox/flox}$*/GnRH*^{cre} mice to entrain to light was also assessed. After constant darkness, the mice were exposed to 12h-light:12h-dark conditions again. This examines the ability of the mice to entrain to the light cues. All control mice entrained normally to light, whereas the cKO mice showed a variety of activity patterns. One mouse entrained normally to light, two mice showed nearly normal entrainment to light, and one mouse exhibited no entrainment to light (Fig. 4.7a). Given the deficit in light entrainment, the visual acuity of *Six6*$^{flox/flox}$*/GnRH*^{cre} was tested using visual evoked potential testing. Fifty percent of the cKO mice tested were blind, while all of the control mice displayed normal visual acuity (Fig. 4.7b).

To determine whether the abnormal circadian rhythm of cKO mice is due to an absence or reduction in the SCN, H&E staining on the SCN was conducted. Analysis revealed a loss of any visible SCN in two of the three cKO mice examined, while the control mice examined showed a visible SCN population (Fig. 4.7c). To further assess the presence of an SCN population, we conducted IHC for the SCN marker

As there is another available cre that specifically targets the GnRH neuron population, we determined whether this LHRH^{cre} also erroneously targets the SCN and the eye. Circadian rhythms were tested again to reveal normal circadian rhythms in all control and *Six6*$^{flox/flox}$*/LHRH*^{cre} (Fig. 4.8a). To assure that the LHRH^{cre} does not target the eye, as does the GnRH^{cre}, we

conducted visual evoked potential testing and found no ocular impairment in the *Six6*$^{flox/flox}$*/LHRH*^{cre} mice (Fig. 4.8b). In addition to a functional SCN and competent vision, *Six6*$^{flox/flox}$*/LHRH*^{cre} mice also have an intact SCN neuronal population with a visible SCN as identified by H&E staining (Fig. 4.8c), and vasoactive intestinal peptide (VIP) staining (Fig. 4.8d).

Discussion

Comparison of the *GnRH*^{cre} and *LHRH*^{cre} in studying GnRH neurons

Our goal here was to determine whether the reported ectopic expression of the *GnRH*^{cre} would alter the previously reported infertility and hypogonadism that resulted from deletion of *Six6* from GnRH neurons using the *LHRH*^{cre}. We therefore compared the two different (GnRH)-driven CRE-expressing vectors, the *LHRH*^{cre} and the *GnRH*^{cre}. Our previous research has enumerated the vast differences between these two vectors and demonstrated the variable conclusions that are drawn depending on which cre vector is chosen to assess the role of a gene. These variances are the result of the two GnRH-driven CRE mouse lines targeting vastly different numbers of neurons in LHRH^{cre} and GnRH^{cre} mice from e12 onward. We demonstrate here that the development, survival, and migration of GnRH neurons are similarly impacted by the *LHRH*^{cre} and the *GnRH*^{cre} vectors. However, the development and function of the SCN and the eyes is only impaired in the *Six6*$^{flox/flox}$*/GnRH*^{cre} model.

These variations in phenotypes of *Six6*$^{flox/flox}$*/GnRH*^{cre} and *Six6*$^{flox/flox}$*/LHRH*^{cre} mice are due to ectopic expression of the *GnRH*^{cre} vector. The *Six6*$^{flox/flox}$*/GnRH*^{cre} vector clearly targets the eye and the SCN, as demonstrated by the defect in ocular entrainment seen in *Six6*$^{flox/flox}$*/GnRH*^{cre} and in lineage tracing conducted using *Rosa*$^{tdTomato/}$*GnRH*^{cre} mice. *Six6* has been shown to be highly expressed in the eye numerous times and mutations in this gene have been associated with impaired eye development (189,192). Similarly, it was recently shown that the *GnRH*^{cre} targets the SCN, and as *Six6* is expressed in the SCN (42), it follows that *Six6*$^{flox/flox}$*/GnRH*^{cre} mice had

aberrant rhythms. Despite these differences, phenotypes of GnRH neuron development and fertility were remarkably similar between these two mouse lines. The *GnRH*^{cre} does not exclusively target the GnRH neuron, and therefore conclusions about the role of *Six6* in this neuronal population cannot be made solely using the *Six6*$^{flox/flox}$*/GnRH*^{cre} mouse. However, as the *LHRH*^{cre} vector is specific to the GnRH neuron, comparison of both cre-expressing vectors sheds light of the role of Six6 within various neuronal populations.

Ectopic expression of Gnrh^{cre} does not contribute to the infertility of mice with Six6 deleted within GnRH neurons

A detailed comparison of the two *Gnrh*-driven Cre alleles (LHRH^{cre} and GnRH^{cre}) revealed extensive expression of Cre in the olfactory bulb, septum, SCN, and, hypothalamus by GnRH^{cre}. Our findings here indicate that this ectopic expression does alter the behavior and physiology of mice. This is evidenced by the severely impaired SCN function and physiology in *Six6*$^{flox/flox}$*/GnRH*^{cre} but not *Six6*$^{flox/flox}$*/LHRH*^{cre} mice. The SCN is a brain structure that is essential in female fertility and the LH surge (86). Our goal here was to assess whether ectopic expression within these structures that are intricately involved in regulating reproduction would alter the fertility of *Six6*$^{flox/flox}$*/GnRH*^{cre} mice. The *Six6*$^{flox/flox}$*/GnRH*^{cre} and the *Six6*$^{flox/flox}$*/LHRH*^{cre} mice displayed comparable lack of GnRH expression and equivalent levels of infertility and hypogonadism. These results offer validity to the use of either of these GnRH-driven Cre expressing alleles for the study of GnRH neuron development. However, we recommend that when studying any system dependent upon the tissues in which aberrant expression of the GnRH^{cre} has been detected, the LHRH^{cre} is more appropriate for use.

Acknowledgements

Chapter 4 is currently being prepared for submission for publication of this material. Pandolfi, Erica C.; Hoffmann, Hanne M.; Mellon, Pamela L. The dissertation author is the primary

investigator and author of this material. Hanne Hoffmann assisted in making the *Six6flox* mouse, and in writing the manuscript. Pamela Mellon supervised the project and provided advice.

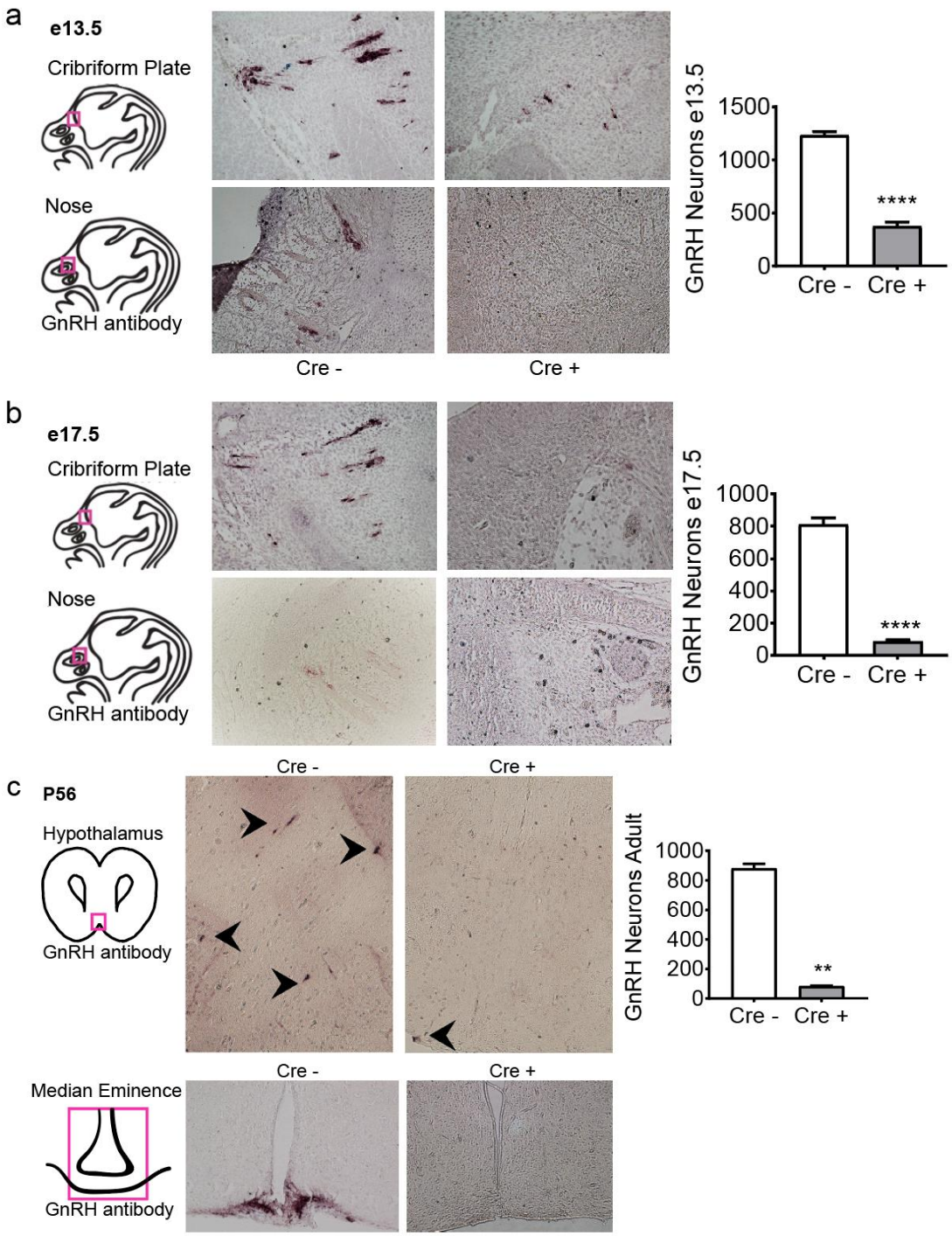

Figure 4.1. Loss of *Six6* specifically from the GnRH neuron results in a loss of ~90% of GnRH neurons. A, GnRH Neurons at e13.5. in Six6-^{flox}/GnRH^{cre} mice (n = 3-4). B, Quantification of GnRH neurons at e15.5 from IHC with anti-GnRH antibody (n = 3-4). C, GnRH neurons in the adult *Six6^{flox}/GnRH^{cre}* mouse (n = 3). (A-C), Drawings to the left of images represent locations in the head/brain where images were taken. Scale bar, 100 μm. Statistical analysis was by Student's t test as compared with control mice. CP, cribriform plate. **, $p < .01$;****, $p < .0001$.

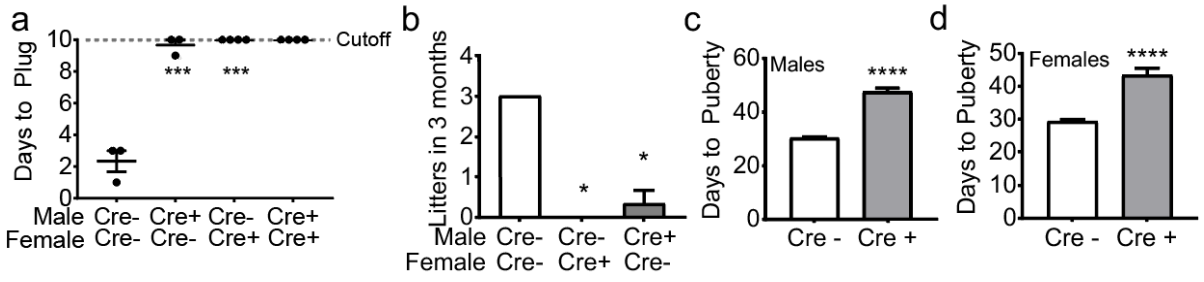

Figure 4.2. *Six6^{flox}/GnRH^{cre}* mice have disrupted fertility and delayed puberty. **a,** Ten-day plugging assay of Cre+ and Cre- mice 3 months of age, as compared to Cre- x Cre- mating (n = 3) Statistical Analysis by Mann-Whitney test. **b,** Number of litters produced in 120-day fertility assay between Cre+ and Cre- mice, as compared to Cre- x Cre- mating. (n = 3-6). **c,** Onset of pubertal opening in male mice measured from day 20 until pubertal onset (n = 3). **d,** Onset of vaginal opening measured from day 20 until pubertal onset (n = 3). **(b-d)** Data were analyzed by Student's t test as compared with control. *, $p < .05$;***, $p < .001$;****, $p < .0001$.

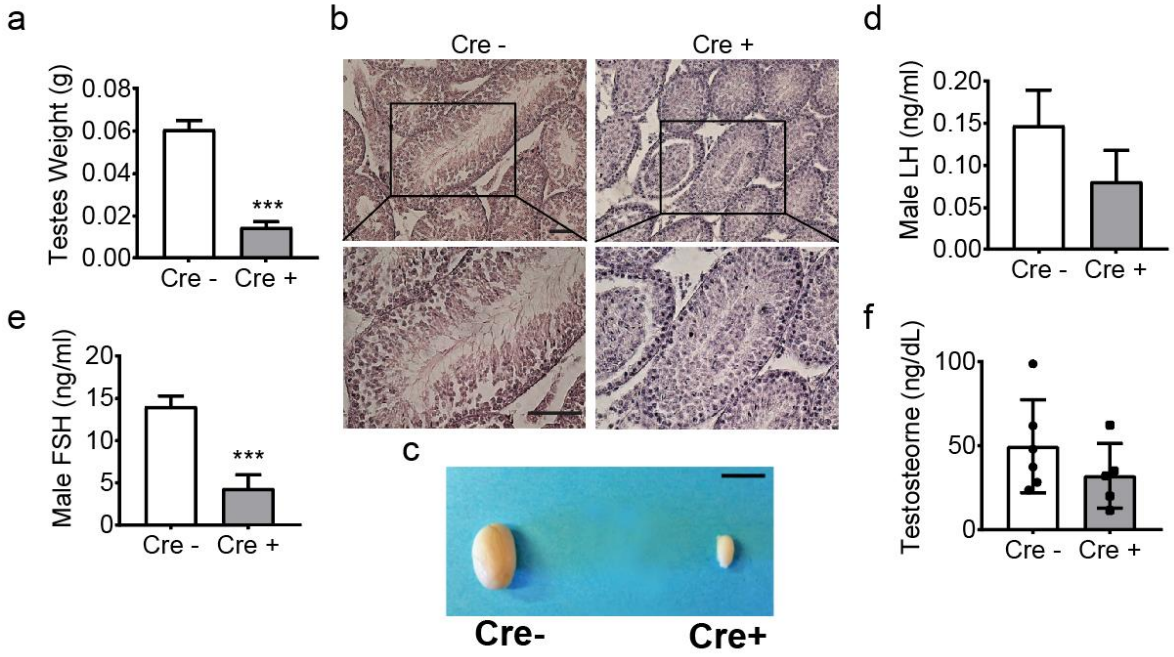

Figure 4.3. *Six6-flox/GnRHcre* male mice are hypogonadal and hypogonadotropic. **a,** Testicular weight of Cre- and Cre+ mice (n = 3). **b,** Images of H&E stained Cre- and Cre+ testicles. **c,** Images of fresh testes Cre- and Cre+ mice. **d,** Serum was collected from adult male mice and assayed for LH (n = 5-6) and **(E)** FSH (n = 5-6) **(F)** Testosterone (4-7) Scale bar, 1cm. All data were analyzed by Student's t test as compared with control. Scale bar, 100 µm. ***, *p*< .001.

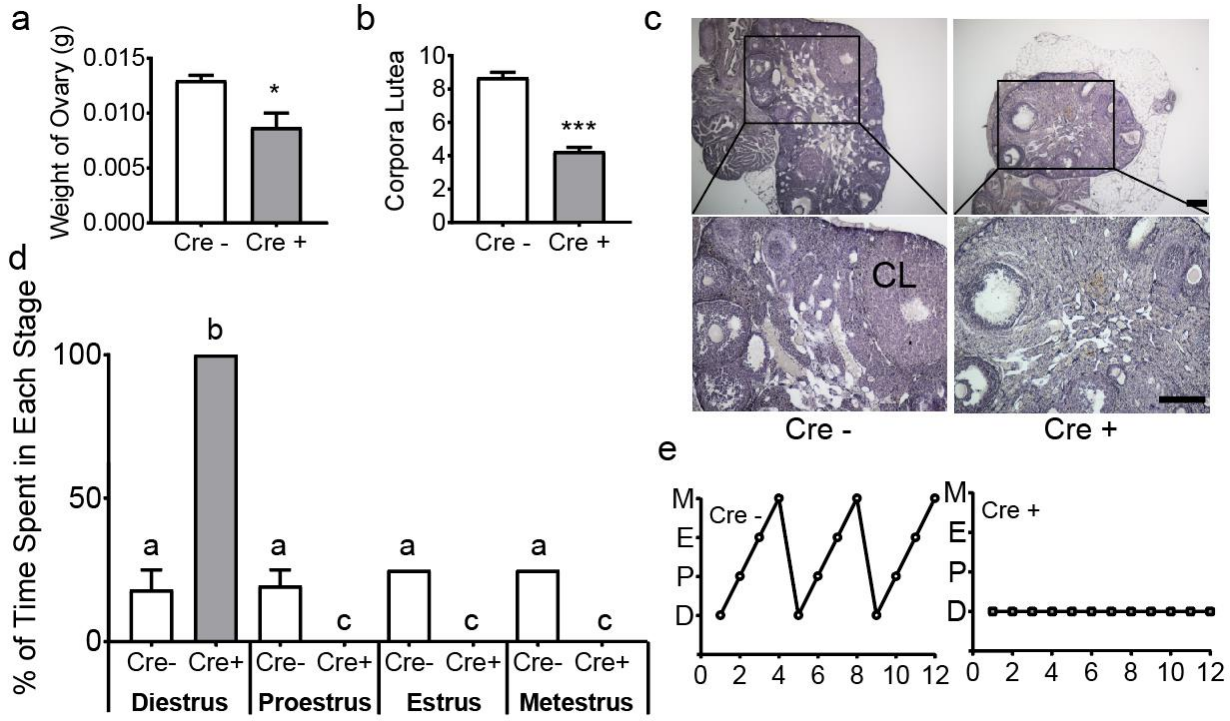

Figure 4.4. *Six6^{flox}/GnRH^{cre}* female mice are hypogonadal and non-cyclic. **a,** Ovarian weights of Cre- and Cre+ mice in grams (n = 3). **b,** Number of corpora lutea in Cre- and Cre+ mice. **(a, b)** Data were analyzed by Student's t test as compared with control. **c,** Images of H&E stained ovaries (3-4). **d,** Estrous cycle was monitored daily in Cre- and Cre+ mice. Statistical analysis by two-way ANOVA followed by Bonferroni, as compared with WT in the same stage of the cycle. **e,** Representative cycles from one Cre- and one Cre+ mouse. **(a, b, and d)** Student's t test as compared with control. D, diestrus; P, proestrus; M, metestrus; E, estrus. Scale bar, 100 µm. *, $p < .05$; ***, $p < .001$.

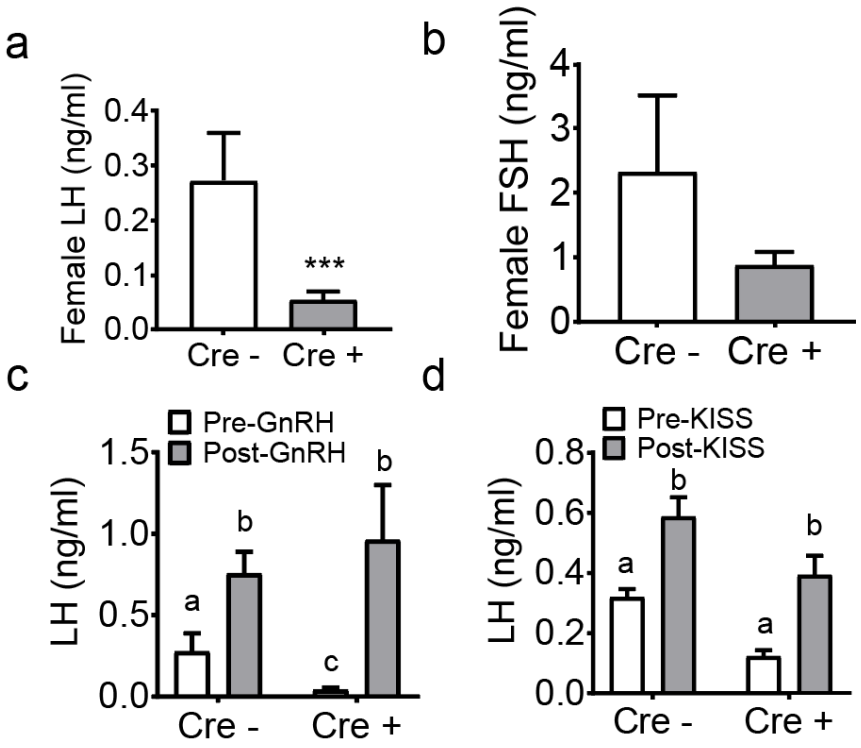

Figure 4.5. *Six6^{flox}/GnRH^{cre}* females are hypogonadotropic due to deficient GnRH. **a,** Serum was collected from adult female diestrus mice and assayed for (A) LH (n = 5-6) and (B) FSH (n = 5-6). **(a, b)** Statistical analysis was by Student's t test as compared with Cre-. **c,** Serum LH was measured immediately prior to, and 10 minutes after a single GnRH challenge in Cre- and Cre+ diestrus females (n = 5-6). **d,** Serum LH was measured prior to and 15 minutes after a single Kisspeptin challenge in Cre- and Cre+ diestrus females (n = 5-6). Statistical analysis by Student's t test as compared with Cre-. *, $p < .05$; **, $P < .01$; ***, $P < .001$.

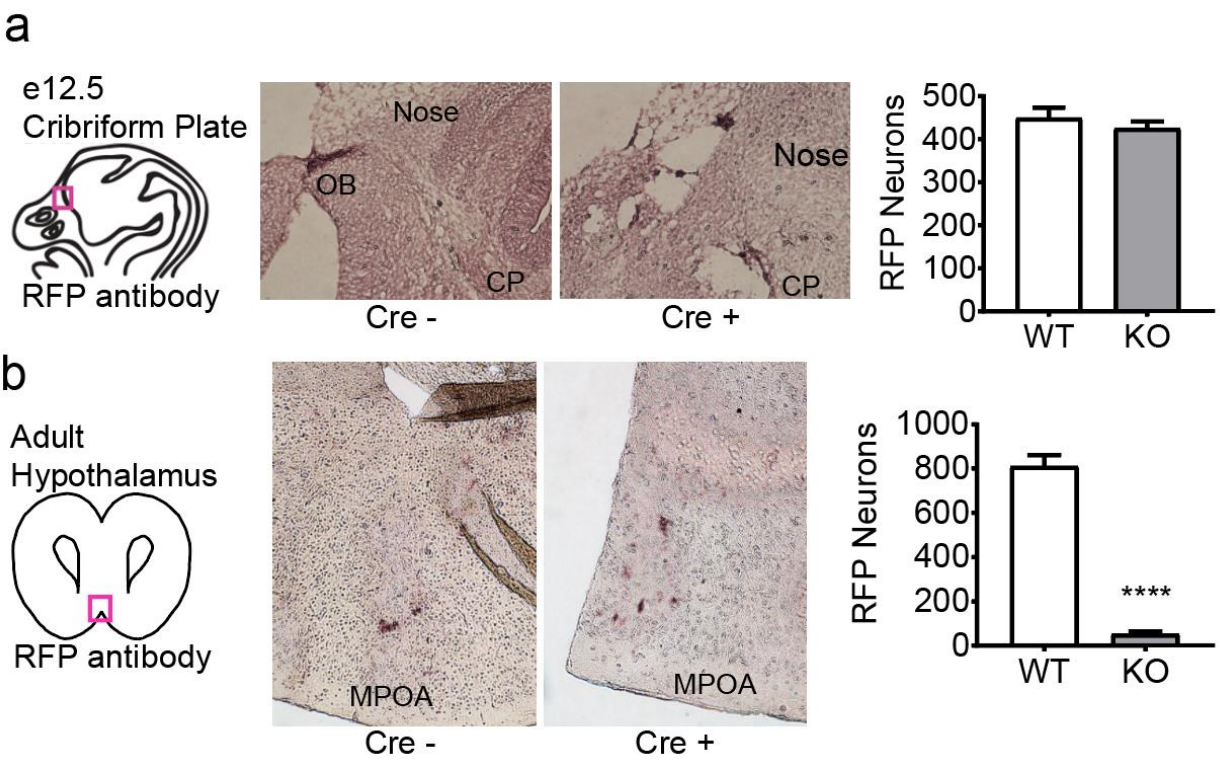

Figure 4.6. *Six6*$^{flox/flox}$*/Rosa*^{tdTomato}*/GnRH*^{cre} mice show a presence of GnRH neurons lacking GnRH expression. **a,** Lineage tracing using tdTomato to mark GnRH neurons regardless of GnRH expression show tdTomato-positive GnRH neurons at e12.5. **b,** tdTomato-positive neurons in the adult. OB, olfactory bulb; CP, cribriform plate; MPOA, medial preoptic area. Scale bar, 100 µm. ****, p <.0001.

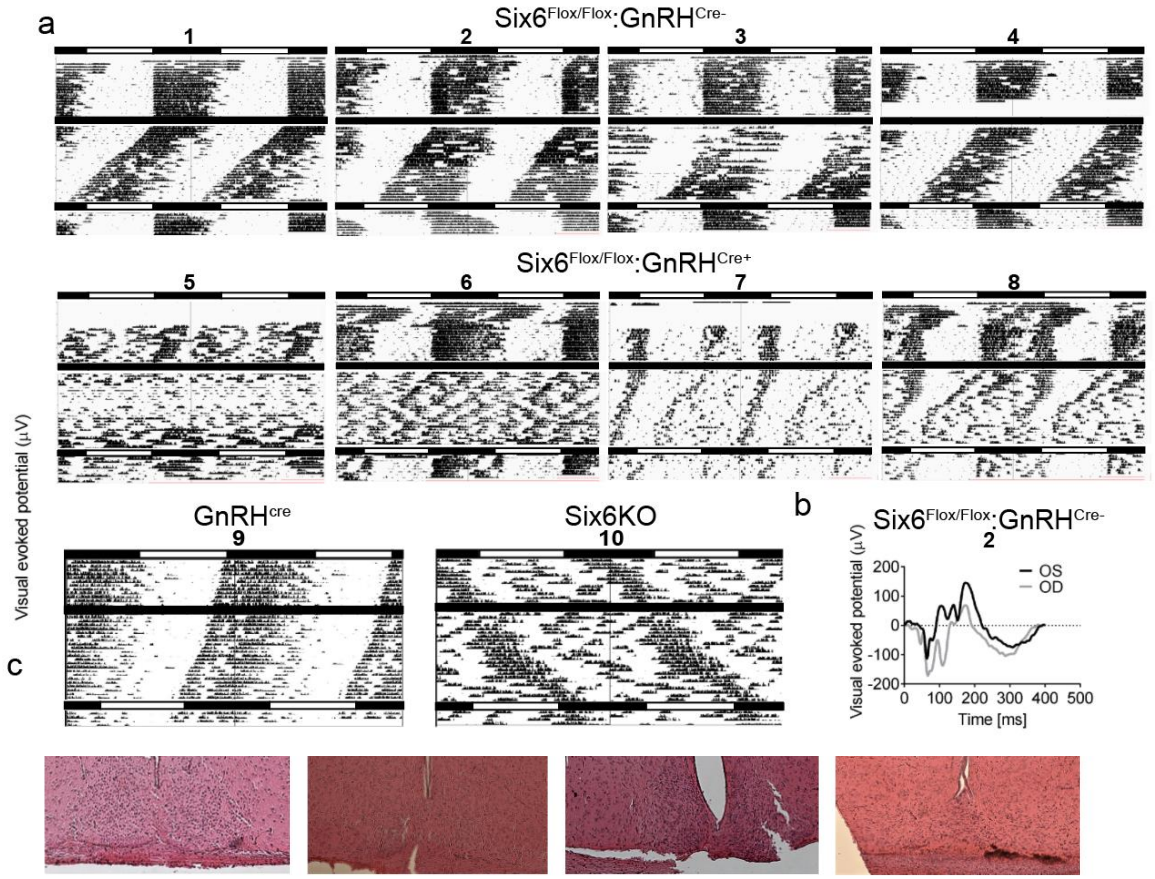

Figure 4.7. *Six6^{flox}/GnRH^{cre}* female mice have abnormal circadian rhythms and impaired vision. A, Mice were placed in cages with wheels in 12-light:12h-dark, then in 24-h constant darkness, then back into 12-light:12-dark to re-entrain them to light. Light exposure is indicated above the plots with a black bar indicating darkness and a white bar indicating light exposure, n=4. B, Visual acuity of *Six6^{flox}/GnRH^{cre}* mice was assessed using evoked visual potential testing, n=1-2. C, H & E staining of SCNs of *Six6^{flox}/GnRH^{cre}* female mice, n=1-3.

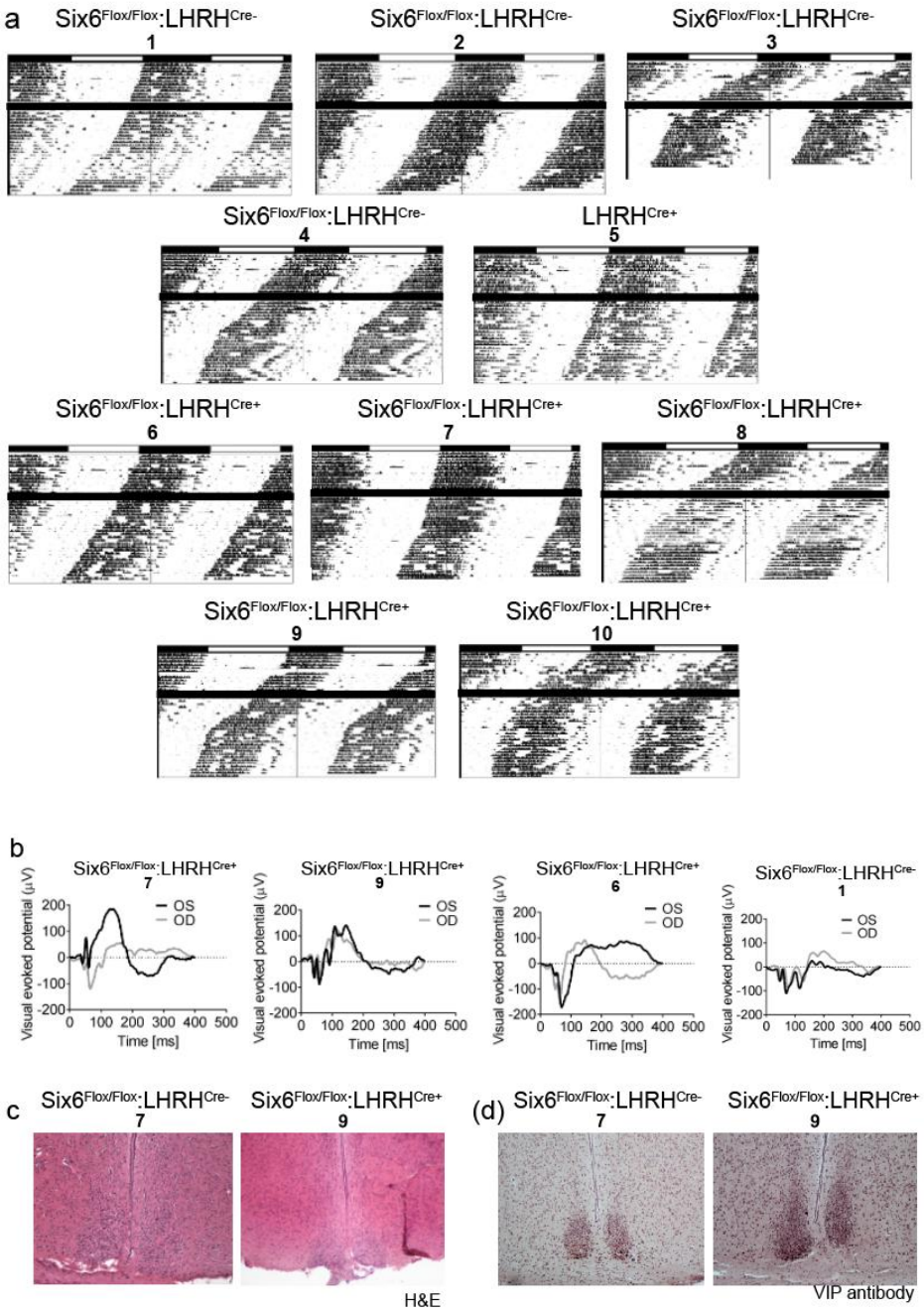

Figure 4.8. *Six6^{flox}/LHRH^{cre}* female mice normal circadian rhythms and normal vision. **a,** Mice were placed in cages with wheels in 12-light:12h-dark, then in 24-h constant darkness, then back into 12-light:12-dark to re-entrain them to light. Light exposure is indicated above the plots with a black bar indicating darkness and a white bar indicating light exposure, n=4-5. **b,** Visual acuity of *Six6^{flox}/GnRH^{cre}* mice was assessed using evoked visual potential testing, n=1-3. **c,** H & E staining of SCNs of *Six6^{flox}/LHRH^{cre}* female mice, n=3. **d,** VIP IHC of *Six6^{flox}/LHRH^{cre}* female mice, n=3.

CONCLUSIONS

The work presented here is an analysis of the roles of homeodomain proteins SIX3 and SIX6 in the development, survival, and migration of GnRH neurons. Our goal herein was to determine whether these proteins are necessary to support the GnRH neuronal network, and therefore determine their potential involvement in the rare genetic disorders of infertility, IHH and Kallmann syndromes. These developmentally linked disorders result in subfertility or infertility and can be paired with anosmia when the development of nasal structures is also impaired This rare condition is congenital and has been linked to a number of genes that are implicated in neuronal development however over 68% of cases of IHH are of an unknown genetic origin. Therefore, our identification of the importance of *Six3* and *Six6* in the development and migration of GnRH neurons adds to our understanding of the etiology of this disease and provides new potential targets for the treatment of IHH.

Chapter 1 investigated the role of *Six3* in IHH using a mouse model with *Six3* removed from the whole-body (*Six3KO*). This mouse model displayed dosage sensitivity of the *Six3* gene in regard to GnRH neuron migration. Complete lack of SIX3 resulted in the total mis-migration of GnRH neurons, while 50% reduction in SIX3 resulted in a 40% reduction in the number of GnRH neurons successfully migrating to the hypothalamus. This reduction in the number of GnRH neurons releasing GnRH into the hypophyseal portal blood system to signal the pituitary was sufficient to alter female fertility, but not male. This was evidenced by the fact that female histology and estrous cycling was abnormal but male gonadal histology was intact. Interestingly, the subfertility observed in males was instead engendered from abnormal development of the MOS, causing impaired olfaction and therefore abnormal mating behavior. These findings are particularly interesting as they closely capitulate the phenotypes of human Kallmann syndrome, where disrupted nasal development leads to GnRH neuron mis-migration and anosmia.

Additionally, it is further evidence for the role of haploinsufficient genes in the etiology of GnRH disorders.

Chapter 2 further investigated the role of *Six3* in the development of GnRH neurons and the olfactory system by specifically deleting *Six3* within the olfactory epithelium using cre-lox technology. The *Six3*$^{flox/flox}$*:Omp*^{cre} mice displayed a modest hyposmia phenotype that clearly impaired their ability to detect odors but was not severe enough to alter their mating behavior. Similarly, they displayed impaired migration early in development but as embryogenesis continued, GnRH neurons of *Six3*$^{flox/flox}$*:Omp*^{cre} mice correct their migration and equivalent numbers were found in the adult hypothalamus. Therefore, no fertility impairment was noted in either sexes other than a defect in male plugging ability, likely due to altered mounting behavior. These findings demonstrated that SIX3 has actions within the olfactory system that illuminate our understanding of the connection between the development of the nose, and the journey of GnRH neurons; but likely would not contribute to the human condition of Kallmann syndrome.

The closely related and homologous gene with a highly overlapping expression pattern, *Six6* was also examined. In Chapter 3, The specific role of *Six6* in the GnRH neuron was examined using a GnRH neuron targeting cre-expressing vector. *Six6*$^{flox/flox}$*:LHRH*^{cre} mice displayed hypogonadism, infertility, and hypogonadotropism. These findings demonstrated the integral role that Six6 play within the GnRH neuron in maintaining GnRH expression. Our work adds to the knowledge of the actions of *Six6* in the development of GnRH neurons, as it was previously known that *Six6* was essential in GnRH neuron development but the specific actions of *Six6* were unknown. This research presented Six6 as another potential target in IHH and revealed that Six6 acts both internally, and externally to the GnRH neuron to preserve fertility.

The experiments detailed in Chapter 4 were conducted to compare to similar GnRH neuron-targeting cre-expressing vectors. This study revealed that the ectopic expression of the

GnRH^{cre} was sufficient to alter phenotypes but not sufficient to worsen the previously observed infertility of the *Six6$^{flox/flox}$:LHRH^{cre}* mice. Our results demonstrate that the GnRH^{cre} targets the SCN and the eye, leading to aberrant circadian rhythms, abnormal SCN morphology, and loss of vision. In addition, these findings further display the importance of *Six3* within these tissues. Chapter 4 serves a reminder to researchers to fully understand the expression patterns of the cre-expressing vectors they select for their experiments. Furthermore, it adds a new perspective to previous studies conducted employing the GnRH^{cre}.

The studies presented here offer a picture of the roles *Six3* and *Six6* play in the GnRH neuron network, and within the GnRH neuron itself. The potential contribution of these proteins to the rare human disease IHH has been examined here. *Six3* was found to be a regulator of olfactory neurogenesis, and GnRH neuron migration. Six6 was identified as a regulator of GnRH expression and GnRH neuron cell survival. This research identifies two new genes that are essential regulators of the GnRH neuronal network, and therefore of fertility.

REFERENCES

1. Balasubramanian R, Dwyer A, Seminara SB, Pitteloud N, Kaiser UB, Crowley WF, Jr. Human GnRH deficiency: a unique disease model to unravel the ontogeny of GnRH neurons. Neuroendocrinology 2010; 92:81-99

2. Bianco SD, Kaiser UB. The genetic and molecular basis of idiopathic hypogonadotropic hypogonadism. Nat Rev Endocrinol 2009; 5:569-576

3. Tobet SA, Bless EP, Schwarting GA. Developmental aspect of the gonadotropin-releasing hormone system. Mol Cell Endocrinol 2001; 185:173-184

4. Cadman SM, Kim SH, Hu Y, Gonzalez-Martinez D, Bouloux PM. Molecular pathogenesis of Kallmann's syndrome. Horm Res 2007; 67:231-242

5. Wray S. Development of gonadotropin-releasing hormone-1 neurons. Front Neuroendocrinol 2002; 23:292-316

6. Wray S. Development of luteinizing hormone releasing hormone neurones. J Neuroendocrinol 2001; 13:3-11

7. Tobet SA, Schwarting GA. Minireview: recent progress in gonadotropin-releasing hormone neuronal migration. Endocrinology 2006; 147:1159-1165

8. Bless E, Raitcheva D, Henion TR, Tobet S, Schwarting GA. Lactosamine modulates the rate of migration of GnRH neurons during mouse development. Eur J Neurosci 2006; 24:654-660

9. Pitteloud N, Quinton R, Pearce S, Raivio T, Acierno J, Dwyer A, Plummer L, Hughes V, Seminara S, Cheng YZ, Li WP, Maccoll G, Eliseenkova AV, Olsen SK, Ibrahimi OA, Hayes FJ, Boepple P, Hall JE, Bouloux P, Mohammadi M, Crowley W. Digenic mutations account for variable phenotypes in idiopathic hypogonadotropic hypogonadism. J Clin Invest 2007; 117:457-463

10. Pitteloud N, Zhang C, Pignatelli D, Li JD, Raivio T, Cole LW, Plummer L, Jacobson-Dickman EE, Mellon PL, Zhou QY, Crowley WF, Jr. Loss-of-function mutation in the prokineticin 2 gene causes Kallmann syndrome and normosmic idiopathic hypogonadotropic hypogonadism. Proc Natl Acad Sci USA 2007; 104:17447-17452

11. Stamou MI, Cox KH, Crowley WF. Discovering Genes Essential to the Hypothalamic Regulation of Human Reproduction Using a Human Disease Model: Adjusting to Life in the "-Omics" Era. Endocr Rev 2015; 36:603-621

12. Papes F, Logan DW, Stowers L. The vomeronasal organ mediates interspecies defensive behaviors through detection of protein pheromone homologs. Cell 2010; 141:692-703

13. Brown RE. Mammalian Social Odors: A Critical Review. In: Rosenblat JS, Hinde RA, Beer C, Busnell M-C, eds. Advances in the Study of Behavior. Vol 10. New York, New York: Academic Press; 1979:107-161.

14. Keller M, Baum MJ, Bakker J. Olfactory control of sex-recognition and sexual behavior in mice. In: Hurst J, Beynon RJ, Roberts SC, Wyatt T, eds. Chemical Signals in Vertebrates Vol 11. New York: Springer; 2008:241-250.

15. Baum MJ, Bakker J. Roles of sex and gonadal steroids in mammalian pheromonal communication. Front Neuroendocrinol 2013; 34:268-284

16. Dulac C, Torello AT. Molecular detection of pheromone signals in mammals: from genes to behaviour. Nat Rev Neurosci 2003; 4:551-562

17. Baum MJ. Contribution of pheromones processed by the main olfactory system to mate recognition in female mammals. Front Neuroanat 2012; 6:20

18. Keller M, Pierman S, Douhard Q, Baum MJ, Bakker J. The vomeronasal organ is required for the expression of lordosis behaviour, but not sex discrimination in female mice. Eur J Neurosci 2006; 23:521-530

19. Yoon H, Enquist LW, Dulac C. Olfactory inputs to hypothalamic neurons controlling reproduction and fertility. Cell 2005; 123:669-682

20. Ma D, Allen ND, Van Bergen YC, Jones CM, Baum MJ, Keverne EB, Brennan PA. Selective ablation of olfactory receptor neurons without functional impairment of vomeronasal receptor neurons in OMP-ntr transgenic mice. Eur J Neurosci 2002; 16:2317-2323

21. Biellmann F, Henion TR, Burki K, Hennet T. Impaired sexual behavior in male mice deficient for the beta1-3 N-acetylglucosaminyltransferase-I gene. Mol Reprod Dev 2008; 75:699-706

22. Matsumoto S, Yamazaki C, Masumoto KH, Nagano M, Naito M, Soga T, Hiyama H, Matsumoto M, Takasaki J, Kamohara M, Matsuo A, Ishii H, Kobori M, Katoh M, Matsushime H, Furuichi K, Shigeyoshi Y. Abnormal development of the olfactory bulb and reproductive system in mice lacking prokineticin receptor PKR2. Proc Natl Acad Sci U S A 2006; 103:4140-4145

23. Keverne EB. Importance of olfactory and vomeronasal systems for male sexual function. Physiol Behav 2004; 83:177-187

24. MacColl G, Quinton R, Bouloux PM. GnRH neuronal development: insights into hypogonadotrophic hypogonadism. Trends Endocrinol Metab 2002; 13:112-118

25. Wray S. From nose to brain: development of gonadotrophin-releasing hormone-1 neurones. J Neuroendocrinol 2010; 22:743-753

26. Cariboni A, Hickok J, Rakic S, Andrews W, Maggi R, Tischkau S, Parnavelas JG. Neuropilins and their ligands are important in the migration of gonadotropin-releasing hormone neurons. J Neurosci 2007; 27:2387-2395

27. Giacobini P. Shaping the Reproductive System: Role of Semaphorins in GnRH Development and Function. Neuroendocrinology 2015; 102:200-215

28. Pitteloud N, Meysing A, Quinton R, Acierno JS, Jr., Dwyer AA, Plummer L, Fliers E, Boepple P, Hayes F, Seminara S, Hughes VA, Ma J, Bouloux P, Mohammadi M, Crowley WF, Jr. Mutations in fibroblast growth factor receptor 1 cause Kallmann syndrome with a wide spectrum of reproductive phenotypes. Mol Cell Endocrinol 2006; 254-255:60-69

29. Chung WC, Moyle SS, Tsai PS. Fibroblast growth factor 8 signaling through fibroblast growth factor receptor 1 is required for the emergence of gonadotropin-releasing hormone neurons. Endocrinology 2008; 149:4997-5003

30. Toba Y, Tiong JD, Ma Q, Wray S. CXCR4/SDF-1 system modulates development of GnRH-1 neurons and the olfactory system. Dev Neurobiol 2008; 68:487-503

31. Falardeau J, Chung WC, Beenken A, Raivio T, Plummer L, Sidis Y, Jacobson-Dickman EE, Eliseenkova AV, Ma J, Dwyer A, Quinton R, Na S, Hall JE, Huot C, Alois N, Pearce SH, Cole LW, Hughes V, Mohammadi M, Tsai P, Pitteloud N. Decreased FGF8 signaling causes deficiency of gonadotropin-releasing hormone in humans and mice. J Clin Invest 2008; 118:2822-2831

32. Hoffmann HM, Tamrazian A, Xie H, Perez-Millan MI, Kauffman AS, Mellon PL. Heterozygous deletion of ventral anterior homeobox (Vax1) causes subfertility in mice. Endocrinology 2014; 155:4043-4053

33. Larder R, Clark DD, Miller NL, Mellon PL. Hypothalamic dysregulation and infertility in mice lacking the homeodomain protein Six6. J Neurosci 2011; 31:426-438

34. Pernasetti F, Vasilyev VV, Rosenberg SB, Bailey JS, Huang HJ, Miller WL, Mellon PL. Cell-specific transcriptional regulation of follicle-stimulating hormone-beta by activin and gonadotropin-releasing hormone in the LbetaT2 pituitary gonadotrope cell model. Endocrinology 2001; 142:2284-2295

35. Radovick S, Wray S, Lee E, Nicols DK, Nakayama Y, Weintraub BD, Westphal H, Cutler J, G B, Wondisford FE. Migratory arrest of gonadotropin-releasing hormone neurons in transgenic mice. Proc Natl Acad Sci USA 1991; 88:3402-3406

36. Wierman ME, Pawlowski JE, Allen MP, Xu M, Linseman DA, Nielsen-Preiss S. Molecular mechanisms of gonadotropin-releasing hormone neuronal migration. Trends Endocrinol Metab 2004; 15:96-102

37. Fang Z, Xiong X, James A, Gordon DF, Wierman ME. Identification of novel factors that regulate GnRH gene expression and neuronal migration. Endocrinology 1998; 139:3654-3657

38. Maggi R, Pimpinelli F, Molteni L, Milani M, Martini L, Piva F. Immortalized luteinizing hormone-releasing hormone neurons show a different migratory activity in vitro. Endocrinology 2000; 141:2105-2112

39. Pimpinelli F, Redaelli E, Restano-Cassulini R, Curia G, Giacobini P, Cariboni A, Wanke E, Bondiolotti GP, Piva F, Maggi R. Depolarization differentially affects the secretory and migratory properties of two cell lines of immortalized luteinizing hormone-releasing hormone (LHRH) neurons. Eur J Neurosci 2003; 18:1410-1418

40. Li X, Perissi V, Liu F, Rose DW, Rosenfeld MG. Tissue-specific regulation of retinal and pituitary precursor cell proliferation. Science 2002; 297:1180-1183

41. Jean D, Bernier G, Gruss P. Six6 (Optx2) is a novel murine Six3-related homeobox gene that demarcates the presumptive pituitary/hypothalamic axis and the ventral optic stalk. Mech Dev 1999; 84:31-40

42. Clark DD, Gorman MR, Hatori M, Meadows JD, Panda S, Mellon PL. Aberrant development of the suprachiasmatic nucleus and circadian rhythms in mice lacking the homeodomain protein six6. J Biol Rhythms 2013; 28:15-25

43. Conte I, Morcillo J, Bovolenta P. Comparative analysis of Six 3 and Six 6 distribution in the developing and adult mouse brain. Dev Dyn 2005; 234:718-725

44. Stowers L, Logan DW. Olfactory mechanisms of stereotyped behavior: on the scent of specialized circuits. Curr Opin Neurobiol 2010; 20:274-280

45. Brennan PA, Zufall F. Pheromonal communication in vertebrates. Nature 2006; 444:308-315

46. Thompson ML, Edwards DA. Olfactory bulb ablation and hormonally induced mating in spayed female mice. Physiol Behav 1972; 8:1141-1146

47. Brennan PA, Keverne EB. Neural mechanisms of mammalian olfactory learning. Prog Neurobiol 1997; 51:457-481

48. Pierman S, Douhard Q, Balthazart J, Baum MJ, Bakker J. Attraction thresholds and sex discrimination of urinary odorants in male and female aromatase knockout (ArKO) mice. Horm Behav 2006; 49:96-104

49. Stowers L, Marton TF. What is a pheromone? Mammalian pheromones reconsidered. Neuron 2005; 46:699-702

50. Lloyd-Thomas A, Keverne EB. Role of the brain and accessory olfactory system in the block to pregnancy in mice. Neuroscience 1982; 7:907-913

51. Rattazzi L, Cariboni A, Poojara R, Shoenfeld Y, D'Acquisto F. Impaired sense of smell and altered olfactory system in RAG-1(--) immunodeficient mice. Front Neurosci 2015; 9:318

52. Forni PE, Wray S. GnRH, anosmia and hypogonadotropic hypogonadism--where are we? Front Neuroendocrinol 2015; 36:165-177

53. Schwanzel-Fukuda M, Pfaff DW. Origin of luteinizing hormone-releasing hormone neurons. Nature 1989; 338:161-164

54. Schwanzel-Fukuda M. Origin and migration of luteinizing hormone-releasing hormone neurons in mammals. Microsc Res Tech 1999; 44:2-10

55. Chan YM, de Guillebon A, Lang-Muritano M, Plummer L, Cerrato F, Tsiaras S, Gaspert A, Lavoie HB, Wu CH, Crowley WF, Jr., Amory JK, Pitteloud N, Seminara SB. GNRH1 mutations in patients with idiopathic hypogonadotropic hypogonadism. Proc Natl Acad Sci USA 2009; 106:11703-11708

56. Diaczok D, DiVall S, Matsuo I, Wondisford FE, Wolfe AM, Radovick S. Deletion of Otx2 in GnRH neurons results in a mouse model of hypogonadotropic hypogonadism. Mol Endocrinol 2011; 25:833-846

57. Hoffmann HM, Trang C, Gong P, Kimura I, Pandolfi EC, Mellon PL. Deletion of Vax1 from GnRH neurons abolishes GnRH expression and leads to hypogonadism and infertility. J Neurosci 2016; 36:3506-3518

58. Larder R, Kimura I, Meadows J, Clark DD, Mayo S, Mellon PL. Gene dosage of Otx2 is important for fertility in male mice. Mol Cell Endocrinol 2013; 377:16-22

59. Lagutin OV, Zhu CC, Kobayashi D, Topczewski J, Shimamura K, Puelles L, Russell HR, McKinnon PJ, Solnica-Krezel L, Oliver G. Six3 repression of Wnt signaling in the anterior neuroectoderm is essential for vertebrate forebrain development. Genes Dev 2003; 17:368-379

60. Oliver G, Mailhos A, Wehr R, Copeland NG, Jenkins NA, Gruss P. Six3, a murine homologue of the sine oculis gene, demarcates the most anterior border of the developing neural plate and is expressed during eye development. Development 1995; 121:4045-4055

61. Anderson AM, Weasner BM, Weasner BP, Kumar JP. Dual transcriptional activities of SIX proteins define their roles in normal and ectopic eye development. Development 2012; 139:991-1000

62. Dubourg C, Lazaro L, Pasquier L, Bendavid C, Blayau M, Le Duff F, Durou MR, Odent S, David V. Molecular screening of SHH, ZIC2, SIX3, and TGIF genes in patients with features of holoprosencephaly spectrum: Mutation review and genotype-phenotype correlations. Hum Mutat 2004; 24:43-51

63. Pasquier L, Dubourg C, Blayau M, Lazaro L, Le Marec B, David V, Odent S. A new mutation in the six-domain of SIX3 gene causes holoprosencephaly. Eur J Hum Genet 2000; 8:797-800

64. Pasquier L, Dubourg C, Gonzales M, Lazaro L, David V, Odent S, Encha-Razavi F. First occurrence of aprosencephaly/atelencephaly and holoprosencephaly in a family with a SIX3 gene mutation and phenotype/genotype correlation in our series of SIX3 mutations. J Med Genet 2005; 42:e4

65. Lewandoski M, Wassarman KM, Martin GR. Zp3-cre, a transgenic mouse line for the activation or inactivation of loxP-flanked target genes specifically in the female germ line. Curr Biol 1997; 7:148-151

66. Wolfe A, Divall S, Singh SP, Nikrodhanond AA, Baria AT, Le WW, Hoffman GE, Radovick S. Temporal and spatial regulation of CRE recombinase expression in gonadotrophin-releasing hormone neurones in the mouse. J Neuroendocrinol 2008; 20:909-916

67. Paxinos G, Franklin KBJ. The mouse brain in stereotxic coordinates. Academic Press.

68. Srinivas S, Watanabe T, Lin CS, William CM, Tanabe Y, Jessell TM, Costantini F. Cre reporter strains produced by targeted insertion of EYFP and ECFP into the ROSA26 locus. BMC Dev Biol 2001; 1:4

69. Yang M, Crawley JN. Simple behavioral assessment of mouse olfaction. Curr Protoc Neurosci 2009; Chapter 8:Unit 8 24

70. Arakawa H, Blanchard DC, Arakawa K, Dunlap C, Blanchard RJ. Scent marking behavior as an odorant communication in mice. Neurosci Biobehav Rev 2008; 32:1236-1248

71. Pankevich DE, Baum MJ, Cherry JA. Olfactory sex discrimination persists, whereas the preference for urinary odorants from estrous females disappears in male mice after vomeronasal organ removal. J Neurosci 2004; 24:9451-9457

72. Stowers L, Holy TE, Meister M, Dulac C, Koentges G. Loss of sex discrimination and male-male aggression in mice deficient for TRP2. Science 2002; 295:1493-1500

73. Poling MC, Kauffman AS. Sexually dimorphic testosterone secretion in prenatal and neonatal mice is independent of kisspeptin-Kiss1r and GnRH signaling. Endocrinology 2012; 153:782-793

74. Kimchi T, Xu J, Dulac C. A functional circuit underlying male sexual behaviour in the female mouse brain. Nature 2007; 448:1009-1014

75. Matsuo T, Hattori T, Asaba A, Inoue N, Kanomata N, Kikusui T, Kobayakawa R, Kobayakawa K. Genetic dissection of pheromone processing reveals main olfactory system-mediated social behaviors in mice. Proc Natl Acad Sci U S A 2015; 112:E311-320

76. Slotnick B, Restrepo D, Schellinck H, Archbold G, Price S, Lin W. Accessory olfactory bulb function is modulated by input from the main olfactory epithelium. Eur J Neurosci 2010; 31:1108-1116

77. Suarez R, Garcia-Gonzalez D, de Castro F. Mutual influences between the main olfactory and vomeronasal systems in development and evolution. Front Neuroanat 2012; 6:50

78. Der-Avakian A, Markou A. The neurobiology of anhedonia and other reward-related deficits. Trends Neurosci 2012; 35:68-77

79. Boden MJ, Kennaway DJ. Circadian rhythms and reproduction. Reproduction 2006; 132:379-392

80. Fueshko S, Wray S. LHRH cells migrate on peripherin fibers in embryonic olfactory explant cultures: an in vitro model for neurophilic neuronal migration. Dev Biol 1994; 166:331-348

81. Strauss JF, Barbieri RL. Yen and Jaffe's Reproductive Endocrinology. 5th ed. Philadelphia, PA: Elsevier Saunders.

82. Walters KA, Allan CM, Jimenez M, Lim PR, Davey RA, Zajac JD, Illingworth P, Handelsman DJ. Female mice haploinsufficient for an inactivated androgen receptor (AR) exhibit age-dependent defects that resemble the AR null phenotype of dysfunctional late follicle development, ovulation, and fertility. Endocrinology 2007; 148:3674-3684

83. Kim HG, Herrick SR, Lemyre E, Kishikawa S, Salisz JA, Seminara S, MacDonald ME, Bruns GA, Morton CC, Quade BJ, Gusella JF. Hypogonadotropic hypogonadism and cleft lip and palate caused by a balanced translocation producing haploinsufficiency for FGFR1. J Med Genet 2005; 42:666-672

84. Pandolfi EC, Hoffmann HM, Schoeller EL, Gorman MR, Mellon PL. Haploinsufficiency of SIX3 abolishes male reproductive behavior through disrupted olfactory development, and impairs female fertility through disrupted GnRH neuron migration. Mol Neurobiol 2018; in press

85. Schwanzel-Fukuda M, Abraham S, Crossin KL, Edelman GM, Pfaff DW. Immunocytochemical demonstration of neural cell adhesion molecule (NCAM) along the migration route of luteinizing hormone-releasing hormone (LHRH) neurons in mice. J Comp Neurol 1992; 321:1-18

86. Kabrita CS, Davis FC. Development of the mouse suprachiasmatic nucleus: determination of time of cell origin and spatial arrangements within the nucleus. Brain Res 2008; 1195:20-27

87. Sonne J, Lopez-Ojeda W. Neuroanatomy, Cranial Nerve. StatPearls. Treasure Island (FL)2018.

88. Wray S, Grant P, Gainer H. Evidence that cells expressing luteinizing hormone-releasing hormone mRNA in the mouse are derived from progenitor cells in the olfactory placode. Proc Natl Acad Sci USA 1989; 86:8132-8136

89. Simonian SX, Herbison AE. Regulation of gonadotropin-releasing hormone (GnRH) gene expression during GnRH neuron migration in the mouse. Neuroendocrinology 2001; 73:149-156

90. Gore AC, Roberts JL, Gibson MJ. Mechanisms for the regulation of gonadotropin-releasing hormone gene expression in the developing mouse. Endocrinology 1999; 140:2280-2287

91. Schwanzel-Fukuda M, Jorgenson KL, Bergen HT, Weesner GD, Pfaff DW. Biology of normal luteinizing hormone-releasing hormone neurons during and after their migration from olfactory placode. Endocrine Rev 1992; 13:623-634

92. Wierman ME, Kiseljak-Vassiliades K, Tobet S. Gonadotropin-releasing hormone (GnRH) neuron migration: initiation, maintenance and cessation as critical steps to ensure normal reproductive function. Front Neuroendocrinol 2011; 32:43-52

93. Seminara SB, Hayes FJ, Crowley WF, Jr. Gonadotropin-releasing hormone deficiency in the human (idiopathic hypogonadotropic hypogonadism and Kallmann's syndrome): pathophysiological and genetic considerations. Endocrine Rev 1998; 19:521-539

94. Mellon PL, Windle JJ, Goldsmith P, Padula C, Roberts J, Weiner RI. Immortalization of hypothalamic GnRH neurons by genetically targeted tumorigenesis. Neuron 1990; 5:1-10

95. Radovick S, Wray S, Lee E, Nicols DK, Nakayama Y, Weintraub BD, Westphal H, Cutler GB, Jr., Wondisford FE. Migratory arrest of gonadotropin-releasing hormone neurons in transgenic mice. Proc Natl Acad Sci USA 1991; 88:3402-3406

96. Hoffmann HM, Gong P, Tamrazian A, Mellon PL. Transcriptional interaction between cFOS and the homeodomain-binding transcription factor VAX1 on the GnRH promoter controls Gnrh1 expression levels in a GnRH neuron maturation specific manner. Mol Cell Endocrinol 2017;

97. Larder R, Mellon PL. Otx2 induction of the gonadotropin-releasing hormone promoter is modulated by direct interactions with Grg co-repressors. J Biol Chem 2009; 284:16966-16978

98. Kim HH, Wolfe A, Cohen RN, Eames SC, Johnson AL, Wieland CN, Radovick S. In vivo identification of a 107 bp promoter element mediating neuron-specific expression of mouse GnRH. Mol Endocrinol 2007; 21:457-471

99. Acampora D, Mazan S, Lallemand Y, Avantaggiato V, Maury M, Simeone A, Brulet P. Forebrain and midbrain regions are deleted in OTX2-/- mutants due to a defective anterior neuroectoderm specification during gastrulation. Development 1995; 121:3279-3290

100. Simeone A, Acampora D, Mallamaci A, Stornaiuolo A, D'Apice R, Nigro V, Boncinelli E. A vertebrate gene related to orthodenticle contains a homeodomain of the bicoid class and demarcates anterior neuroectoderm of the gastrulating mouse embryo. EMBO J 1993; 12:2735-2774

101. Frantz GD, Weimann JM, Levin ME, McConnell SK. Otx1 and Otx2 define layers and regions in developing cerebral cortex and cerebellum. J Neurosci 1994; 14:5725-5740

102. Puelles E, Annino A, Tuorto F, Usiello A, Acampora D, Czerny T, Brodski C, Ang SL, Wurst W, Simeone A. Otx2 regulates the extent, identity and fate of neuronal progenitor domains in the ventral midbrain. Development 2004; 131:2037-2048

103. Mallamaci A, DiBlas E, Briata P, Boncinelli E, Corte G. OTX2 homeoprotein in the developing central nervous system and migratory cells of the olfactory area. Mech Devel 1996; 58:165-178

104. Dateki S, Kosaka K, Hasegawa K, Tanaka H, Azuma N, Yokoya S, Muroya K, Adachi M, Tajima T, Motomura K, Kinoshita E, Moriuchi H, Sato N, Fukami M, Ogata T. Heterozygous orthodenticle homeobox 2 mutations are associated with variable pituitary phenotype. J Clin Endocrinol Metab 2010; 95:756-764

105. Dateki S, Fukami M, Sato N, Muroya K, Adachi M, Ogata T. OTX2 mutation in a patient with anophthalmia, short stature, and partial growth hormone deficiency: functional studies using the IRBP, HESX1, and POU1F1 promoters. J Clin Endocrinol Metab 2008; 93:3697-3702

106. Diaczok D, Romero C, Zunich J, Marshall I, Radovick S. A novel dominant negative mutation of OTX2 associated with combined pituitary hormone deficiency. J Clin Endocrinol Metab 2008; 93:4351-4359

107. Ang S-L, Jin O, Rhinn M, Daigle N, Stevenson L, Rossant J. A targeted mouse OTX2 mutation leads to severe defects in gastrulation and formation of axial mesoderm and to deletion of rostral brain. Development 1996; 122:243-252

108. Matsuo I, Kuratani S, Kimura C, Takeda N, Aizawa S. Mouse OTX2 functions in the formation and patterning of rostral head. Genes & Dev 1995; 9:2646-2658

109. Fossat N, Chatelain G, Brun G, Lamonerie T. Temporal and spatial delineation of mouse Otx2 functions by conditional self-knockout. EMBO Rep 2006; 7:824-830

110. Kelley CG, Lavorgna G, Clark ME, Boncinelli E, Mellon PL. The Otx2 homeoprotein regulates expression from the gonadotropin-releasing hormone proximal promoter. Mol Endocrinol 2000; 14:1246-1256

111. Taglialatela P, Soria JM, Caironi V, Moiana A, Bertuzzi S. Compromised generation of GABAergic interneurons in the brains of Vax1-/- mice. Development 2004; 131:4239-4249

112. Soria JM, Taglialatela P, Gil-Perotin S, Galli R, Gritti A, Verdugo JM, Bertuzzi S. Defective postnatal neurogenesis and disorganization of the rostral migratory stream in absence of the Vax1 homeobox gene. J Neurosci 2004; 24:11171-11181

113. Bertuzzi S, Hindges R, Mui SH, O'Leary DD, Lemke G. The homeodomain protein vax1 is required for axon guidance and major tract formation in the developing forebrain. Genes Dev 1999; 13:3092-3105

114. Hallonet M, Hollemann T, Pieler T, Gruss P. Vax1, a novel homeobox-containing gene, directs development of the basal forebrain and visual system. Genes Dev 1999; 13:3106-3114

115. Geoghegan F, Xavier GM, Birjandi AA, Seppala M, Cobourne MT. Vax1 Plays an Indirect Role in the Etiology of Murine Cleft Palate. J Dent Res 2017; 96:1555-1562

116. Zhao L, Saitsu H, Sun X, Shiota K, Ishibashi M. Sonic hedgehog is involved in formation of the ventral optic cup by limiting Bmp4 expression to the dorsal domain. Mech Dev 2010; 127:62-72

117. Bharti K, Gasper M, Bertuzzi S, Arnheiter H. Lack of the ventral anterior homeodomain transcription factor VAX1 leads to induction of a second pituitary. Development 2011; 138:873-878

118. Slavotinek AM, Chao R, Vacik T, Yahyavi M, Abouzeid H, Bardakjian T, Schneider A, Shaw G, Sherr EH, Lemke G, Youssef M, Schorderet DF. VAX1 mutation associated with microphthalmia, corpus callosum agenesis, and orofacial clefting: the first description of a VAX1 phenotype in humans. Hum Mutat 2012; 33:364-368

119. Butali A, Suzuki S, Cooper ME, Mansilla AM, Cuenco K, Leslie EJ, Suzuki Y, Niimi T, Yamamoto M, Ayanga G, Erkhembaatar T, Furukawa H, Fujiwawa K, Imura H, Petrin AL, Natsume N, Beaty TH, Marazita ML, Murray JC. Replication of genome wide association

identified candidate genes confirm the role of common and rare variants in PAX7 and VAX1 in the etiology of nonsyndromic CL(P). Am J Med Genet A 2013; 161A:965-972

120. de Aquino SN, Messetti AC, Bagordakis E, Martelli-Junior H, Swerts MS, Graner E, Coletta RD. Polymorphisms in FGF12, VCL, CX43 and VAX1 in Brazilian patients with nonsyndromic cleft lip with or without cleft palate. BMC Med Genet 2013; 14:53

121. Zhang BH, Shi JY, Lin YS, Shi B, Jia ZL. VAX1 gene associated non-syndromic cleft lip with or without palate in Western Han Chinese. Arch Oral Biol 2018; 95:40-43

122. VanDunk C, Hunter LA, Gray PA. Development, maturation, and necessity of transcription factors in the mouse suprachiasmatic nucleus. J Neurosci 2011; 31:6457-6467

123. Gallardo ME, Lopez-Rios J, Fernaud-Espinosa I, Granadino B, Sanz R, Ramos C, Ayuso C, Seller MJ, Brunner HG, Bovolenta P, Rodriguez de Cordoba S. Genomic cloning and characterization of the human homeobox gene SIX6 reveals a cluster of SIX genes in chromosome 14 and associates SIX6 hemizygosity with bilateral anophthalmia and pituitary anomalies. Genomics 1999; 61:82-91

124. Tsai PS, Gill JC. Mechanisms of disease: Insights into X-linked and autosomal-dominant Kallmann syndrome. Nat Clin Pract Endocrinol Metab 2006; 2:160-171

125. Kramer PR, Wray S. Novel gene expressed in nasal region influences outgrowth of olfactory axons and migration of luteinizing hormone-releasing hormone (LHRH) neurons. Genes Dev 2000; 14:1824-1834

126. Xu N, Kim HG, Bhagavath B, Cho SG, Lee JH, Ha K, Meliciani I, Wenzel W, Podolsky RH, Chorich LP, Stackhouse KA, Grove AM, Odom LN, Ozata M, Bick DP, Sherins RJ, Kim SH, Cameron RS, Layman LC. Nasal embryonic LHRH factor (NELF) mutations in patients with normosmic hypogonadotropic hypogonadism and Kallmann syndrome. Fertil Steril 2011; 95:1613-1620

127. Silveira LG, Noel SD, Silveira-Neto AP, Abreu AP, Brito VN, Santos MG, Bianco SD, Kuohung W, Xu S, Gryngarten M, Escobar ME, Arnhold IJ, Mendonca BB, Kaiser UB, Latronico AC. Mutations of the KISS1 gene in disorders of puberty. J Clin Endocrinol Metab 2010; 95:2276-2280

128. Mandiyan VS, Coats JK, Shah NM. Deficits in sexual and aggressive behaviors in Cnga2 mutant mice. Nat Neurosci 2005; 8:1660-1662

129. Herbison AE, Porteous R, Pape JR, Mora JM, Hurst PR. Gonadotropin-releasing hormone (GnRH) neuron requirements for puberty, ovulation and fertility. Endocrinology 2008; 149:597-604

130. Pingault V, Bodereau V, Baral V, Marcos S, Watanabe Y, Chaoui A, Fouveaut C, Leroy C, Verier-Mine O, Francannet C, Dupin-Deguine D, Archambeaud F, Kurtz FJ, Young J, Bertherat J, Marlin S, Goossens M, Hardelin JP, Dode C, Bondurand N. Loss-of-function mutations in SOX10 cause Kallmann syndrome with deafness. Am J Hum Genet 2013; 92:707-724

131. Givens ML, Rave-Harel N, Goonewardena VD, Kurotani R, Berdy SE, Swan CH, Rubenstein JL, Robert B, Mellon PL. Developmental regulation of gonadotropin-releasing hormone gene expression by the MSX and DLX homeodomain protein families. J Biol Chem 2005; 280:19156-19165

132. Ng KL, Li JD, Cheng MY, Leslie FM, Lee AG, Zhou QY. Dependence of olfactory bulb neurogenesis on prokineticin 2 signaling. Science 2005; 308:1923-1927

133. Dode C, Rondard P. PROK2/PROKR2 Signaling and Kallmann Syndrome. Front Endocrinol (Lausanne) 2013; 4:19

134. Layman WS, McEwen DP, Beyer LA, Lalani SR, Fernbach SD, Oh E, Swaroop A, Hegg CC, Raphael Y, Martens JR, Martin DM. Defects in neural stem cell proliferation and olfaction in Chd7 deficient mice indicate a mechanism for hyposmia in human CHARGE syndrome. Hum Mol Genet 2009; 18:1909-1923

135. Edwards DA, Burge KG. Olfactory control of the sexual behavior of male and female mice. Physiol Behav 1973; 11:867-872

136. Zhu CC, Dyer MA, Uchikawa M, Kondoh H, Lagutin OV, Oliver G. Six3-mediated auto repression and eye development requires its interaction with members of the Groucho-related family of co-repressors. Development 2002; 129:2835-2849

137. Restrepo D, Zviman M, Rawson NE. Imaging of Intracellular Calcium in Chemosensory Receptor Cells. In: Spielman AI, Brand JG, eds. Experimental Cell Biology of Taste and Olfaction: Current Techniques and Protocols. Boca Raton, FL: CRC Press; 1995:387–398.

138. Butler A, Hoffman P, Smibert P, Papalexi E, Satija R. Integrating single-cell transcriptomic data across different conditions, technologies, and species. Nat Biotechnol 2018; 36:411-420

139. Fan J, Salathia N, Liu R, Kaeser GE, Yung YC, Herman JL, Kaper F, Fan JB, Zhang K, Chun J, Kharchenko PV. Characterizing transcriptional heterogeneity through pathway and gene set overdispersion analysis. Nat Methods 2016; 13:241-244

140. Wickham H. ggplot2, Elegant Graphics for Data Analysis. 2 ed. Switzerland: Springer International Publishing.

141. Wray S, Key S, Qualls R, Fueshko SM. A subset of peripherin positive olfactory axons delineates the luteinizing hormone releasing hormone neuronal migratory pathway in developing mouse. Dev Biol 1994; 166:349-354

142. Henion TR, Raitcheva D, Grosholz R, Biellmann F, Skarnes WC, Hennet T, Schwarting GA. Beta1,3-N-acetylglucosaminyltransferase 1 glycosylation is required for axon pathfinding by olfactory sensory neurons. J Neurosci 2005; 25:1894-1903

143. Whitlock KE. Origin and development of GnRH neurons. Trends Endocrinol Metab 2005; 16:145-151

144. Chen CR, Kachramanoglou C, Li D, Andrews P, Choi D. Anatomy and cellular constituents of the human olfactory mucosa: a review. J Neurol Surg B Skull Base 2014; 75:293-300

145. Kam JW, Raja R, Cloutier JF. Cellular and molecular mechanisms regulating embryonic neurogenesis in the rodent olfactory epithelium. Int J Dev Neurosci 2014; 37:76-86

146. Calof AL, Bonnin A, Crocker C, Kawauchi S, Murray RC, Shou J, Wu HH. Progenitor cells of the olfactory receptor neuron lineage. Microsc Res Tech 2002; 58:176-188

147. Liu W, Cvekl A. Six3 in a small population of progenitors at E8.5 is required for neuroretinal specification via regulating cell signaling and survival in mice. Dev Biol 2017; 428:164-175

148. Kumar JP. The sine oculis homeobox (SIX) family of transcription factors as regulators of development and disease. Cell Mol Life Sci 2009; 66:565-583

149. Kawakami K, Sato S, Ozaki H, Ikeda K. Six family genes--structure and function as transcription factors and their roles in development. Bioessays 2000; 22:616-626

150. Ikeda K, Ookawara S, Sato S, Ando Z, Kageyama R, Kawakami K. Six1 is essential for early neurogenesis in the development of olfactory epithelium. Dev Biol 2007; 311:53-68

151. Ikeda K, Kageyama R, Suzuki Y, Kawakami K. Six1 is indispensable for production of functional progenitor cells during olfactory epithelial development. Int J Dev Biol 2010; 54:1453-1464

152. Geng X, Acosta S, Lagutin O, Gil H, Oliver G. Six3 dosage mediates the pathogenesis of holoprosencephaly. Development 2016;

153. Carl M, Loosli F, Wittbrodt J. Six3 inactivation reveals its essential role for the formation and patterning of the vertebrate eye. Development 2002; 129:4057-4063

154. Cheyette BN, Green PJ, Martin K, Garren H, Hartenstein V, Zipursky SL. The Drosophila sine oculis locus encodes a homeodomain-containing protein required for the development of the entire visual system. Neuron 1994; 12:977-996

155. Zhu X, Rosenfeld MG. Transcriptional control of precursor proliferation in the early phases of pituitary development. Curr Opin Genet Dev 2004; 14:567-574

156. Schwob JE, Jang W, Holbrook EH, Lin B, Herrick DB, Peterson JN, Hewitt Coleman J. Stem and progenitor cells of the mammalian olfactory epithelium: Taking poietic license. J Comp Neurol 2017; 525:1034-1054

157. Beites CL, Kawauchi S, Crocker CE, Calof AL. Identification and molecular regulation of neural stem cells in the olfactory epithelium. Exp Cell Res 2005; 306:309-316

158. Belluscio L, Gold GH, Nemes A, Axel R. Mice deficient in G(olf) are anosmic. Neuron 1998; 20:69-81

159. Cariboni A, Maggi R, Parnavelas JG. From nose to fertility: the long migratory journey of gonadotropin-releasing hormone neurons. Trends Neurosci 2007; 30:638-644

160. Tarozzo G, Peretto P, Perroteau I, Andreone C, Varga Z, Nicholls J, Fasolo A. GnRH neurons and other cell populations migrating from the olfactory neuroepithelium. Ann Endocrinol (Paris) 1994; 55:249-254

161. Solomon BD, Lacbawan F, Jain M, Domene S, Roessler E, Moore C, Dobyns WB, Muenke M. A novel SIX3 mutation segregates with holoprosencephaly in a large family. Am J Med Genet A 2009; 149A:919-925

162. Wallis DE, Roessler E, Hehr U, Nanni L, Wiltshire T, Richieri-Costa A, Gillessen-Kaesbach G, Zackai EH, Rommens J, Muenke M. Mutations in the homeodomain of the human SIX3 gene cause holoprosencephaly. Nat Genet 1999; 22:196-198

163. Mason AJ, Pitts SL, Nikolics K, Szonyi E, Wilcox JN, Seeburg PH, Stewart TA. The hypogonadal mouse: Reproductive functions restored by gene therapy. Science 1986; 234:1372-1378

164. Valdes-Socin H, Rubio Almanza M, Tome Fernandez-Ladreda M, Debray FG, Bours V, Beckers A. Reproduction, smell, and neurodevelopmental disorders: genetic defects in

different hypogonadotropic hypogonadal syndromes. Front Endocrinol (Lausanne) 2014; 5:109

165. Hardelin JP. Kallmann syndrome: towards molecular pathogenesis. Mol Cell Endocrinol 2001; 179:75-81

166. Gonzalez-Martinez D, Hu Y, Bouloux PM. Ontogeny of GnRH and olfactory neuronal systems in man: novel insights from the investigation of inherited forms of Kallmann's syndrome. Front Neuroendocrinol 2004; 25:108-130

167. Kobayashi M, Taniura H, Yoshikawa K. Ectopic expression of necdin induces differentiation of mouse neuroblastoma cells. J Biol Chem 2002; 277:42128-42135

168. Rodriguez CI, Buchholz F, Galloway J, Sequerra R, Kasper J, Ayala R, Stewart AF, Dymecki SM. High-efficiency deleter mice show that FLPe is an alternative to Cre-loxP. Nat Genet 2000; 25:139-140

169. Tsai PS, Moenter SM, Postigo HR, El Majdoubi M, Pak TR, Gill JC, Paruthiyil S, Werner S, Weiner RI. Targeted expression of a dominant-negative fibroblast growth factor (FGF) receptor in gonadotropin-releasing hormone (GnRH) neurons reduces FGF responsiveness and the size of GnRH neuronal population. Mol Endocrinol 2005; 19:225-236

170. Gill JC, Wadas B, Chen P, Portillo W, Reyna A, Jorgensen E, Mani S, Schwarting GA, Moenter SM, Tobet S, Kaiser UB. The gonadotropin-releasing hormone (GnRH) neuronal population is normal in size and distribution in GnRH-deficient and GnRH receptor-mutant hypogonadal mice. Endocrinology 2008; 149:4596-4604

171. Gill JC, Moenter SM, Tsai PS. Developmental regulation of gonadotropin-releasing hormone neurons by fibroblast growth factor signaling. Endocrinology 2004; 145:3830-3839

172. Novaira HJ, Fadoju D, Diaczok D, Radovick S. Genetic mechanisms mediating kisspeptin regulation of GnRH gene expression. J Neurosci 2012; 32:17391-17400

173. DiVall SA, Herrera D, Sklar B, Wu S, Wondisford F, Radovick S, Wolfe A. Insulin receptor signaling in the GnRH neuron plays a role in the abnormal GnRH pulsatility of obese female mice. PLoS One 2015; 10:e0119995

174. Schinckel AP, Johnson RK, Kittok RJ. Relationships among measures of testicular development and endocrine function in boars. J Anim Sci 1984; 58:1255-1261

175. Beaver LM, Gvakharia BO, Vollintine TS, Hege DM, Stanewsky R, Giebultowicz JM. Loss of circadian clock function decreases reproductive fitness in males of Drosophila melanogaster. Proc Natl Acad Sci USA 2002; 99:2134-2139

176. MacColl G, Bouloux P, Quinton R. Kallmann syndrome: adhesion, afferents, and anosmia. Neuron 2002; 34:675-678

177. Schwarting GA, Wierman ME, Tobet SA. Gonadotropin-releasing hormone neuronal migration. Semin Reprod Med 2007; 25:305-312

178. Wierman ME, Bruder JM, Kepa JK. Regulation of gonadotropin-releasing hormone (GnRH) gene expression in hypothalamic neuronal cells. Cell Mol Neurobiol 1995; 15:79-88

179. Wolfe A, Kim HH, Radovick S. The GnRH neuron: molecular aspects of migration, gene expression and regulation. Prog Brain Res 2002; 141:243-257

180. Tobet SA, Hanna IK, Schwarting GA. Migration of neurons containing gonadotropin releasing hormone (GnRH) in slices from embryonic nasal compartment and forebrain. Brain Res Dev Brain Res 1996; 97:287-292

181. Branda CS, Dymecki SM. Talking about a revolution: The impact of site-specific recombinases on genetic analyses in mice. Dev Cell 2004; 6:7-28

182. Pogoda HM, Hammerschmidt M. Molecular genetics of pituitary development in zebrafish. Semin Cell Dev Biol 2007; 18:543-558

183. Wang H, Yang H, Shivalila CS, Dawlaty MM, Cheng AW, Zhang F, Jaenisch R. One-step generation of mice carrying mutations in multiple genes by CRISPR/Cas-mediated genome engineering. Cell 2013; 153:910-918

184. Dubois NC, Hofmann D, Kaloulis K, Bishop JM, Trumpp A. Nestin-Cre transgenic mouse line Nes-Cre1 mediates highly efficient Cre/loxP mediated recombination in the nervous system, kidney, and somite-derived tissues. Genesis 2006; 44:355-360

185. Rempe D, Vangeison G, Hamilton J, Li Y, Jepson M, Federoff HJ. Synapsin I Cre transgene expression in male mice produces germline recombination in progeny. Genesis 2006; 44:44-49

186. Whitlock KE, Wolf CD, Boyce ML. Gonadotropin-releasing hormone (GnRH) cells arise from cranial neural crest and adenohypophyseal regions of the neural plate in the zebrafish, Danio rerio. Dev Biol 2003; 257:140-152

187. Messina A, Langlet F, Chachlaki K, Roa J, Rasika S, Jouy N, Gallet S, Gaytan F, Parkash J, Tena-Sempere M, Giacobini P, Prevot V. A microRNA switch regulates the rise in hypothalamic GnRH production before puberty. Nat Neurosci 2016; 19:835-844

188. Soriano P. Generalized *lacZ* expression with the ROSA26 Cre reporter strain. Nature Genetics 1999; 21:70-71

189. Carnes MU, Liu YP, Allingham RR, Whigham BT, Havens S, Garrett ME, Qiao C, Investigators NC, Katsanis N, Wiggs JL, Pasquale LR, Ashley-Koch A, Oh EC, Hauser MA. Discovery and functional annotation of SIX6 variants in primary open-angle glaucoma. PLoS Genet 2014; 10:e1004372

190. Mahoney MM. Shift work, jet lag, and female reproduction. Int J Endocrinol 2010; 2010:813764

191. Miller BH, Olson SL, Turek FW, Levine JE, Horton TH, Takahashi JS. Circadian clock mutation disrupts estrous cyclicity and maintenance of pregnancy. Curr Biol 2004; 14:1367-1373

192. Skowronska-Krawczyk D, Zhao L, Zhu J, Weinreb RN, Cao G, Luo J, Flagg K, Patel S, Wen C, Krupa M, Luo H, Ouyang H, Lin D, Wang W, Li G, Xu Y, Li O, Chung C, Yeh E, Jafari M, Ai M, Zhong Z, Shi W, Zheng L, Krawczyk M, Chen D, Shi C, Zin C, Zhu J, Mellon PL, Gao W, Abagyan R, Zhang L, Sun X, Zhong S, Zhuo Y, Rosenfeld MG, Liu Y, Zhang K. P16INK4a upregulation mediated by SIX6 defines retinal ganglion cell pathogenesis in glaucoma. Mol Cell 2015; 59:931-940